EXPERIMENTS ON SEPARATED FLOWS:

A NEW PROBE AND UPSTREAM EFFECTS OF SEPARATION

BY

RAMESH P. GUPTA

DEPARTMENT OF MECHANICAL ENGINEERING
INDIAN INSTITUTE OF TECHNOLOGY, KANPUR

MAY 1973

EXPERIMENTS ON SEPARATED FLOWS:
A NEW PROBE AND UPSTREAM EFFECTS OF SEPARATION

A Thesis Submitted
In Partial Fulfilment of the Requirements
for the Degree of

DOCTOR OF PHILOSOPHY

BY

RAMESH P. GUPTA

to the

DEPARTMENT OF MECHANICAL ENGINEERING

INDIAN INSTITUTE OF TECHNOLOGY, KANPUR

MAY 1973

CERTIFICATE

Certified that this work has been carried out under my supervision and that this has not been submitted elsewhere for a degree.

K.S. Yajnik

Dr. K.S. Yajnik
Associate Professor
Department of Mechanical Engineering
Indian Institute of Technology Kanpur

(Presently at
National Aeronautical Laboratory, Bangalore)

ACKNOWLEDGEMENTS

It is a great pleasure for me to express gratitude to Dr. K.S.Yajnik for his invaluable guidance and continuing encouragement. I am indebted to him in many ways, for suggesting the problem, for informal discussions, for critical appraisal and most important for being an unending source of inspiration.

I am thankful to the Departments of Mechanical and Aeronautical Engineering for permitting me to use the laboratory facilities. I especially wish to acknowledge that the Aeronautical Engineering wind tunnel facility, was made available to me for two and a half years, involving 700 hours of tunnel running for the experiments.

I am grateful to many of my colleagues for their invaluable help, especially Shri B.S.Rohewal (Fluid Mechanics Laboratory), M.M.Singh, D.K.Sarkar, Shrivastava, Krishnamurthy, Muthappa, Choudhary and Pande.

The help of Dr. A.K. Gupta (Aeronautical Engineering) for hot-wire work is highly appreciated.

The editorial suggestions of Mrs. Yajnik for improving the manuscript are appreciated.

Thanks are due to Shri S.S.Rao for drawing excellent figures and to Shri L.Pathiyappa for careful typing of the thesis.

Partial support of CSIR for this work under scheme 25(4)/69-GAU-II on separated flows during 1970-71 is acknowledged.

TABLE OF CONTENTS

PART II

UPSTREAM EFFECTS IN SEPARATION INDUCED BY A FORWARD-FACING WALL JET

LIST OF TABLES

PARAMETERS OF UPSTREAM EFFECT

LIST OF FIGURES

PART II

LIST OF SYMBOLS

C	Additive constant in the logarithmic velocity law in wall coordinates
C_f	Skin friction coefficient
C_p	Static pressure coefficient $=(p-p_\infty)/\frac{1}{2}\rho U_\infty^2$
$C_{p_{max}}$	Maximum value of C_p
$C_{p_{min}}$	Minimum value of C_p
d	Inner diameter of probe tube
D	Outer diameter of probe tube
h	Maximum height of the dividing streamline from test surface
H	Shape factor δ^*/θ
k	vonKārmān constant in the logarithmic velocity law in wall coordinates
L	A characteristic length of free stream boundary-layer
p	Static pressure
p_o	Pressure at the central tube of the three-tube probe
p_1, p_2	Pressures at the side tubes of the three tube probe

p_{ref}	Static pressure at first wall tap location in unseparated flow
p_{st}	Static pressure of pitot-static tube at reference station
p_{∞}	Free-stream static pressure
q_{∞}	Free-stream dynamic pressure
R_{θ}	Reynold number based on momentum thickness θ
R_{∞}	Reynold number based on U_{∞} and L
t_j	Wall jet height at exit
U	X component of mean velocity
U_e, U_1	Velocity at the edge of boundary-layer
U_j	Maximum wall jet velocity at jet exit
U_{∞}	Free stream velocity
U_{τ}	Friction velocity $=\sqrt{\tau_w/\rho}$
X	Coordinate parallel to the test surface
X_o	X location of $C_p = 0$
X_m	X location of $C_{p_{max}}$
X_s	X location of separation point
Y	Coordinate perpendicular to the test surface
α	Angle of the false wall with the X direction (radians)
δ	Boundary-layer thickness
δ^*	Displacement thickness
δ^{**}	Energy thickness
θ	Momentum thickness

Φ	Flow angle
$\bar{\Phi}$	Probe angle
Ψ	Stream function
ν	Kinematic viscosity
ρ	Density
τ_w	Wall shear stress
λ	Ratio of wall jet to free-stream velocity = U_j/U_∞

EXPERIMENTS ON SEPARATED FLOWS:
A NEW PROBE AND UPSTREAM EFFECTS OF SEPARATION
A Thesis Submitted
In Partial Fulfilment of the Requirements
for the Degree of
DOCTOR OF PHILOSOPHY
by
RAMESH P. GUPTA
to the
DEPARTMENT OF MECHANICAL ENGINEERING
INDIAN INSTITUTE OF TECHNOLOGY KANPUR
May 1973

SYNOPSIS

It is well-known that despite considerable technological interest in separated flows, there are very few experimental surveys of separated flows which can guide the development of prediction methods. Experimental results are given for a separated flow field with emphasis on the upstream effects of separation. A new pressure probe was developed during the investigation for making rapid surveys of separated flows. As the probe is expected to be of a more general interest, it is described in the first part of the work. The second part deals with the upstream effects.

The new three-tube pressure probe is asymmetric unlike all known probes. Two chamfered tubes are asymmetrically arranged flanking a central total-pressure tube. This configuration considerably reduces the transverse probe dimension, and enables it to be used in thin shear layers

and close to a wall. Further, errors due to transverse shear are reduced. It is capable of providing simultaneous measurements of flow direction, speed and total pressure in two-dimensional or axisymmetric flows. A parallelogram pitching apparatus was developed to align the probe in the flow direction.

Measurements of the probe were compared with well-known empirical laws and also pitot-probe measurements in zero pressure gradient turbulent boundary-layer and pipe flow. They suggested that the probe can be effectively used outside a region of about two tube diameters from a wall. Further measurements in a separating turbulent boundary-layer demonstrate the probe capability for making surveys of separated flow fields.

Upstream effects were studied by inducing separation from a flat surface by a two-dimensional forward-facing wall jet. The free-stream flow separated and the jet flow curved back forming a large recirculating region. Wall pressure distributions upstream of the separation point were studied as a function of three parameters, namely the ratio of jet to free-stream velocity, the free-stream Reynolds number and a pressure gradient parameter.

Wall pressure distributions in suitable non-dimensional coordinates showed a distinct trend towards similarity at large upstream distances. This distribution agreed, to a

first approximation, with the calculations based on inviscid flow models, which described in simple ways the displacement of the external flow by the recirculating region. There was however a region close to the separation point, typically extending about ten boundary-layer thicknesses, where a distinctly different trend was observed. It is therefore concluded that the upstream effect is governed by two length scales. The smaller scale describes the region where the comparatively larger rate of thickening of the layer near the wall influences the pressure distribution, although within the framework of classical boundary-layer theory, such an effect would be of a higher order.

It was observed that the pressure gradient near separation for the free-stream wall-layer was favourable. While this can be viewed as a consequence of the separation of the wall jet under adverse pressure gradient, a predictio procedure for the free-stream boundary-layer would have to predict separation in favourable pressure gradient. On the other hand, a classical argument holds that adverse pressure gradient is necessary for separation. It is argued that the classical argument applies only to velocity profiles which are monotonic before separation, while non-monotonic profiles were observed in this experiment.

The applicability of the observed upstream effects to other flow configurations is also discussed.

PART I

A NEW TECHNIQUE FOR FLOW MEASUREMENT IN SEPARATED FLOWS

ABSTRACT

A new three-tube pressure-probe is developed for measurement of flow direction, and dynamic and total pressure in two-dimensional separated flows. Unlike all earlier probes, it is asymmetric. The arrangement of side tubes, which is responsible for the asymmetry, allows it to be used in thin shear layers and close to wall, where earlier probes tended to be inaccurate. A pitching apparatus is designed to align the probe in the flow direction.

Measurements with the new probe are compared with classical pitot tube measurements and well-known empérical laws in zero-pressure-gradient turbulent boundary-layer and fully developed pipe flow. The comparison shows that the new probe can be effectively used, with uniform flow calibration, in a shear flow outside a region of about two probe-tube diameter thickness from a wall.

The capability of the new probe in surveying complex flow fields is demonstrated by measurements in wall-jet induced separation.

CHAPTER 1

A NEW ASYMMETRIC PRESSURE-PROBE FOR SEPARATED FLOWS

1.1 INTRODUCTION

Since separation frequently occurs in turbomachine components and fluidic devices, and is unavoidable at the base of the rear fuselage of certain aircraft, there is significant technological interest in the development and improvement of prediction methods for separated flows. As in the case of turbulent boundary-layers, detailed surveys of representative types of separated flows are indispensable for the assessment of such prediction methods and for guiding their improvement.

However, unlike extensive data (Coles, 1968) available for turbulent boundary-layers, data for separated flows are very scanty. The difference is mainly due to the relative complexity of measurements in separated flows. The simple method of measuring the velocity profile with a pitot-probe and a static wall tap is adequate for the mean flow field in two-dimensional boundary-layers. But transverse variations of static pressure and flow direction in two-dimensional separated flows increase the number of quantities to be measured at interior points from one to three.

A majority of the velocity and flow direction measuring techniques can be broadly categorised into three classes depending on whether they rely on pressure-probes or they use the hot-wire or laser-doppler anemometer. The first category has the advantages of simplicity and the possibility of simultaneous measurement of all mean flow quantities. The second category gives measurements of greater precision, but difficulties arise when velocity fluctuations are not very small in comparison with the mean. The third category has received considerable attention recently (e.g. Durst and Whitelaw, 1971) and is believed to have great potential as a high precision technique. The last two categories however require separate measurements for static pressure for a complete survey of the flow field. Hence they are likely to be useful in a few test flows requiring greater precision rather than in surveys of large number of representative types of flow.

The simplest of pressure-probe methods using either a pitot-static tube or a pitot tube with a wall tap tends to be inaccurate in separated flows for two reasons. First, the normal velocity component, which is in general not insignificant, leads to errors of nonalignment. Second, the transverse variation of static pressure can cause significant errors in the second method. More complex probes like yawmeter probes or combination probes have their limitations. While they are suitable for approximately

uniform flows, their large transverse dimensions introduce errors in a shear layer or in the vicinity of the separation point. Morever, if they are not aligned in the flow direction, they are unsatisfactory for pitch angles larger than about $\pm 20°$ (Bryer et.al., 1958). If they are to be aligned in the flow direction, the mechanical problems in designing the pitch-cum-traverse apparatus are difficult to solve.

The first part of this work is devoted to a new pressure-probe for separated flows.* Unlike all known pressure-probes, it is asymmetric. This probe was developed in the context of a study of upstream effects which is the theme of the second part of this work. The context is explained briefly in the next section, but as the probe is expected to be useful in a wide range of separated flows, the first part is largely independent of the second.

The probe and the pitching apparatus are described in sections 3 and 4 of this chapter. Calibration procedures, installation and operation are taken up in the last two sections. Probe performance and typical measurements are described in the second chapter.

1.2 THE ORIGIN OF THE PROBE

A survey of the flow field was desired during an investigation of upstream effects of boundary-layer

---

* A preliminary account is given by Vajnik & Gupta (1973).

separation. In particular, velocity profile surveys upstream of separation were required to find the development of boundary-layer parameters. The flow field is shown in Figure 1, where an approximately two-dimensional wall-jet orposes an uniform stream. The free stream boundary-layer separates due to the action of the wall-jet and the jet flow curves back forming a large recirculating region.

A pitot-static tube or a pitot tube with a wall tap were not considered suitable for reasons given earlier. The next alternative was to use a pressure sensing combination probe with a suitable orientation mechanism. Probes for two-dimensional flows shown in Figure 2 were considered after a literature survey. Although they are suitable for uniform flows, significant errors can arise due to shear in separated flows as explained in the next section. Further, the transverse dimension of the probes introduce difficulties in measurements in thin shear layers or close a separation point. These considerations suggested the need for a new probe.

1.3 THE EFFECT OF SHEAR

Figure 3 (b) shows a three-tube Conrad type of probe in a parallel flow with shear. When the probe is aligned in the flow direction, the side tubes will indicate a pressure difference depending on the shear and the distance between the axes of the tubes. If the pressure difference

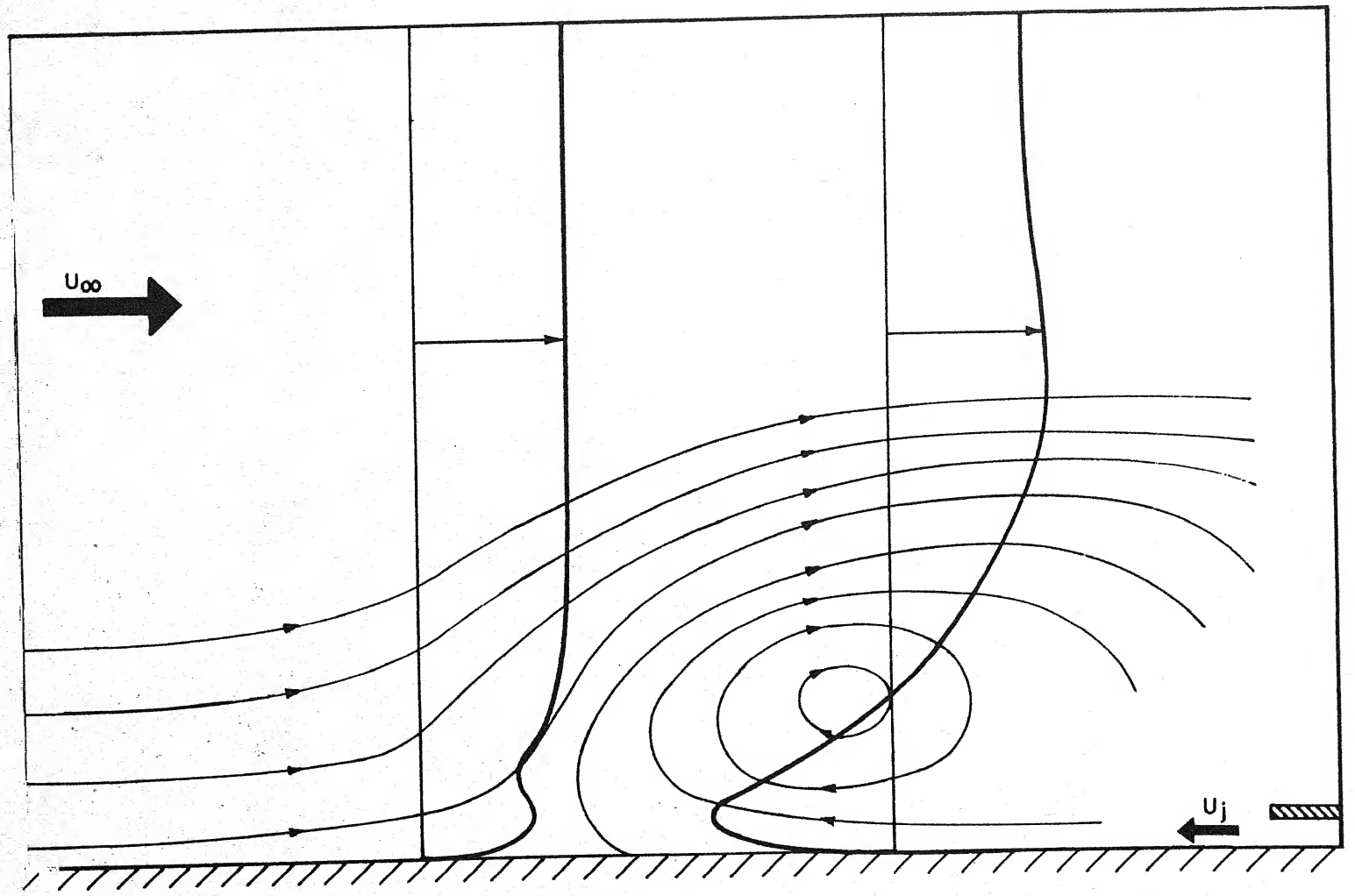

FIG.1 WALL JET INDUCED SEPARATION
(SCHEMATIC)

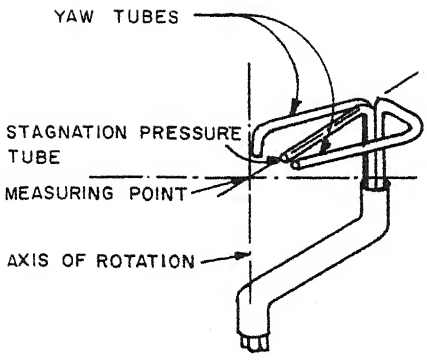

(a) TWO-DIMENSIONAL CLAW PROBE

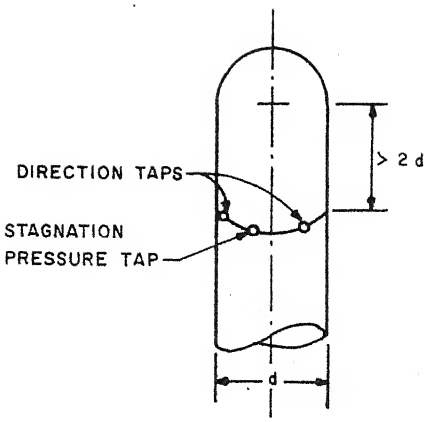

(b) 3-HOLE YAW PROBE

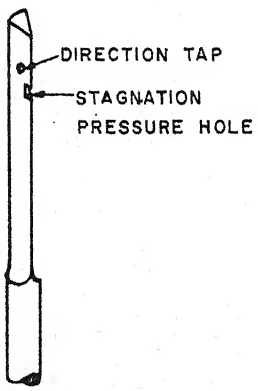

(c) WEDGE PROBE

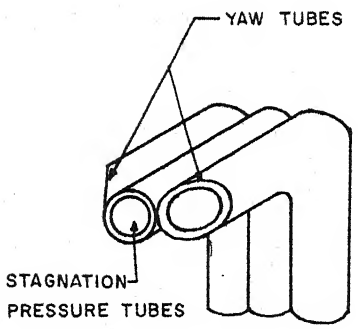

(d) CONRAD PROBE

FIG.2 PRESSURE PROBES FOR TWO-DIMENSIONAL FLOWS

is used as an indication of the probe alignment, an error in the flow direction will result. Also, the pressure difference between the central and a side tube is influenced by shear and this leads to errors in the velocity measurements based on calibration in uniform flow.

Even a pitot probe experiences the effect of shear in velocity measurements. The error is described in terms of the effective centre of the probe. The effective centre is defined as the point where the local total pressure is equal to the total-pressure sensed by the probe. The effective centre is found to be displaced from the geometric centre towards the region of increased total-pressure. This distance ΔY is given by (Young and Maas, 1936)

$$\Delta Y/D = 0.13 + 0.08\, d/D$$

and it is independent of shear. Investigations of the effect of shear were carried out by MacMillan (1956), Hall (1956), Lighthill (1957), Davies (1958) and Dhawan et al (1959).

Viscous effects in pressure probes are significant when Reynolds number based on outer tube diameter is less than about 40 (Dean 1953, Hurd 1953, MacMillan 1954, Ower and Pankhurst 1966). For a probe diameter of 1 mm this effect is significant when the velocities are less than about 60 cm/s. Since larger velocities were used in the present investigation, viscous effects were negligible.

Similarly compressibility effects were of no consequence. Since the turbulence intensity of the tunnel was 0.4%, turbulence effects (Goldstein 1936) were expected to be small and were not considered.

1.4 THE ASYMMETRIC PROBE

Since a reduction in the transverse dimension brings about reduction in shear errors and improves the suitability of the probe for thin shear layers and the vicinity of a wall, a new probe configuration (Figure 3 (a)) was invented to reduce the transverse distance between the side tubes to zero. The axes of the three tubes lie in a plane normal to the plane of motion and the chamfered faces are asymmetrically arranged.

If the asymmetric configuration (Figure 3 (a)) is compared with the symmetric three-tube Conrad type configuration (Figure 3 (b)) for a given tube diameter, the first arrangement has one third the transverse dimension of the second. Hence, the first arrangement can be used closer to the wall and with smaller interference.

One way of using the probe is to align it in flow direction. This type of usage is dealt with in this work. There is also another type of usage in which the probe is held fixed in a known direction and the pitching apparatus is then not needed. The second method is used when space restrictions do not permit the probe rotation and the

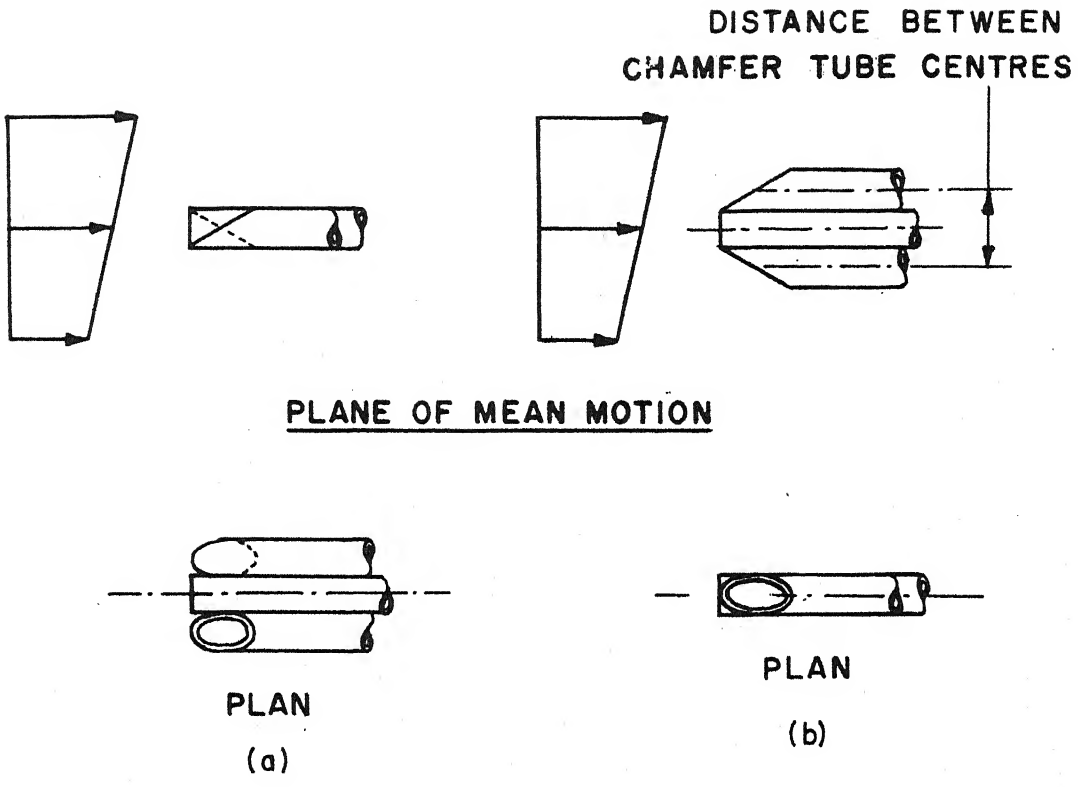

FIG.3 ASYMMETRIC AND SYMMETRIC CONFIGURATION IN SHEAR

pitching apparatus. Furthermore, it eliminates alignment time and is therefore suitable for intermittent high speed tunnels with limited run times. The pressure differences between the tubes are used to obtain the flow direction and the dynamic pressure using uniform flow calibration. But this usage is influenced by the flow conditions like shear and turbulence and the angle between the flow direction and probe axis may have to be less than a critical value (usually $\pm 20°$) depending on the probe geometry. Whenever possible the first method is preferred (Bryer et.al. 1958).

A probe with the asymmetric configuration was made from stainless steel tubes of 0.5 mm inner diameter d and 0.8 mm outer diameter D ($d/D = 0.625$). The side tubes had a chamfer angle of 45°. The chamfered face was carefully prepared on a vertical milling machine and then carefully hand-finished using a jig and oil-stone. This gave a good finish to the chamfered faces and freedom from burrs. The angles were checked in an optical profile projector with a magnification of 50. The tubes were held together by soldering and the external surface was carefully hand-finished and checked for proper alignment in the optical projector and with a projection microscope.

Common requirements of a combination probe are small size, rapid response, sturdy and simple construction, ability to take measurements close to one point etc.

These requirements are satisfactorily met by the new probe in a way similar to the Conrad probe which was the best available in view of these requirements (Pryer et.al. 1958).

1.5 THE ORIENTATION APPARATUS

The selection of a suitable orientation apparatus is rather important. In a two-dimensional flow, the probe has to be aligned either for yaw or for pitch depending on the orientation of the probe support with respect to the flow. Rotation about an axis passing through the probe support is usually called yaw rotation and rotation about an axis perpendicular to the probe support is termed pitch rotation. The mechanical problems involved in designing an orientation mechanism for pitch angles are more difficult to solve than those for yaw.

Two of the common orientation mechanisms are shown in Figure 4. The cranked cantilever orientation mechanism (Figure 4 (a)) is suitable for yaw angles. But the pitching orientation is required for the present experiment, and in general for two-dimensional separated flow studies near a wall. The orientation mechanism of Figure 4 (b) can be used for pitch alignment but it has certain imitations. It is convenient for calibration in uniform flow, but not for general purpose usage with a rectilinear traverse. An alternative mechanism proposed by Salter et.al. (1965) has similar limitations.

(a) TRAVERSE FOR DIRECTION PROBE IN 2D FLOWS

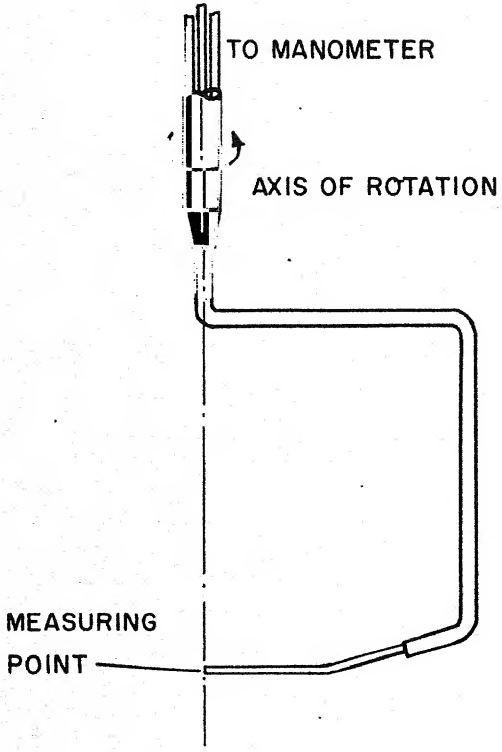

(b) TRAVERSE FOR DIRECTION PROBE IN 3D FLOWS

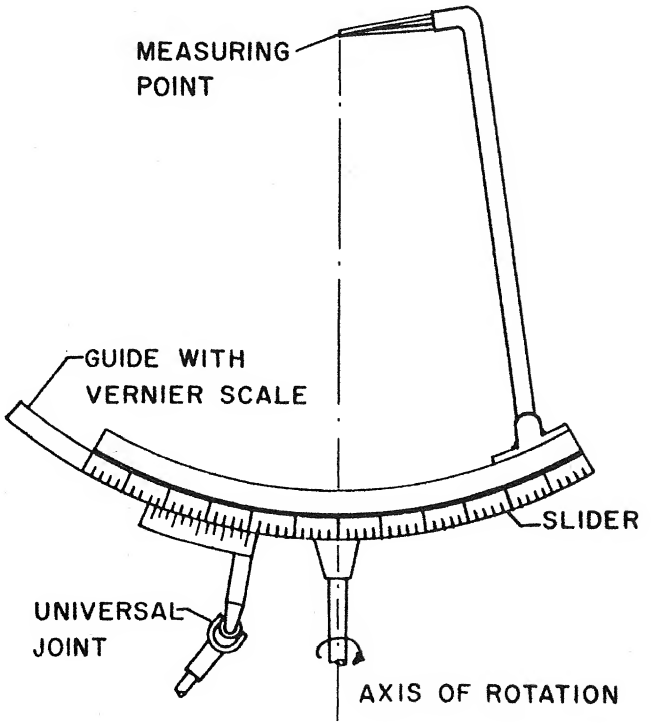

FIG.4 COMMON PROBE TRAVERSES

An apparatus was designed to pitch the probe. It is based on a modification of a parallelogram linkage (Figure 5). It consists of three vertical links, DGK, BEM and CFI, and three parallel links, GHI, DEF and ABC of variable inclination. When the apparatus is installed, link DGK is normal to the solid surface and the plane of mechanism is in the plane of motion. An auxiliary link HJ is connected to a slider J moving in a supporting tube soldered to link DGK. The slider is moved by a metal wire. The supporting tube also encloses flexible tubes connecting the three probe tubes. (Figure 6)

Since the apparatus is a plane mechanism, obstruction of the flow is reduced and installation and operation are easier than with a space mechanism having a similar function. Also, redundancy of links reduces clearance errors and increases rigidity. Perhaps the principal advantage is that rotation of the probe about the probe tip is achieved with little intereference to the flow near the probe tip, even when it is near a solid wall.

The links of the apparatus were made with brass strips of 6 mm width and 1.5 mm thickness. Pin joints were made from brass pins and care was taken to minimise clearance. The pins were 5 cm apart on a vertical link and 4 cm on an inclined link.

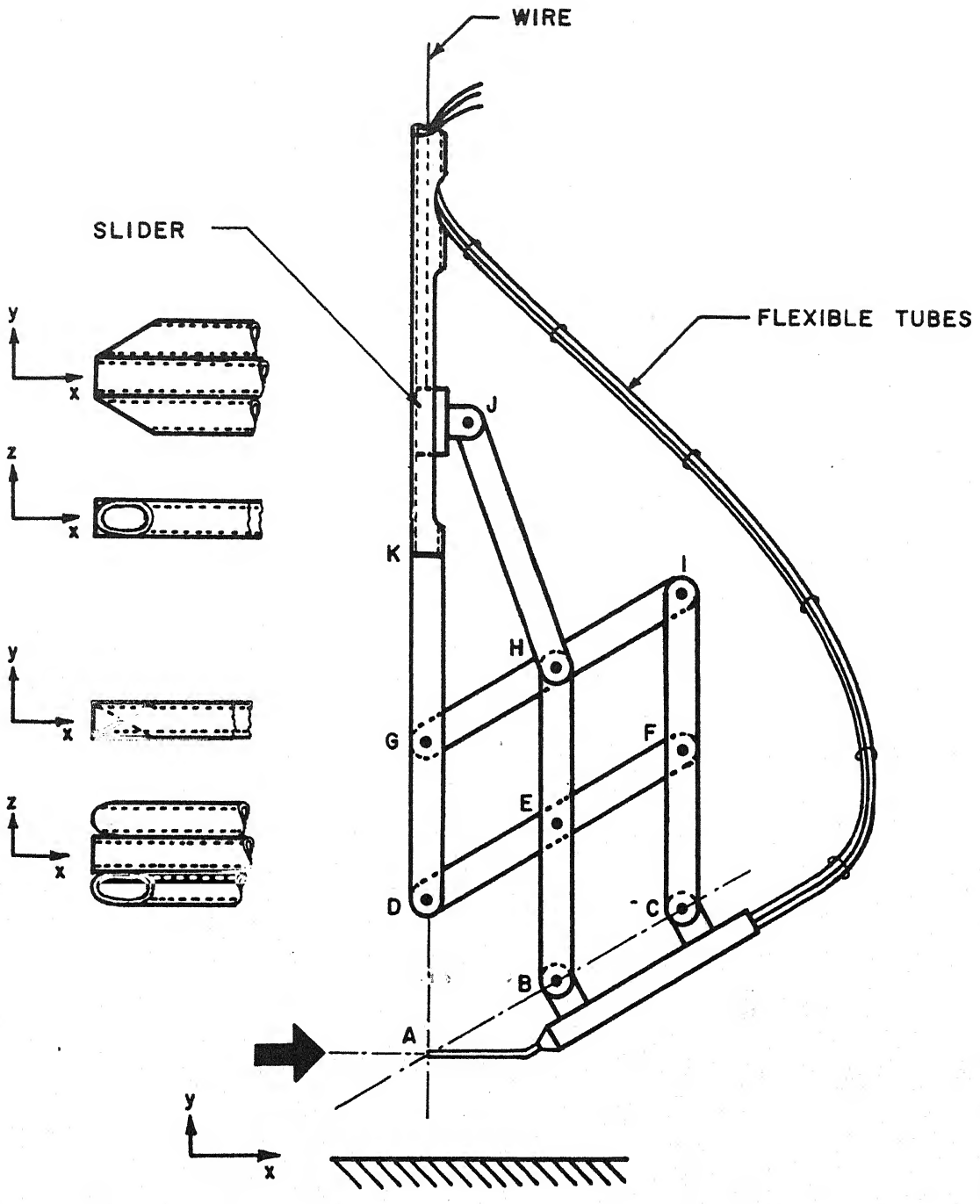

FIG.5 PROBE AND PITCHING APPARATUS

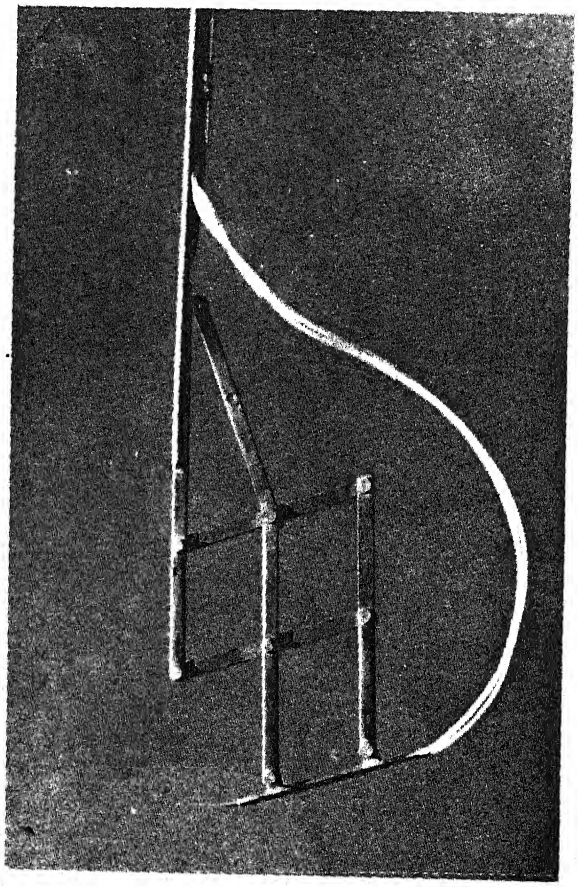

FIG. 6 VIEW OF THE PROBE AND THE PITCHING APPARATUS

The probe was held in a stiff copper tube attached to pin joints B and C of the pitching apparatus. The probe tip A was adjusted during installation so that A is on the intersection of GD and CB.

1.6 CALIBRATION PROCEDURES

The total pressure was measured directly with the central tube. Calibration for dynamic pressure was done in a uniform flow with the probe aligned in the flow direction. Calibration for the probe angle was done in an optical profile projector to relate the probe angle to the linear displacement of wire. Details of procedures employed in the present study are given below.

(a) Calibration for dynamic pressures

The probe assembled with the pitching apparatus was mounted in the test section of the wind tunnel A (test section - 1 x 1.2 m, length 1.5 m, maximum speed 60 m/s). The supporting tube was held normal to the free stream direction with the pitching apparatus in the plane of mean flow and the probe was first aligned in the flow direction till the differential pressure in the side tubes was shown to be zero in a micromanometer. This probe direction was maintained during the entire calibration for dynamic pressure.

The tunnel velocity was varied, first in increasing and then in decreasing steps. The pressure difference

The probe was held in a stiff copper tube attached to pin joints B and C of the pitching apparatus. The probe tip A was adjusted during installation so that A is on the intersection of GD and CB.

1.6 CALIBRATION PROCEDURES

The total pressure was measured directly with the central tube. Calibration for dynamic pressure was done in a uniform flow with the probe aligned in the flow direction. Calibration for the probe angle was done in an optical profile projector to relate the probe angle to the linear displacement of wire. Details of procedures employed in the present study are given below.

(a) Calibration for dynamic pressures

The probe assembled with the pitching apparatus was mounted in the test section of the wind tunnel A (test section - 1 x 1.2 m, length 1.5 m, maximum speed 60 m/s). The supporting tube was held normal to the free stream direction with the pitching apparatus in the plane of mean flow and the probe was first aligned in the flow direction till the differential pressure in the side tubes was shown to be zero in a micromanometer. This probe direction was maintained during the entire calibration for dynamic pressure.

The tunnel velocity was varied, first in increasing and then in decreasing steps. The pressure difference

between the central tube and one side tube was measured for each step. The dynamic pressure in the test section was measured by a pitot probe in the settling chamber and a static hole in the test section wall. The curve of the pressure difference between the central and the side tubes against the dynamic pressure (Figure 7) was linear to a first good approximation in the range 10-50 mm of alcohol. The curve was slightly nonlinear near the origin, but the nonlinearity was reproducible in several calibration tests. The straight line approximating the curve had a small intercept on the ordinate axis which could be reduced by further development. There was no noticeable difference between measurements in increasing and decreasing steps. Also, the pressure difference between the side tubes remained within 0.05 mm during the calibration procedure.

(b) Calibration for probe angle

An optical profile projector of magnification 20 was used. It had a circular screen with cross-wires which could be rotated and the rotation could be measured. The probe with the pitching apparatus was placed in the projector, the probe being in the zero position of the previous calibration. The probe tip was first projected at the cross-wire centre and one wire was aligned with the centreline of the probe shadow. The wire connected to the slider J (Figure 5) was moved to rotate the probe about its tip and the wire displacement was noted on a vernier of

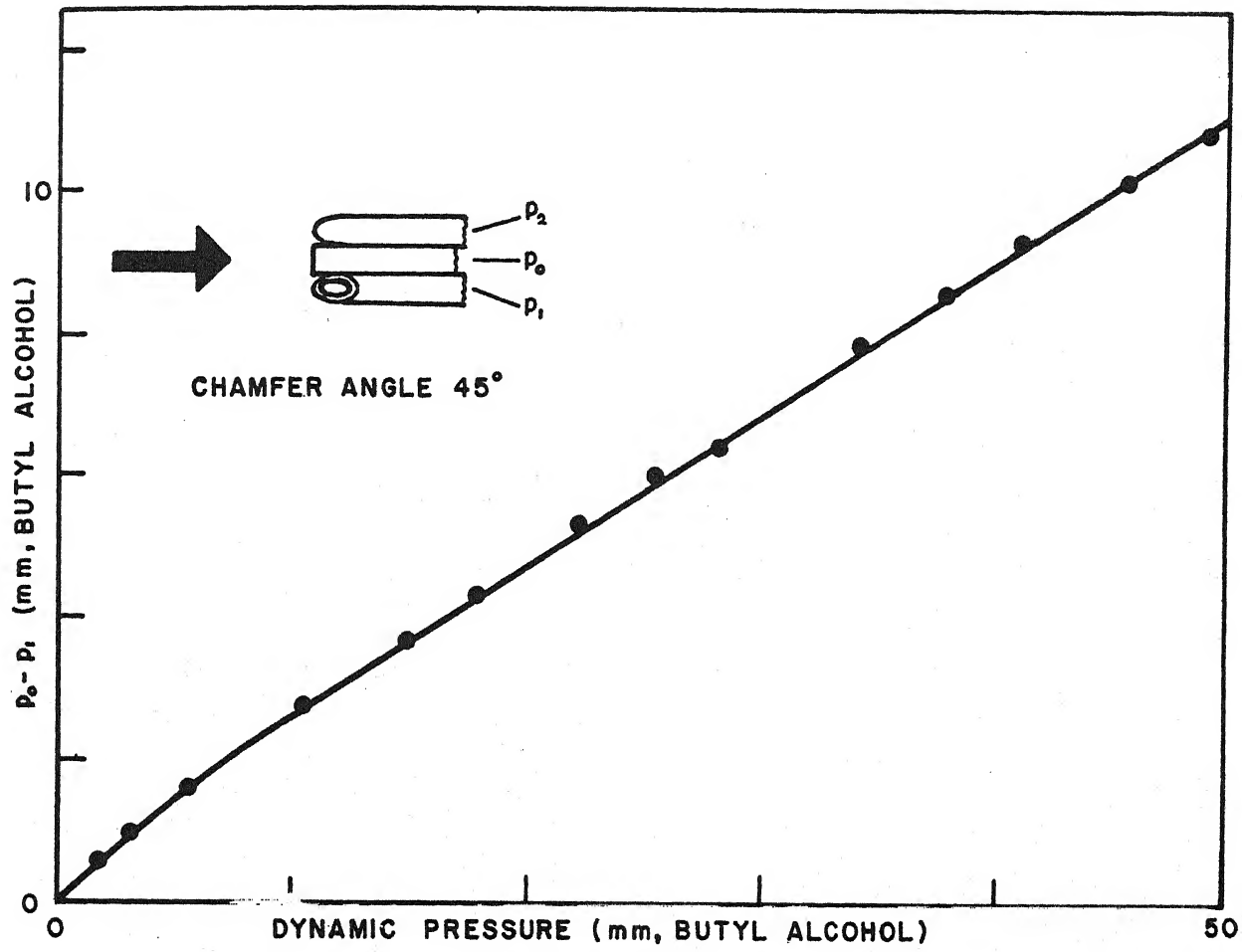

FIG.7 DYNAMIC PRESSURE CALIBRATION

least count 0.05 mm. The screen was then turned till the cross-wire was again aligned with the probe axis, and the screen rotation was measured. The process was repeated for several angular displacements in the clockwise and anticlockwise directions. The probe tip image was seen to remain almost at the cross-wire centre for all such rotations. The calibration (Figure 8) was carried out from +60° to -30° and the linear range was found to extend from +20° to -20°. An angular displacement of 1° gave rise to a linear displacement of about 0.74 mm. Thus an angular displacement of about 0.07° could be detected. The probe angle sensitivity is distinct from the sensitivity to flow angles. The former is essentially determined by the mechanical amplification built into the pitching apparatus, but the latter is influenced by probe geometry, flow velocity, manometer sensitivity etc.

1.7 INSTALLATION AND OPERATION

The general orientation of the probe and the pitching apparatus is shown in Figure 9. The apparatus with the probe was inserted into the test section from a slot in the upper wall at a chosen streamwise location. The apparatus could be traversed in the vertical direction. When the probe tip was at a point of interest, the probe axis was rotated by moving the wire till the side tubes showed equal pressure. The wire displacement was noted and the flow angle $\emptyset$ was obtained using the calibration curve (Figure 8).

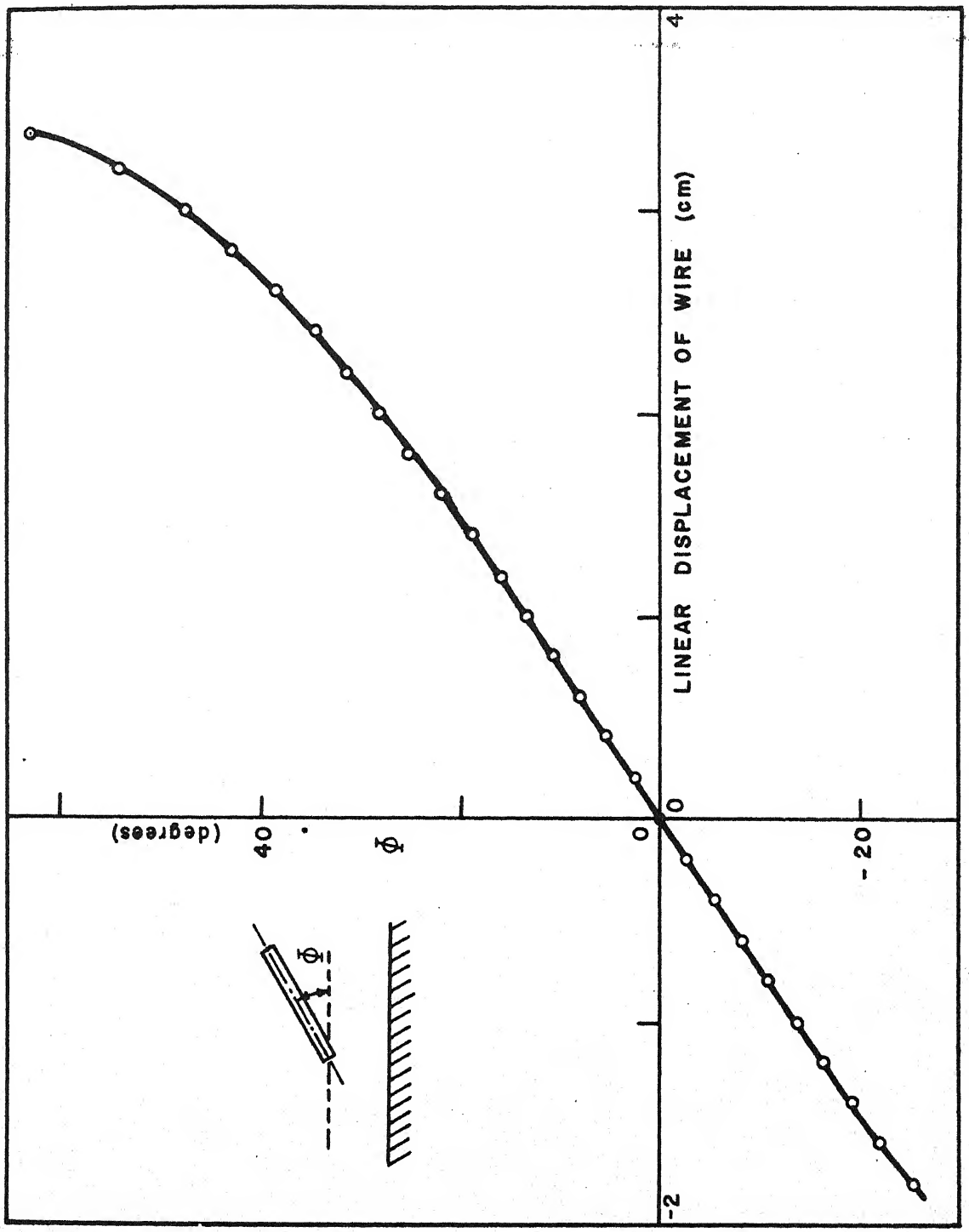

FIG.8 PROBE ANGLE CALIBRATION

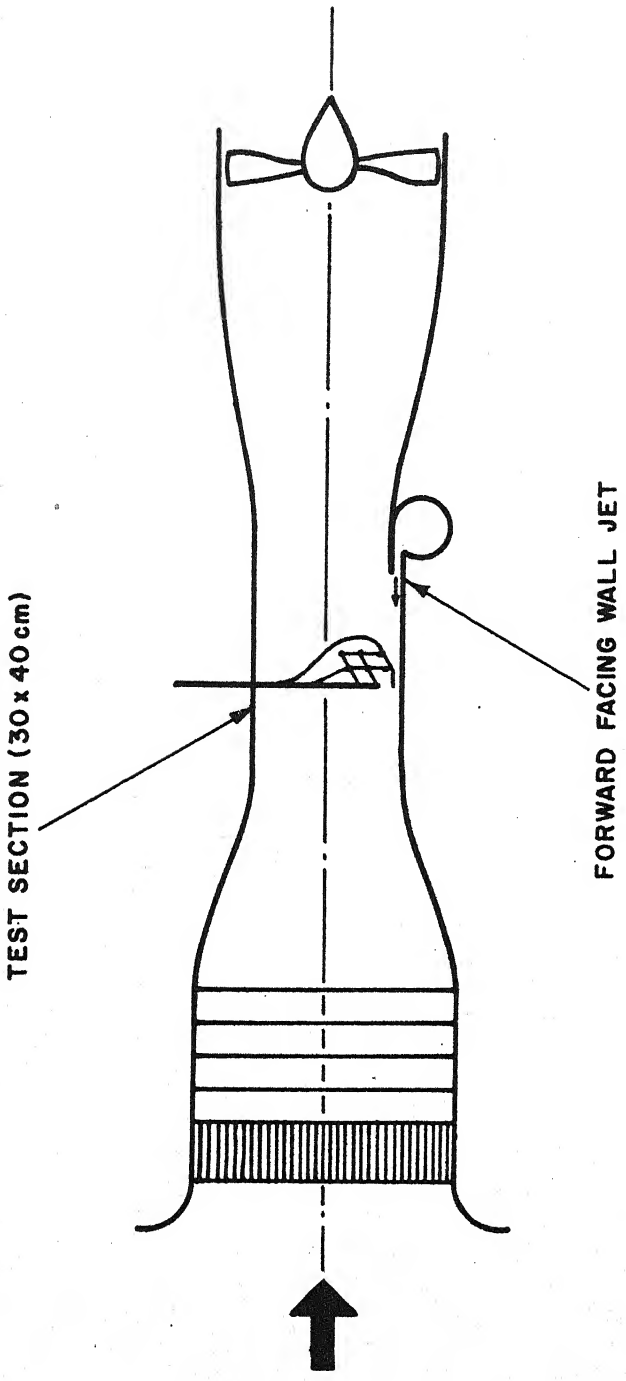

FIG.9 PROBE IN THE TUNNEL

The central tube gave the total pressure, and the dynamic pressure was obtained from the measured ($p_o - p_1$) and the calibration curve (Figure 7). The installation and operation were found to be simple and rapid.

CHAPTER 2

PROBE PERFORMANCE AND TYPICAL MEASUREMENTS

2.1 INTRODUCTION

Since an asymmetric probe configuration was used for the first time, it was desirable to compare the new probe measurements with conventional probe measurements in some well-known flows. If the measurements indicate satisfactory probe performance, the probe can be used with confidence in flows which have not been extensively investigated. However, a critical and definitive evaluation of probe performance requires extensive studies in sensitivity to flow features like yaw and shear and parametric studies for optimisation. Such an evaluation was not attempted.

Further, new probe measurements in wall-jet induced separation are presented to demonstrate the probe capability in surveying complex flow fields. The plan of the chapter is to examine in the next section pitch sensitivity which indicates the resolution of flow angle. The next three sections compare the new probe measurements with the empirical laws and pitot probe measurements in zero pressure gradient turbulent boundary-layer and fully developed pipe flow. The comparative measurements indicate errors in total-pressure, dynamic pressure and flow angle.

Finally, new probe measurements in a separating turbulent boundary-layer are compared with pitot measurements in section 2.6. Calculated boundary-layer parameters provided a further indication of the accuracy of the new probe. Illustrative measurements close to and beyond separation point are given in section 2.7.

2.2 PITCH SENSITIVITY

Pitch sensitivity and boundary-layer measurements were carried out in tunnel B (test section - 40 cm x 30 cm, length 100 cm, maximum speed 16 m/s). A speed of 780 cm/s was used due to the limited range of the available micromanometer. The probe was located at the centre and aligned in the flow direction. It was then rotated in steps and the pressure difference (p_1-p_2) was noted. Figure 10 shows the probe sensitivity to pitch angles in the range -20° to +60°. An angle of 1° is seen to result in a pressure difference of 0.16 mm of butyl alcohol even at this low speed. Hence an angle of about 0.2° can be sensed with a micromanometer of 0.025 mm least count.

The pitch sensitivity of the probe ($(p_1-p_2)/\frac{1}{2}\rho V^2\phi$) is equal to 0.038 per degree of probe rotation. Also, approximately linear behaviour over a large range suggests that the probe can be used in non-aligned mode with suitable calibration. (see section 1.4)

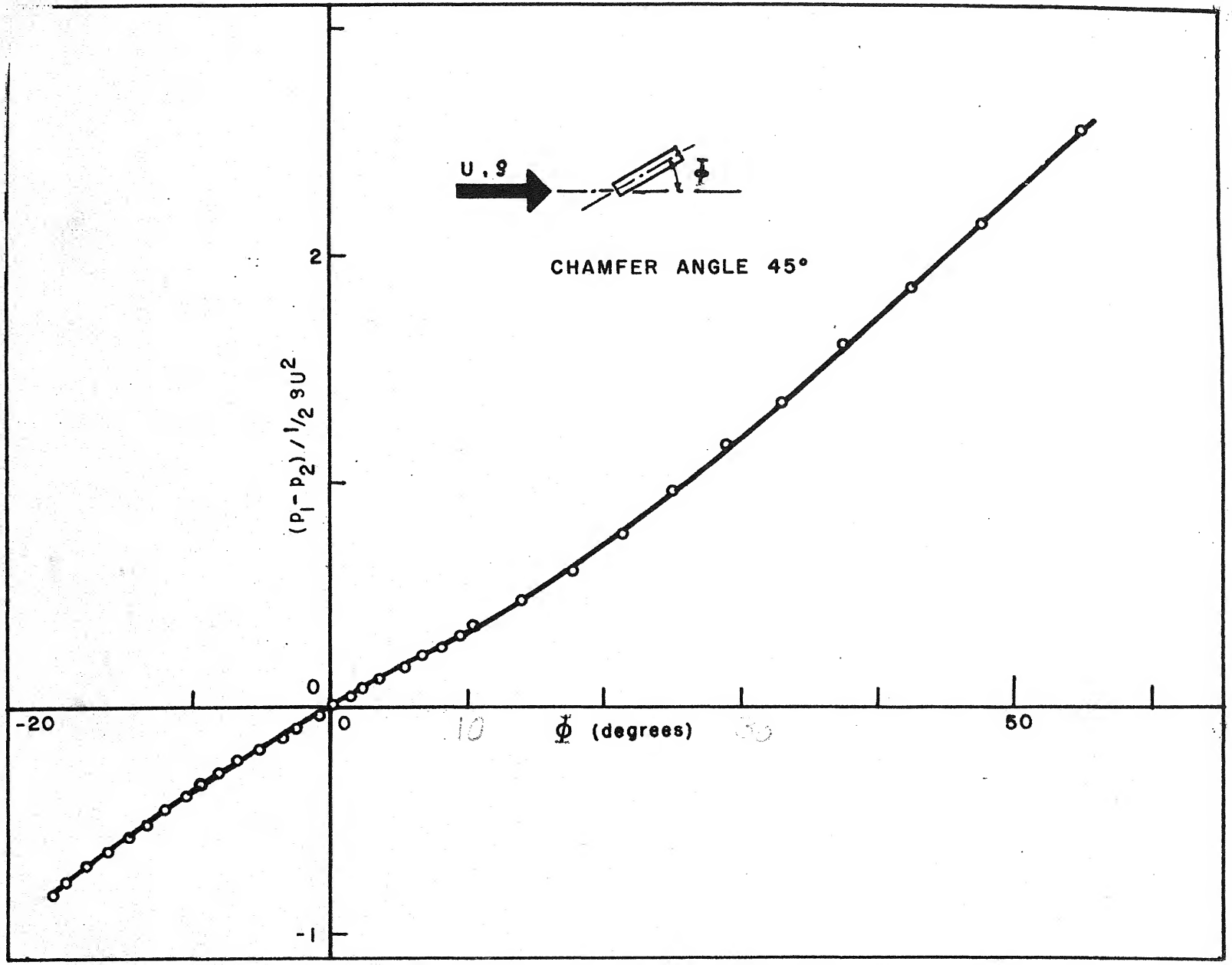

FIG.10 PITCH SENSITIVITY

2.3 COMPARATIVE MEASUREMENTS OF TOTAL PRESSURE

The intereference of the side tubes to the central tube was expected to be negligible. However, it was desirable to test the intereference in presence of shear and near a solid wall. Central tube measurements were compared with a pitot probe having the same outer and inner diameters.

Measurements were carried out in a turbulent boundary-layer with zero pressure gradient. Reynolds number based on momentum thickness was 310. However a comparison of velocity profiles measured with the conventional probe and well-known empirical laws suggested that the effects of moderate Reynolds numbers were not serious.

Total pressure profiles obtained with the two probes are shown in Figure 11. The close agreement indicates that the interference of the side tubes was not significant even in presence of shear and wall.

2.4 COMPARATIVE MEASUREMENTS OF VELOCITY

The velocity profile obtained with the new probe using uniform flow calibration was compared with the logarithmic law (Figure 12). The coefficients of the logarithmic law were taken to be 0.41 and 5.0 as recommended by Coles (1968). The velocity profile obtained with the pitot tube and a static wall tap was also used for

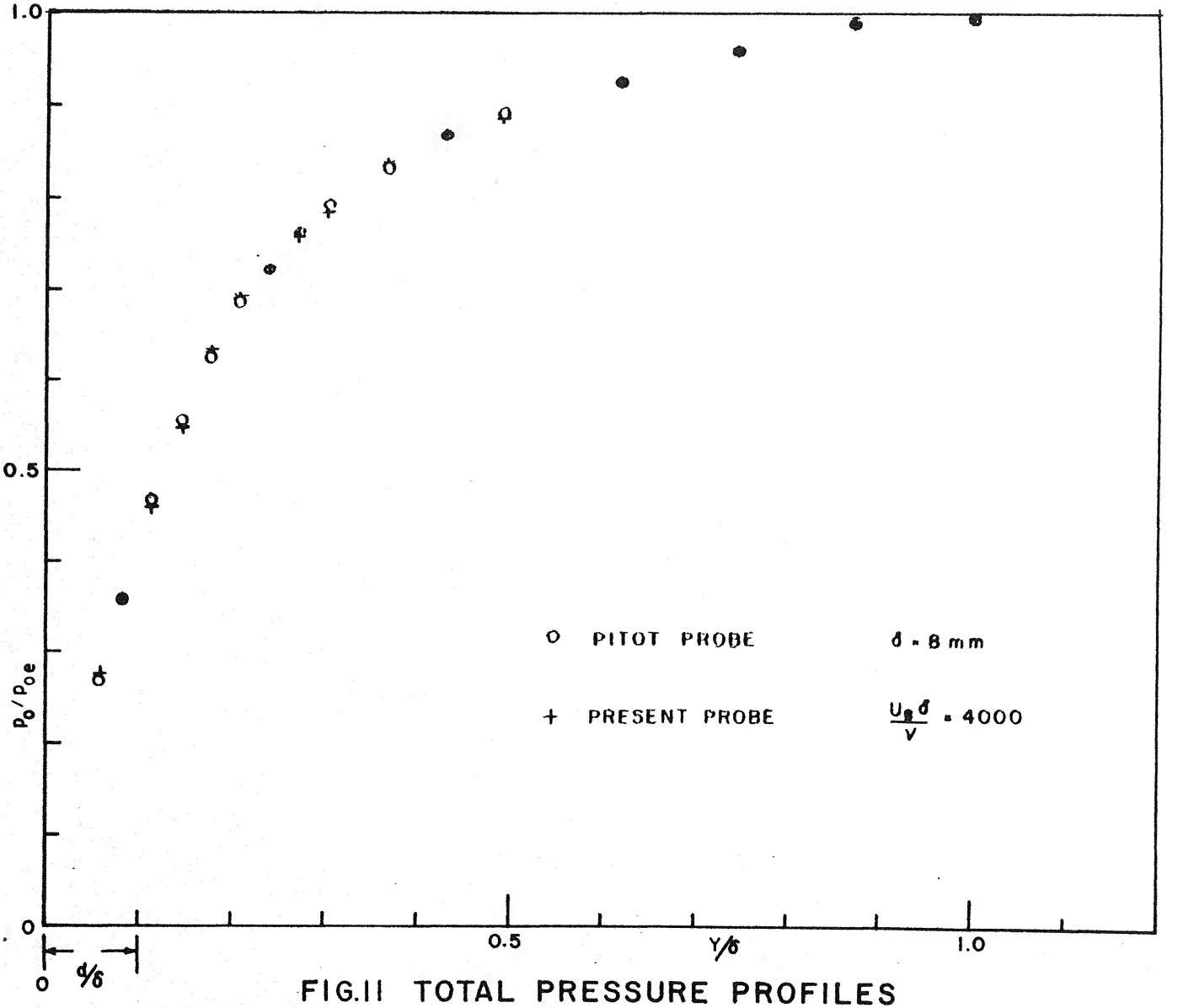

FIG.11 TOTAL PRESSURE PROFILES

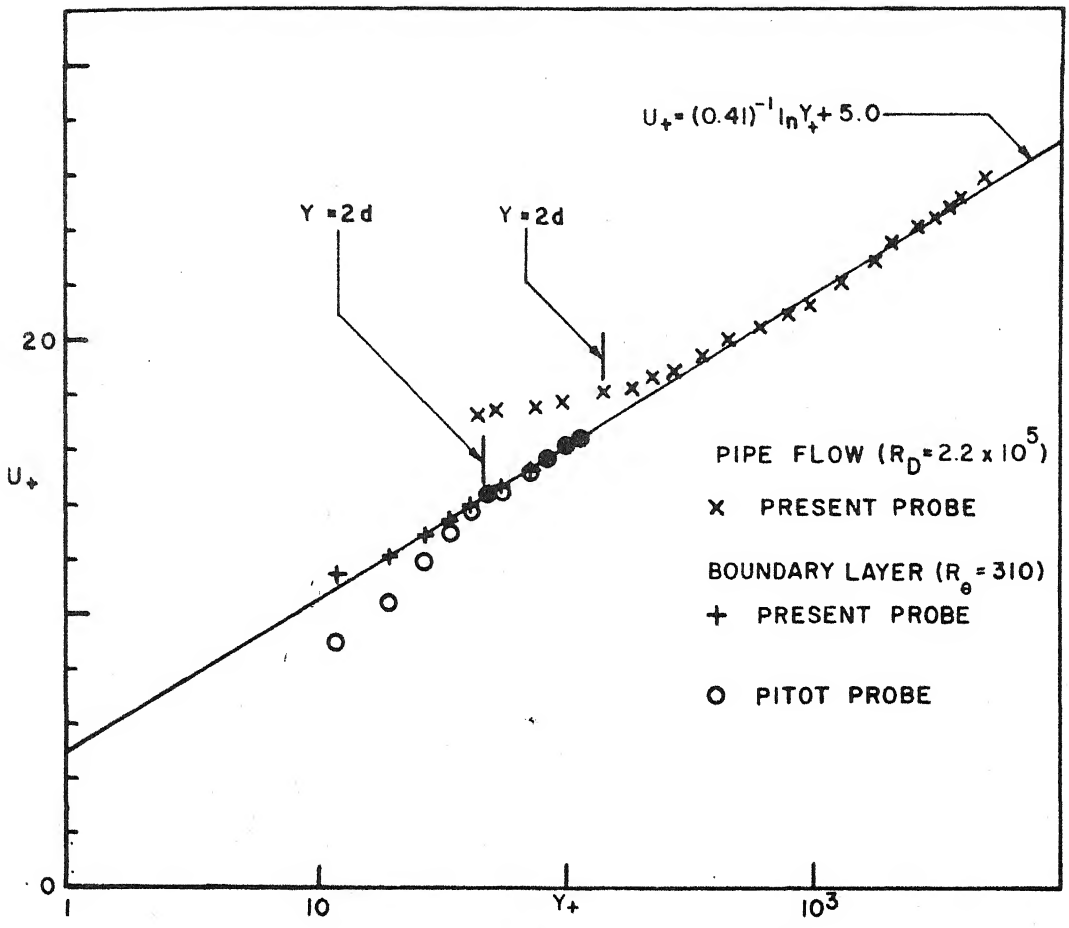

FIG.12 VELOCITY IN WALL CO-ORDINATES

comparison. Friction velocity for both the profiles was calculated by a method suggested by Bradshaw (1959). Velocity measurements at a distance larger than two tube diameters were found to be in good agreement with the wall law and the pitot tube measurements.

Velocity measurements were also made in a turbulent pipe flow at a section 50 pipe diameters from entry. Reynolds number based on pipe diameter was 0.22×10^6. The velocity profile in wall coordinates was obtained by finding the friction velocity using Bradshaw's method. The curve UY = constant drawn for this method was found to intersect the velocity profile in the logarithmic region and at a point more than two tube diameters from the wall. Agreement with the logarithmic law was found to be fairly good outside a region of two tube diameters from the wall (Figure 12).

Velocity measured with the new probe was systematically larger than pitot probe values very close to the wall. Maximum error occured when the probe touched the wall, and was about 25% in the boundary-layer. Estimates were made to see whether this difference should be attributed to the well-known displacement effect (Thwaites 1960, Davies 1968). The shear parameter α as defined by Davies is equal to the ratio of the difference of the velocities at the extreme ends of the probe to twice the velocity at the centre of

the probe. The velocities were calculated assuming the log law for $Y_+ > 45$. The shear parameter was found to vary from 0.19 at Y = 0.05 cm to 0.0305 at Y = 0.16 cm. Displacements of effective centres necessary to bring the data into conformity with the wall law were 1.2 and 0.6 times the tube diameter at these locations. Thus if the effects of chamfered ends and the probe angle with the wall can give rise to a displacement of this order, the difference could be interpreted as a displacement effect, and a correction procedure could be developed as for pitot probes.

2.5 ACCURACY IN FLOW DIRECTION

The effect of shear and wall proximity on the chamfered tubes can be expected to cause errors in flow direction, although these errors would be considerably smaller than in comparable earlier probes. Pipe flow measurements were used to obtain information about the accuracy of flow direction measurements. Mean flow was assumed to be parallel to the pipe axis and the probe angle ϕ with the axis in nulled position was regarded as the error in measurement of flow direction. The probe angle ϕ is shown against distance Y from the wall in Figure 13. Errors were less than 1°, excluding the wall proximity ($Y < 2D$), where the maximum error was about 2°. Hence the effect of the displaced effective centres led to errors less than 1°, while wall interference errors were less than 2°.

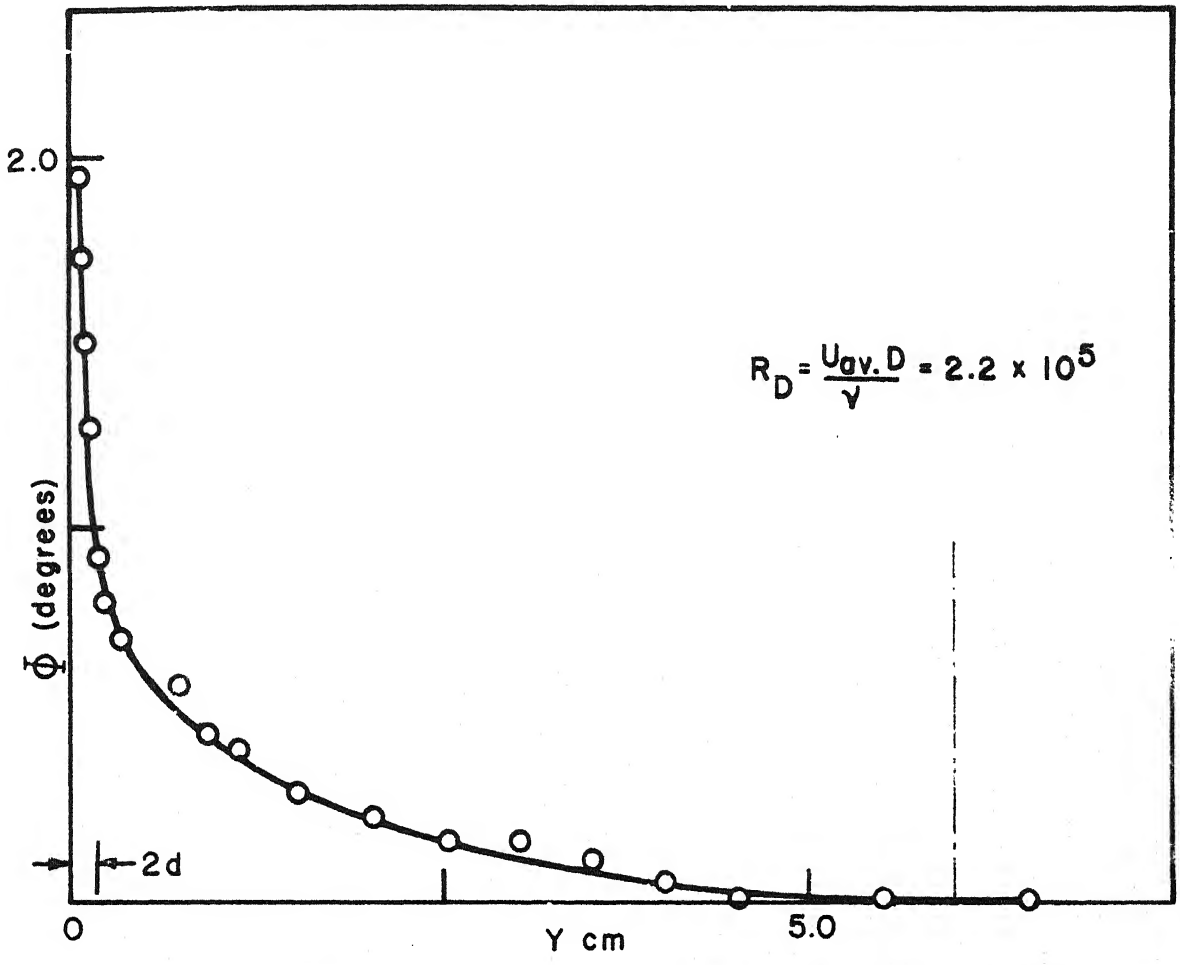

FIG.13 MEASURED PROBE ANGLES IN PIPE FLOW

2.6 MEASUREMENTS IN A SEPARATING TURBULENT BOUNDARY-LAYER

The probe was used for the measurement of velocity profiles in a separating turbulent boundary-layers where the flow direction varied significantly.

The flow was described in section 1.2. The free stream and jet velocities were 550 and 2700 cm/s. Turbulence intensity in absence of wall jet was about 0.4 percent. Measurements of dynamic pressures and flow angles were made at five stations at 30, 35, 40, 42.5 and 45 cm from the beginning of the test section. The separation point was found to be at 48.6 $\pm$0.1 cm with a two-headed probe held close to the wall.

Measurements were also made at the 45 cm station with a pitot probe having the same outer and inner diameters as the tubes in the new probe. Figure 14 (a) shows the flow angle profile obtained with the new probe and Figure 14 (b) shows the dynamic pressure profiles obtained with the two probes.

Dynamic pressure profiles of both showed an unusual valley. This feature was attributed to the strong reversed flow created by the forward-facing wall-jet. The flow angles were larger than 30° at some points and the use of a conventional pitot probe (say, with inner to outer diameter ratio of 0.6) would result in errors of the order of fifteen percent in total pressure. Dynamic pressure

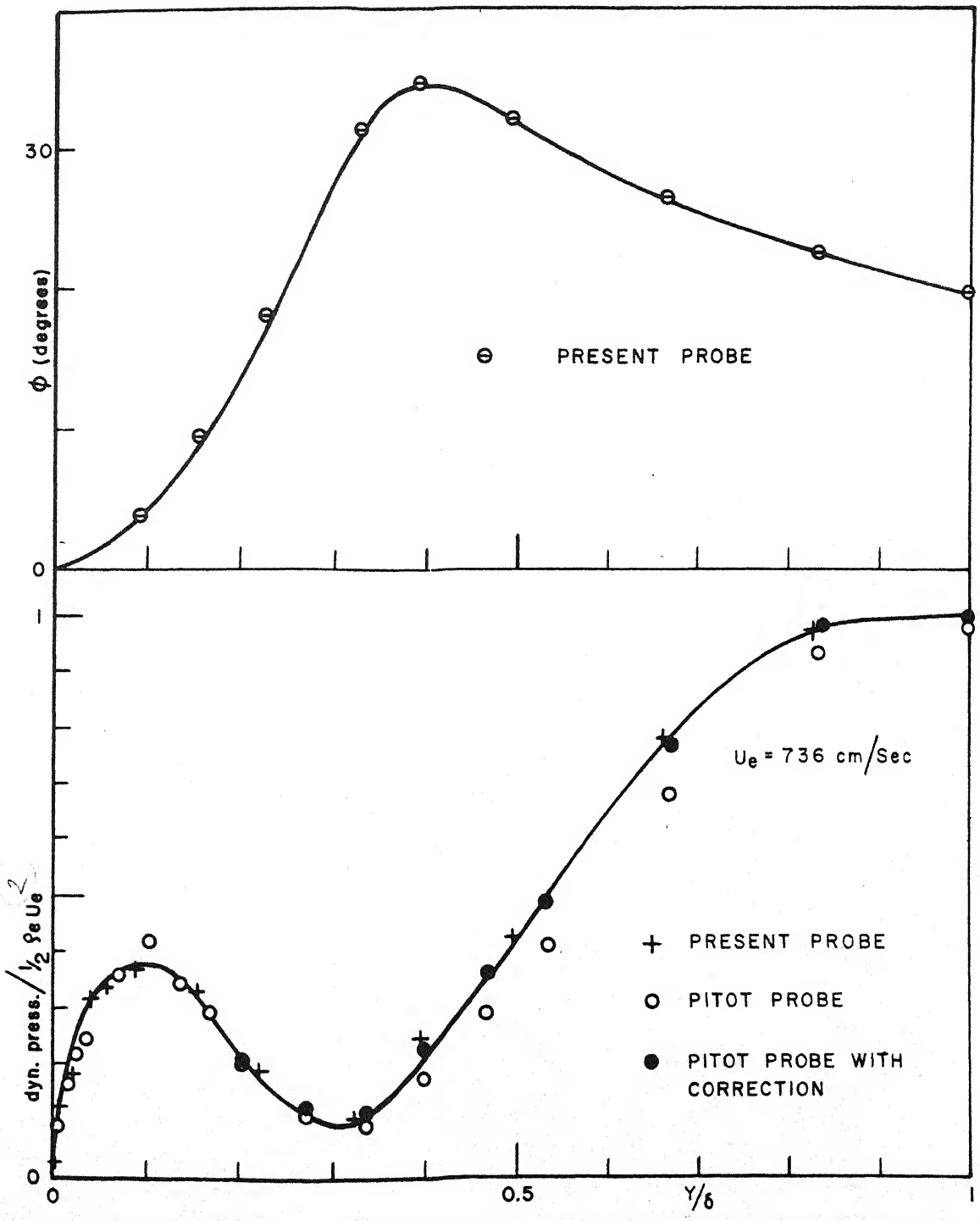

FIG.14 FLOW DIRECTION AND DYNAMIC PRESSURE

obtained with the pitot probe and a static pressure rake was systematically less than the new probe value and the difference was significant wherever the flow angle was more than about 10°. The difference was attributed to the lack of alignment of the pitot probe. A correction was applied following Fan hurst and Holder (1968, p.180) to the pitot prove values for $Y/\delta > 0.15$, where flow angles were greater than 10°, using the values given by the new probe. Corrected values were found to be in good agreement (Figure 14 b) with the new probe values. The agreement suggests that the new probe can be used with confidence in a shear flow with varying flow direction.

Flow angle profiles measured with the new probe are shown in Figure 15. They developed systematically as the separation point was approached and the maximum flow angle was found to be about 36° at 40 percent of the layer thickness at the last station 3.6 cm upstream of the separation point.

Figure 16 shows the development of velocity profiles (X component) obtained by the new probe. A growing dip in the profile is a consequence of the wall jet which peels off from the wall and curls itself to form a strong vortex. The growing dip also results in the occurence of reversed flow at an interior point.

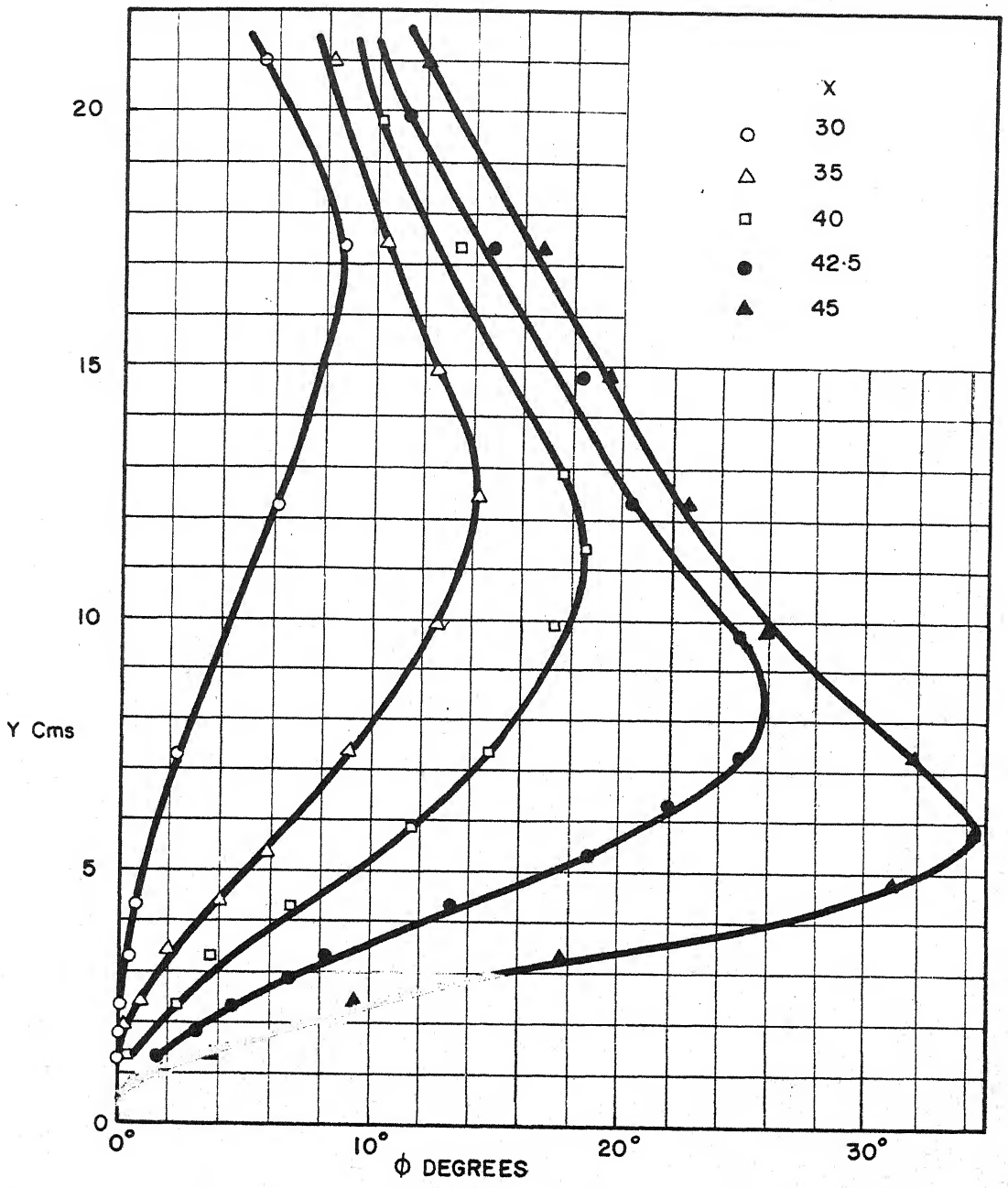

FIG.15 FLOW ANGLES

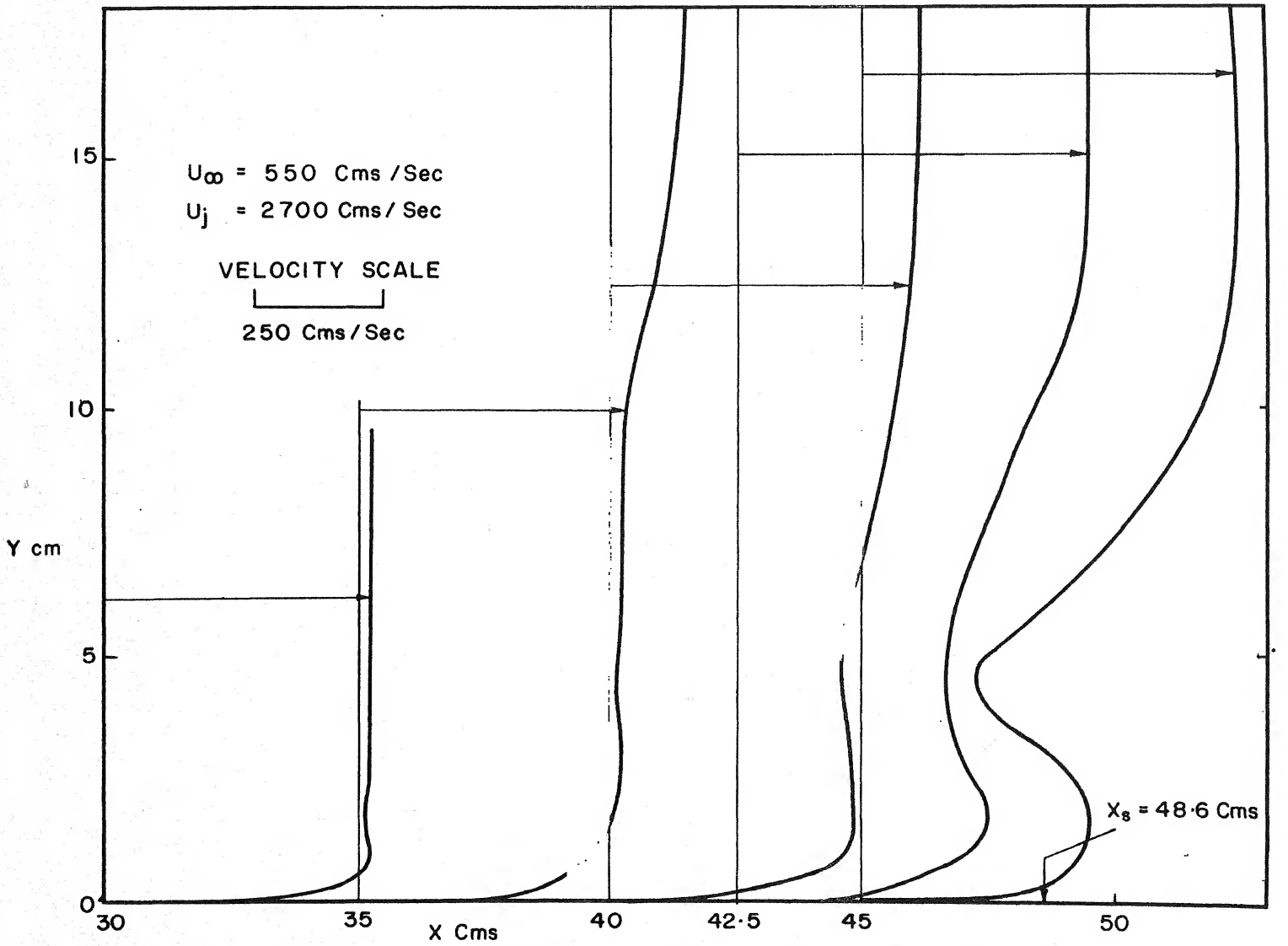

FIG. 16 VELOCITY PROFILES (X COMPONENT)

Various boundary-layer parameters are shown in Figure 17. The parameters were calculated by numerical integration of U-velocity profiles using a programme of modified Simpson's rule with variable step size. The accuracy of the programme was tested on well-known laminar and turbulent profiles and was estimated to be better than 0.5 percent. Skin friction was calculated from these parameters by applying the Ludweig-Tillman formula.

The behaviour of H and C_f gave important conclusions. The value of the shape factor H increased continuously and had a value of about 2.5 close to the separation point. This is a reasonable value of the shape factor for a separating turbulent boundary-layer, as given by Van Deonshoff (1943, H = 2.6), Schaubar and Kiebanoff (1951, H = 2.7) and Clauser (1956, H = 2.5). Further, C_f decreased monotonically and was practically zero at the separation point. These results support the view that the new probe can be effectively used close to the wall near the separation point and in presence of large shear.

2.7 PROFILES CLOSE TO AND BEYOND THE SEPARATION POINT

Flow angles and velocity profiles were also measured at 47.5, 50, 55, 60 and 70 cm locations and are given in Figure 18 and Figure 19. The last four stations were after the separation point while the first station was about 1 cm ahead of the separation point. When the flow angles were

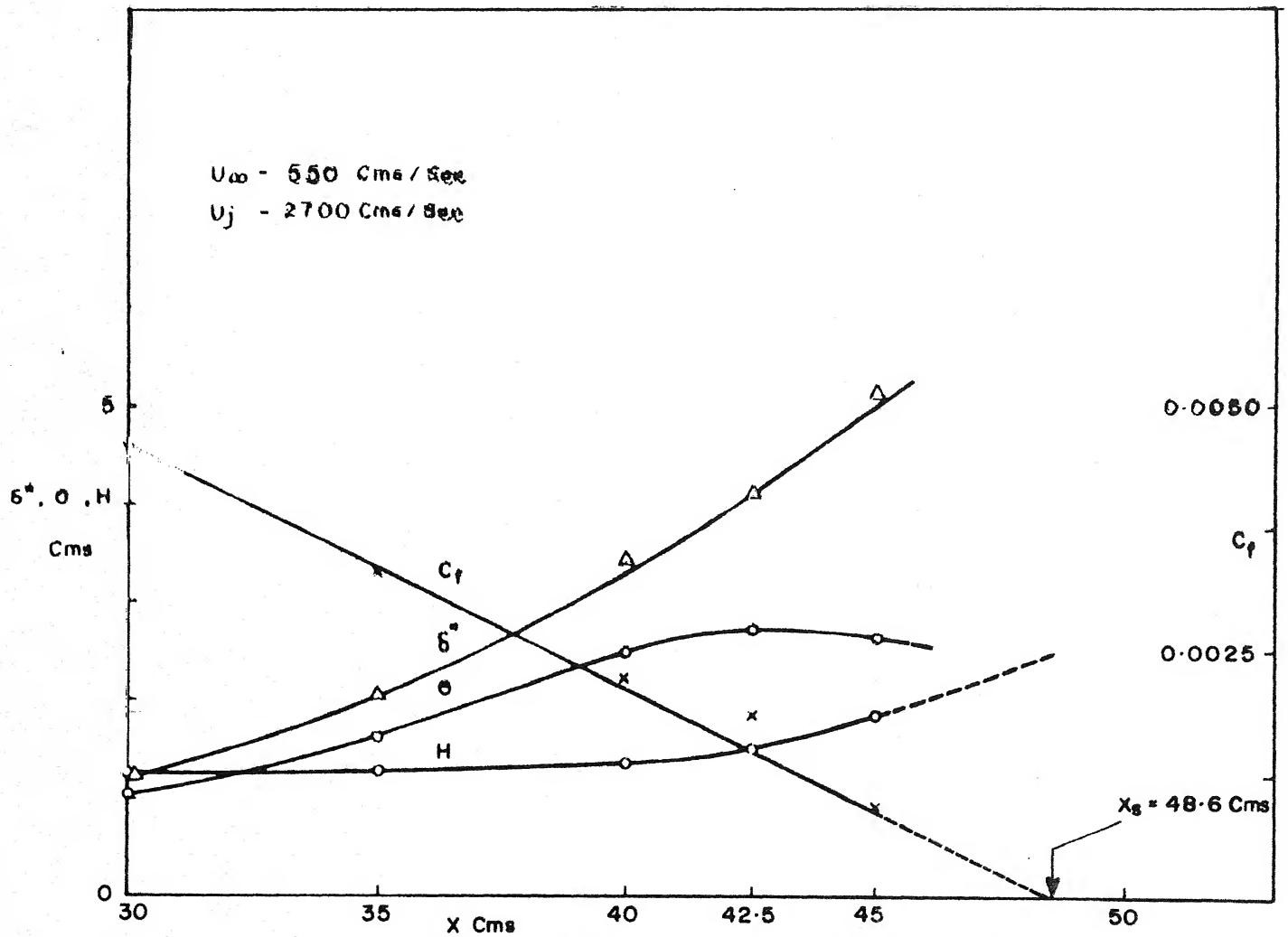

FIG.17 BOUNDARY-LAYER PARAMETERS

more than 60° or less than -30°, the mechanical design of the pitching apparatus did not permit probe alignment in the local flow direction. Consequently, there were gaps in the range from Y = 3.5 to 5 cms. Dotted lines in Figure 19 correspond to these ranges. Flow angles in the range of 120° to 210° were obtained by turning the probe around to face the downstream direction.

The profiles just ahead of separation at X = 47.5 cm show an unusual behaviour. The reversed flow begins at an interior point and the region of reversed flow is sandwiched between two regions of forward flow for a short distance.

The flow angle profiles at the last two stations are qualitatively different from the preceeding two. In the latter the flow angle increases continuously from zero to 180° as the wall is approached. Hence the flow is away from the wall at all points on the station. But for the last two stations, the flow angles decrease from +5° to -30°, the flow being in the forward direction. For values at Y less than about 5 cm the flow opposes the freestream direction. There is a region close to wall where the flow angles are in the range of 170° to 180°. (representing the jet flow spreading away from the wall). Outside this region, the flow is towards the wall. This is due to the effect of the vortex which is upstream of these two stations.

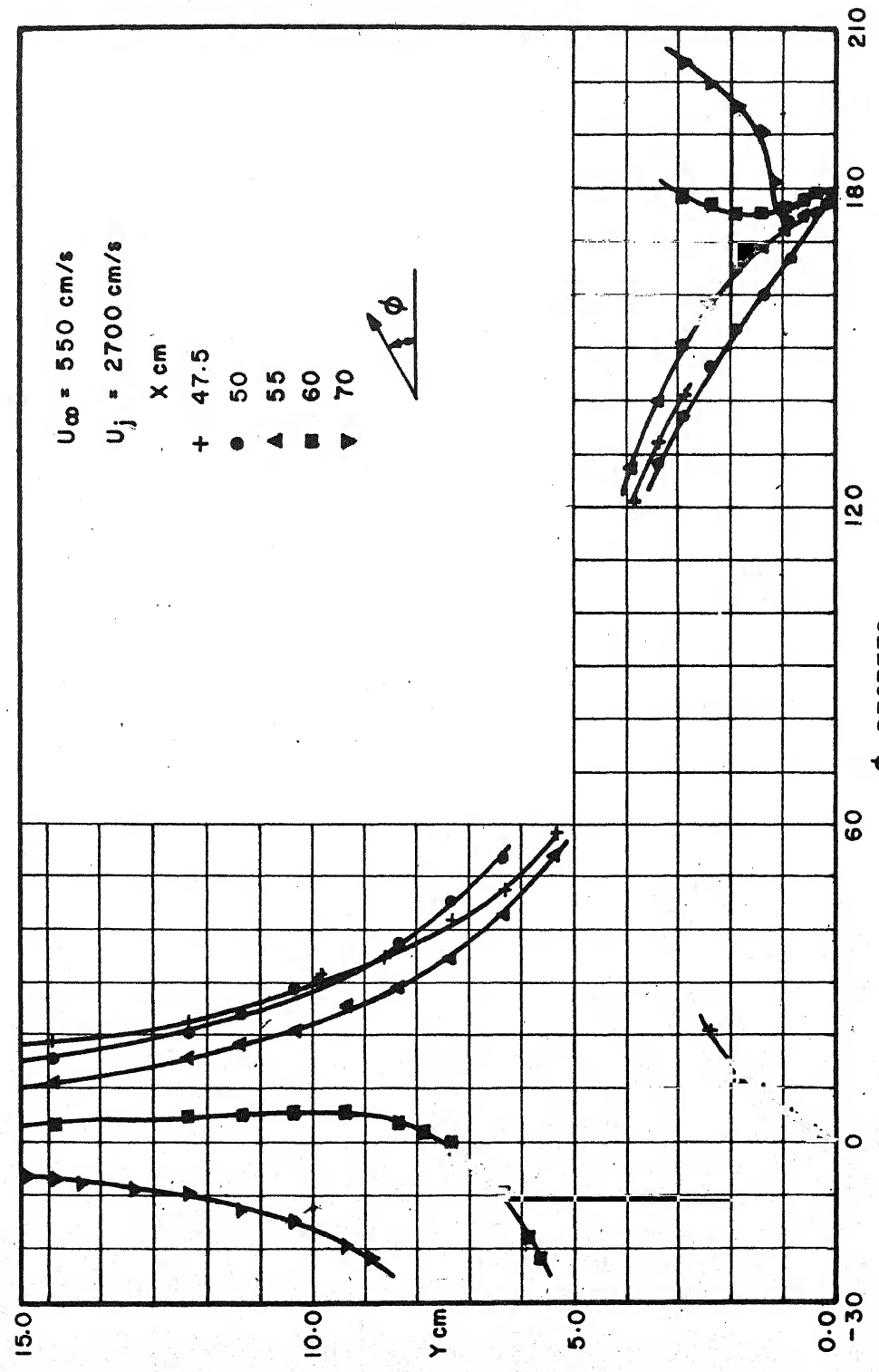

FIG.18 FLOW ANGLES

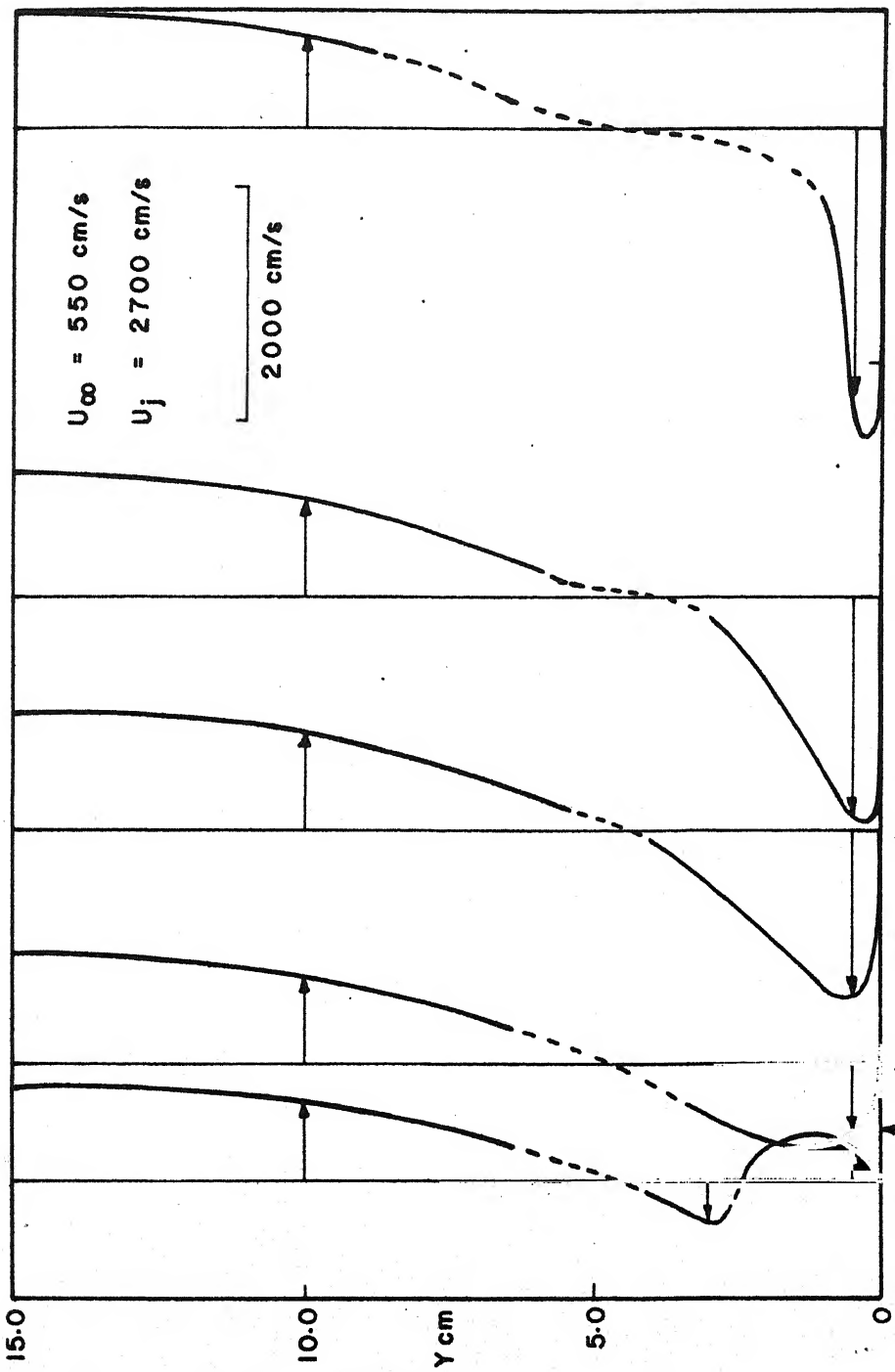

FIG.19 VELOCITY (X COMPONENT) PROFILES AFTER SEPARATION

Figure 20 shows the overall flow features for the entire field. The vectors show to scale the speed as well as direction at the points indicated by dots. The flow features agree well with the streamline pattern (Figure 1) and vividly demonstrate the probe capability.

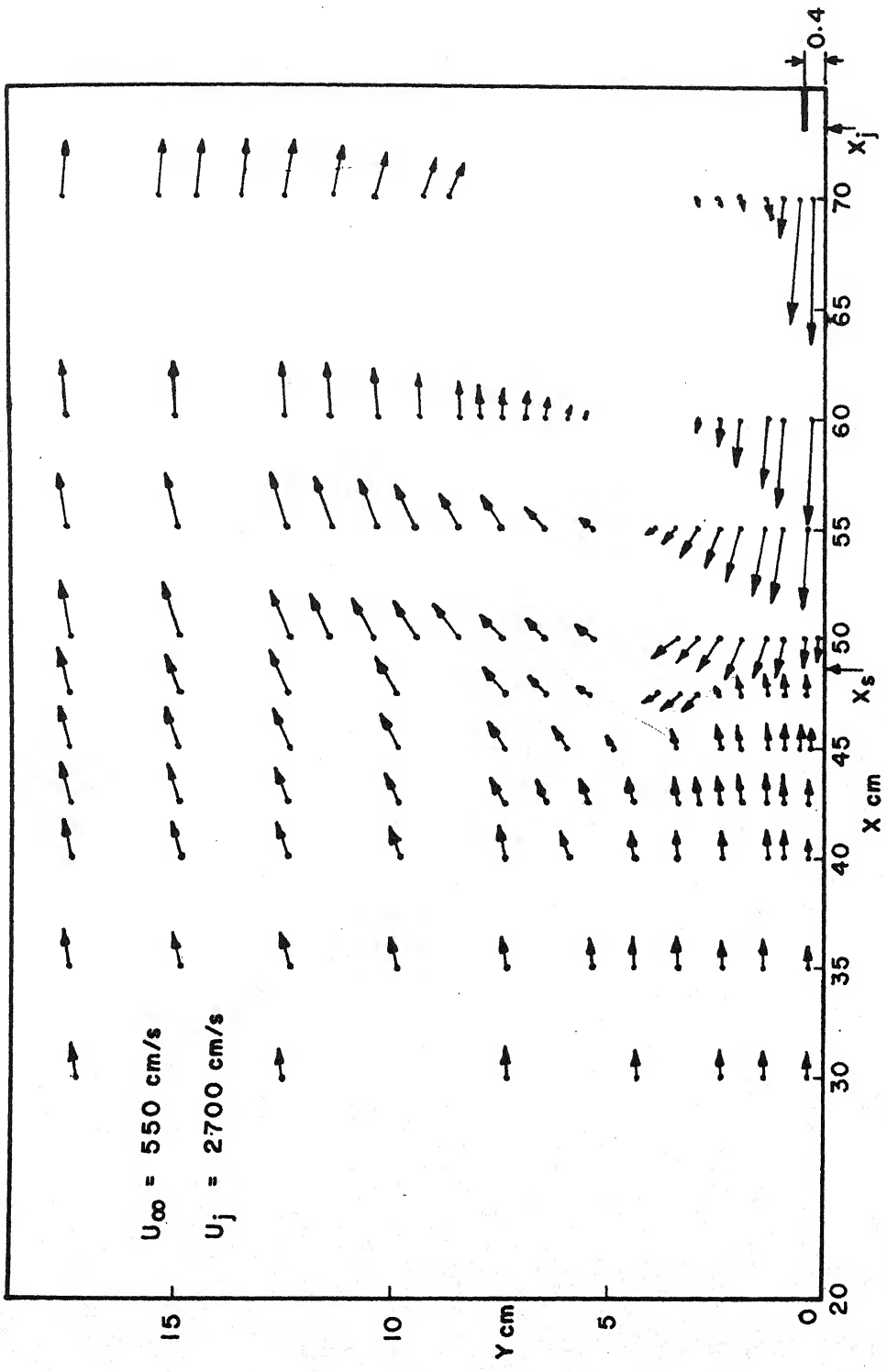

FIG.20 VELOCITY VECTORS IN WALL JET INDUCED SEPARATION

REFERENCES

1. Bradshaw P. 1959, A simple method for determining turbulent skin friction from velocity profiles, J. Aero Space Sci. Vol.26, 841.

2. Bryer D.W., Walshe D.E. and Gardner H.O. 1958, Pressure Probes selected for three-dimensional flow measurement, ARC R and M. 3037.

3. Clauser F.H. 1954, Turbulent boundary layers in adverse pressure gradients, J. Aero. Soc. Vol.21, No. 2, 91-108.

4. Coles D. 1968, Conference, Computation of turbulent boundary-layers, Stanford AFOSR-IFP Vol.2.

5. Davies P.O.A.L. 1958, The behaviour of pitot in transverse shear, J. Fluid Mechanics, Vol.3, part 5, 441.

6. Dean R.C. 1953, Aerodynamic measurements (MIT Press).

7. Dhawan S. and Vasudeva B.R. 1959, The pitot tube displacement effect in boundary layer flows, J. Aero. Soc. India, Vol.11, No. 1, 1-18.

8. Durst F. and Whitelaw J.M. 1971, Optimisation of optical anemometers. Proc. Royal Soc. A 325, 154-81.

9. Goldstein S. 1936, A note on the measurement of total head and static pressure in a turbulent stream, Proc. Roy. Soc. (A), Vol.155, 570.

10. Hall I.M. 1956, The displacement effect of a sphere in a two-dimensional shear flow, J. Fluid Mechanics, Vol.1, part 2, 142-162.

11. Hurd C.N., Chesky K.P. and Shapiro A.H. 1953, Influence of viscous effects on impact tubes, J. Appl. Mech., Vol.20, 253.

12. Lighthill M.J. 1957, Contribution to the theory of the pitot tube displacement effect. J. Fluid Mechanics, Vol.2, part 5, 493-512.

13. MacMillan F.A. 1954, Viscous effects on a pitot tube at low speeds. J. Roy. Aero. Soc. Vol.58, 570.

14. MacMillan F.A. 1956, Experiments on pitot tubes in shear flow. ARC R and M 3028.

15. Ower E. and Pankhurst R.C. 1966, The measurement of air flow, (Pergamon).

16. Pankhurst R.C. and Holder D.W. 1968, Wind-tunnel technique, (Pitman).

17. Salter C., Warsap J.H. and Goodman D.G. 1965, A discussion of pitot-static tubes and their calibration factors with a description of various versions of new design, ARC R and M 3365.

18. Yajnik K.S. and Gupta R.P. (1973) A new probe for the measurement of velocity and flow direction in separated flows. J. Phy. E: Scientific Instruments, Vol.6, No. 1.

19. Young A.D. and Maas J.N. 1936, The behaviour of a pitot tube in a transverse total pressure gradient. ARC R and M 1770.

PART II

UPSTREAM EFFECTS IN SEPARATION INDUCED BY A FORWARD-FACING WALL JET

ABSTRACT

Experiments were conducted to study the upstream effects in two-dimensional separated flow of an incompressible fluid. The development of the vortical layer upstream of the separation point, the location of the separation point, and the initial conditions of the separated shear layer are strongly influenced by the pressure distribution of the surface. Emphasis was therefore placed on studying the way in which the wall pressure distribution is altered by separation.

A forward-facing two-dimensional wall jet was employed to separate the turbulent boundary-layer of the main stream from a flat smooth surface. The main stream and wall jet velocities were varied in ranges of 4 to 12 m/s and 14 to 30 m/s, the ratio of the latter to the former varying from 1.5 to 7.2. Further experiments were conducted by varying the angle of an opposite wall by -2.5° and 2.5° to study the influence of the pressure gradient of the corresponding unseparated flow field on the upstream effects.

Detailed checks were carried out to assess the departures from two-dimensionality, the effects of Reynolds number and non-equilibrium on the unseparated turbulent

boundary-layer and on the wall jet. They showed that these effects were not significant.

For the case in which wall pressure gradients were absent in the unseparated flow, the data suggested that the upstream wall pressure in corresponding separated flow is given by $C_p = f\ (X/t_j, \lambda\ )$ to a good approximation almost upto the separation point. The wall pressure distribution in suitable nondimensional coordinates showed a distinct trend towards similarity. The far upstream effect agreed with the predictions based on inviscid flow models describing the dividing streamline approximately, and the agreement improved with increasing upstream distances. Thus this effect can be attributed to the displacement of the external inviscid flow by the reversed flow region. Further, this wall pressure distribution closely resembled that of a forward facing step, suggesting that details in the method of inducing separation do not have a significant effect in the far upstream range. However, a distinctly different trend was observed close to the separation point over a region of the order of twenty boundary-layer thicknesses. It was therefore concluded that the upstream effect is governed by at least two length scales, the smaller describing the region where the rapid rate of thickening of the vortical layer at the wall affects the pressure distribution.

Further, it was noticed that the charge in the inviscid external velocity distribution at far upstream distances due to separation was independent of the pressure gradient of the corresponding unseparated flow.

CHAPTER 1

INTRODUCTION

1.1 SEPARATED FLOWS AND UPSTREAM EFFECTS

When a boundary-layer separates from a body, the region where the effect of viscosity is critically important no longer remains thin. Consequently, the form-drag of a body in a fluid stream is considerably larger than the skin-friction drag. Also, the displacement effect of the separated region reduces circulation and lift. Further, separation adversely affects the performance of internal flow devices like diffusers. Prevention of separation has therefore been an important objective in the design of airborne and marine vehicles and fluid machinery.

Separation can sometimes be used to advantage. For instance, the working principle of several fluidic devices depends on the reattachment of a separated layer. The subsonic performance of thin airfoils which are suitable for supersonic flight can be improved by the formation of a short separation bubble.

With the technological developments in transonic and supersonic aircrafts and gas turbines, the need for basic

studied extensively (Lighthill 1953, Chapman et.al. 1958, Zukoski 1967 and Carpentor 1968). The hyperbolic equations of inviscid supersonic flow make the strong interaction local and hence simpler than that in subsonic flow.

1.2 REVIEW OF EARLIER WORK

There does not seem to be any investigation of upstream effects in separated flows of the type of the present work. The following brief review gives general background of the present state of related knowledge.

Classical studies were largely concerned with two types of information depending on whether the separation took place from a sharp corner or from a smooth surface. The free streamline theory of Kirchoff (1869), Helmholtz (1868), Batchelor (1956), and Roshko (1955) in general dealt with the first type of problem. The effect of the separated region on the outer flow was described by a dynamical condition on the interface streamlines. Pressure distribution and drag coefficient were usually obtained as a function of a parameter whose value was not determined by the theory. The other type of investigation dealt with the question of whether a boundary-layer starting from given initial conditions and external pressure distribution would separate from a smooth surface. The investigation further sought to determine the location of separation point, if the boundary-layer separated.

The present work is concerned with separation from a smooth surface.* The problem of two-dimensional laminar boundary-layer of an incompressible fluid has been extensively discussed in the literature (Brown, 1969). There is a diversity of opinion regarding the validity of the boundary-layer equations near the separation point. Early calculations (Howarth 1938, Hartree 1939, Leigh 1955, Terrill 1960) indicated that numerical integration of the boundary-layer equations ran into difficulties as the skin-friction value approached zero. The calculations were terminated at a suitable low value of skin-friction and the point of zero skin-friction was determined by extrapolation. The behaviour of skin-friction near the separation point and the breakdown of the process of integration gave rise to the view that the point of zero skin-friction is a singular point. This point has some significance and has been called the separation point.** The nature of singularity has been discussed by

---

* In the present context, this phrase merely distinguishes separation from a geometrically singular point like a corner from the separation taking place at a regular point. The surface need not be hydraulically smooth.

** There are many subtle and somewhat unresolved issues in adopting a suitable definition of the separation point. They are discussed in Appendix A.

Goldstein (1948), Stewartson (1958), Terrill (1960) and Catherall, Stewartson and Williams (1965).

Catherall and Mangler (1966) obtained a numerical solution of the boundary-layer equations which proceeded beyond the point of zero skin-friction. It is therefore not certain whether the separation point is always a singular point. It was suggested (Stewartson 1958, Catherall and Mangler 1966, Klemp and Acrivos 1971) that a distinction needs to be made between two types of situations. In one case, the streamlines leave the surface but the separated region still remains thin $O(R^{-1/2})$, as in shallow bubbles within boundary-layers. No difficulty about the validity of the boundary-layer equations is expected in this case, except possibly in the immediate neighbourhood of the point of zero skin-friction. Solutions of boundary-layer equations with reversed flow (Klemp and Acrivos 1972) have shown that flow reversal is compatible with boundary-layer equations.

The procedure of Catherall and Mangler (1966) was to specify the displacement thickness some distance upstream of the separation point and to determine the pressure distribution as a part of the numerical integration procedure. Many investigations (Brown 1969) suggest that in general an incompressible boundary-layer is singular at separation when the pressure gradient is arbitrarily prescribed.

The problem of the separation of a turbulent boundary-layer is more complicated due to the auxiliary equation or closure hypothesis for turbulence and also possibly the effects of normal Reynolds stresses near the separation point. An extensive comparative study of contemporary prediction methods was carried out at the Stanford Conference (Kline et.al. 1968). Twentynine methods were tested for a selected data of thirtythree flow fields. While the methods differed in the use of differential or integral equations and the type of the auxiliary equation, all the methods assumed the external pressure distribution. Although the overall judgement of the evaluation committee was favourable, it was pointed out that none of the methods directly dealt with the strong interaction taking place near the separation point. The general performance of the methods was not very satisfactory near the separation point.

Special analyses have been constructed to deal with turbulent boundary-layer near the separation point. For example, the analysis of Stratford (1959), Townsend (1962) and Nishida & Iida (1972) divides the layer in two parts. The outer part behaves like an inviscid layer of almost constant total pressure. Reynolds stress enters in the force balance only in the inner layer. As pointed by Townsend (1962), this analysis does not attempt to describe the upstream effects of separation.

Turbulent boundary-layers subjected to adverse pressure gradient have been experimentally studied by many workers. Well-known works include those of Ludwieg and Tillman (1950), Schubauer and Klebanoff (1951), Newman (1951), Clauser (1954), Fraser (1954), Stratford (1959), Schubauer and Spangenberg (1960), Moses (1964), Perry (1966) and Sandborn (1969). Many of the investigations dealt with attached flows and the main concern was in the gross properties of the boundary-layer. Mean velocity profiles were usually obtained by a total-head probe and wall taps. As pointed out by Coles (Stanford Conference, 1968) the measurements were often terminated before the separation point was reached, and effects like transverse static pressure variations or the flow angle relative to the wall were usually not considered. Further, there were sometimes difficulties in obtaining two-dimensional or axisymmetric flows. When the region of adverse pressure gradient is long, slight three-dimensionality can have considerable effects, as was revealed in the works of Schubauer and Klebanoff (1951) and Clauser (1954). Another problem is the measurement of skin-friction in adverse pressure gradient. The preston tube needs a sufficiently long logarithmic portion in the mean velocity profile. Direct measurement of skin-friction in adverse pressure gradient also has associated difficulties (Brown and Joubert, 1969), and the heat transfer gauge is rather insensitive to small values of skin-friction (Drinkuth and Pierce 1966, McCroskey 1972).

The development of a boundary-layer ahead of a forward-facing step (Bradshaw and Galea 1967, Robertson and Taulbee 1969) and a bluff plate (Good 1968) has drawn attention recently.

The attainment of a maximum pressure rise with a given initial boundary-layer without causing separation or the attainment of a given pressure rise over the shortest distance is of engineering interest in the context of compressor and wing design. Experimental studies of incipient separation were undertaken by Stratford (1959) and Spangenberg et.al. (1967).

If the reattaching separated layer leaves a long slender region, it is called a separation bubble. Wall pressure measurements of separation bubbles and characterisation of the conditions under which they are formed have also been extensively reported (Tani 1964, Ojha 1967).

Experimental data on the upstream effects of separation is known to be very scanty (Kline et.al. 1968) and any prediction procedure which attempts to locate the separation point needs to take these effects into account. The present experiments are designed with a view to understand the general properties of the upstream effects. The separated flow was approximately two-dimensional and the separating boundary-layer was turbulent.

1.3 BASIC IDEAS UNDERLYING THE PRESENT EXPERIMENTS

Consider the separation of a boundary-layer of an incompressible fluid from a smooth surface. The outer inviscid flow is assumed to be steady and two-dimensional. Let the outer flow with separation and a corresponding inviscid flow without separation be given by stream-functions Ψ and ψ'.

Then

$$\Psi = \psi' + \Delta\psi \qquad (1)$$

where the difference $\Delta\psi$ describes the effect of separation. Ψ, ψ' and hence $\Delta\psi$ satisfy the Laplace equation. Since the study of $\Delta\psi$ must be through measurement of Ψ, it was decided to keep the unseparated flow ψ' as simple as possible. To make ψ' correspond approximately to uniform flow, separation was induced by a forward-facing wall jet on a flat surface, which was the test section floor of a wind tunnel. Control of the wall jet velocity gave a simple direct control on the reversed flow region without affecting ψ'. The upper test-section wall was adjusted initially to make ψ' correspond to a uniform flow in the region of interest. In the latter stages the angle of the upper wall was altered to study the effect of ψ' on $\Delta\psi$.

In supersonic separated flow problems, there is a free interaction zone where the pressure distribution is not

affected to any detectable extent by the details of how separation is caused (i.e. by an impinging shock, step, ramp etc.). If there are similar regions in subsonic flow, the findings could be general and need not be restricted to particular methods of causing separation.

Figure 1 shows the essential configuration of the experiment and the notations used. Control of U_∞, U_j and α gave control on the three major flow parameters namely λ, R_∞ and α.

Let I denote the outer flow which is approximately inviscid, II the viscous layer ahead of the separation point, and III the remaining region. For the present qualitative discussion it is not necessary to consider how the boundaries are determined. The region I influences the viscous layer II through pressure distribution, which determines the separation point. Hence, considerable emphasis is laid on investigation of the properties of the wall pressure distribution upstream of the separation point.

An important question is how the wall pressure distribution in region II upstream of separation is influenced by region III. The effect could be displacement effect on region I which modifies the inviscid flow upstream of the separation point and hence the pressure distribution. This effect can be approximated to some extent by describing the dividing streamline in several simple ways. If the

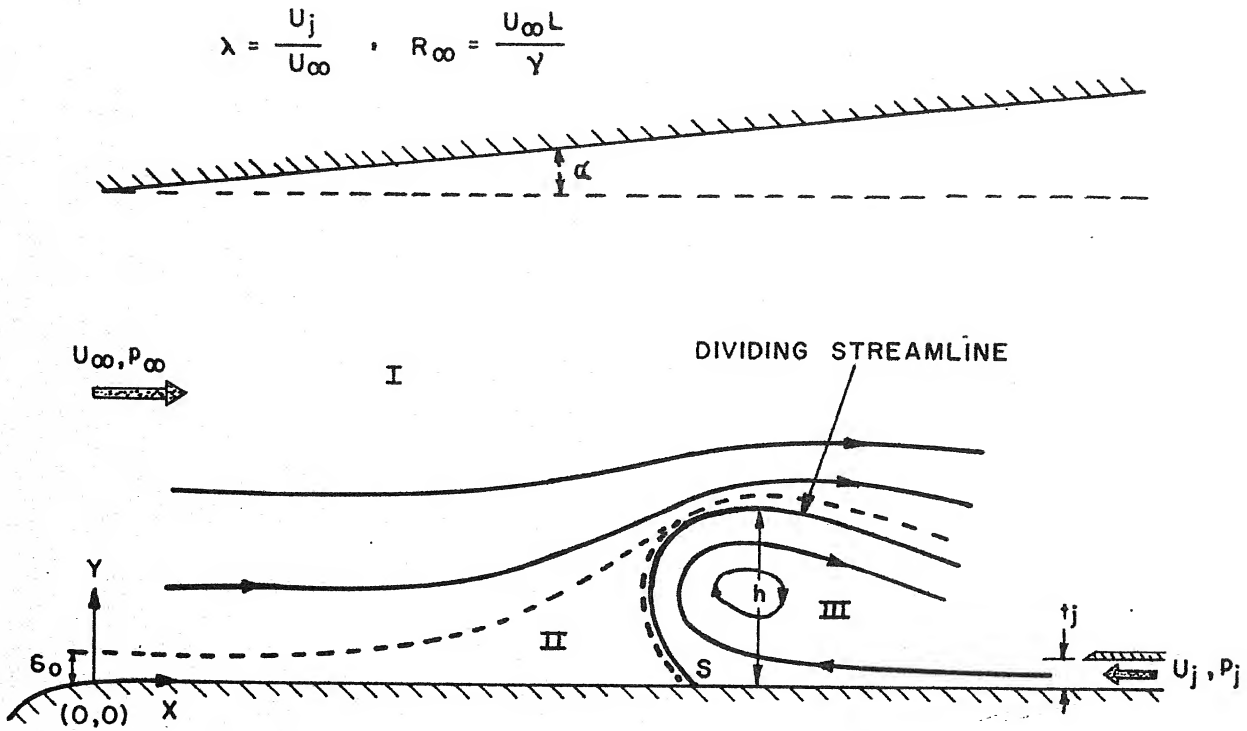

FIG.1 FLOW CONFIGURATION AND SYMBOLS

observed pressure distribution shows some properties which are at variance with the effects produced by widely varying descriptions of the dividing streamline, the conclusion would be that there is also a strong interaction between regions I and II or II and III. The classical framework of thin boundary-layer does not permit a strong interaction between regions I and II. However, such a strong interaction theory using integral methods has been very successful in supersonic flows (Crocco and Lees 1952, Lees and Reeves 1964).

Direct influence of region III on the pressure distribution in II would require propagation of upstream influences within the boundary-layer. The classical framework of the boundary-layer uses parabolic equations and upstream influences within the layer are not permissible. A more refined asymptotic framework which allows a switchback effect of higher order terms or alteration in the parabolic nature of the equations by normal Reynolds stress terms near the separation point can permit the propagation of upstream effects within the layer.

1.4 OUTLINE OF THE WORK

Details of the experimental programme is described in chapter 2. This includes the description of the experimental set up, apparatus and instrumentation. Preliminary experimental results for boundary-layer study, two-dimensionality of flow, and effects of Reynolds number

on unseparated turbulent boundary-layer and on wall jet are also given. Hot wire results for turbulence measurements and an oil film method for flow visualisation are also described.

Chapter 3 describes the results and includes a discussion. Emphasis is on the upstream wall pressure distribution, its parameters and existence of similarity. Results are compared with pressure distribution upstream of stagnation point in inviscid flow models.

Upstream pressure distribution is compared with similar earlier experiments. Last section summarises the results.

CHAPTER 2

EXPERIMENTAL PROGRAMME

2.1 APPARATUS

The experiments were conducted in a 30 cm x 40 cm smoke tunnel (Figure 2). Air was sucked in the open-circuit tunnel from an essentially closed room and discharged into the room. The tunnel therefore acted like a closed-circuit tunnel. It had a honey-comb of 25 mm square mesh and two screens in a settling chamber followed by two two-dimensional contraction sections with an overall contraction ratio of 9. The 100 cm long test-section was followed by a diffuser-cum-transition section and an axial flow fan driven by a DC motor.

The maximum attainable speed in the test-section was 16 m/s and free-stream unit Reynolds numbers ranged from 2.6×10^5 to 8.0×10^5 per meter during the experiment. The variation of dynamic pressure in the test-section at a typical section was less than 2% of the free-stream dynamic pressure outside the wall boundary-layers which were typically 10 mm thick. The turbulence intensity based on streamwise fluctuation was less than 0.5%.

The top and bottom walls of the test-section, which were modified for the experiment, consisted of 6 mm thick perspex

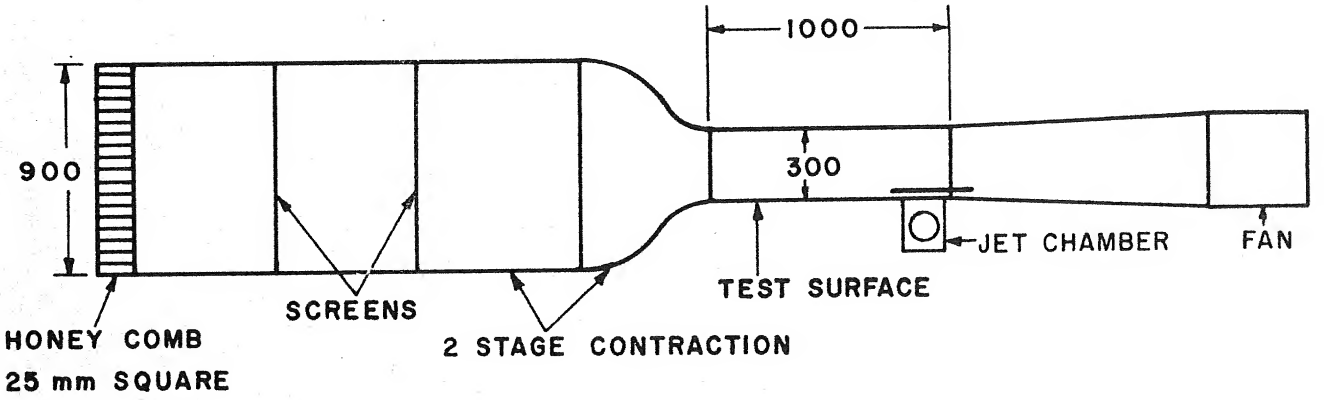

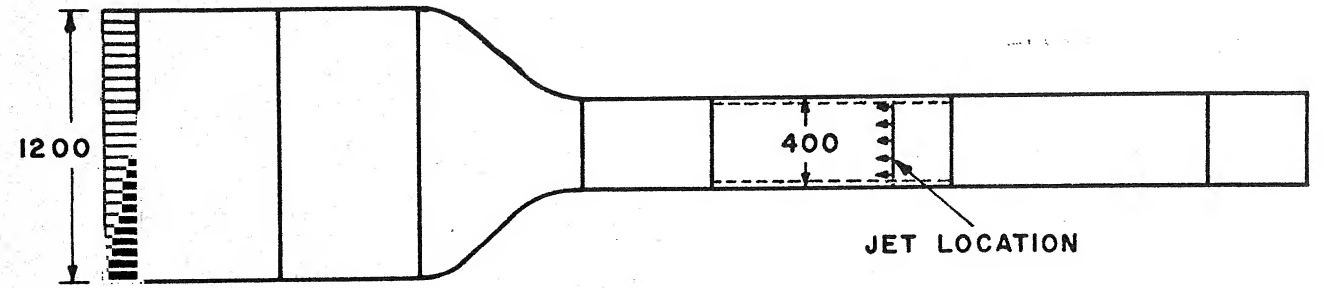

FIG.2 A SKETCH OF THE WIND TUNNEL

ALL DIMENSIONS IN mm

sheets. The upper sheet contained slots for spanwise and longitudinal traverse of probes. The bottom test surface was provided with 0.3 mm diameter brass wall pressure tappings. Beginning at x = 6 cm from the end of contraction, the first 8 taps were at 2 cm pitch, the next 28 at 1 cm pitch, and the remaining 12 at 2 cm pitch. Taps and smoke injection tubes were also provided at 5 cm pitch in the spanwise direction on either side of the centreline (Figure 3).

A 4 cm wide sand-paper strip spanning the contraction was fixed on the lower surface about 10 cm upstream of the test-section for triggering transition of the boundary-layer.

A wall jet facing the main stream was located at x = 73.2 cm. Two vertical false walls were provided at 30 cm spanwise distance as the width of the wall jet was restricted by the tunnel construction. They extended throughout the entire height and length of the test-section. They also reduced the effective thickness of the side-wall boundary-layers.

A 3/4 HP blower supplied air to the wall jet through a first settling chamber with a honeycomb and two screens, and through two 130 mm diameter symmetrical ducts (Figure 5). The air then passed through a second settling chamber which was connected to the tunnel floor, the top surface of the chamber being a 6 mm thick bakelite sheet with a sharp edge forming the upper surface of the wall jet. The height of

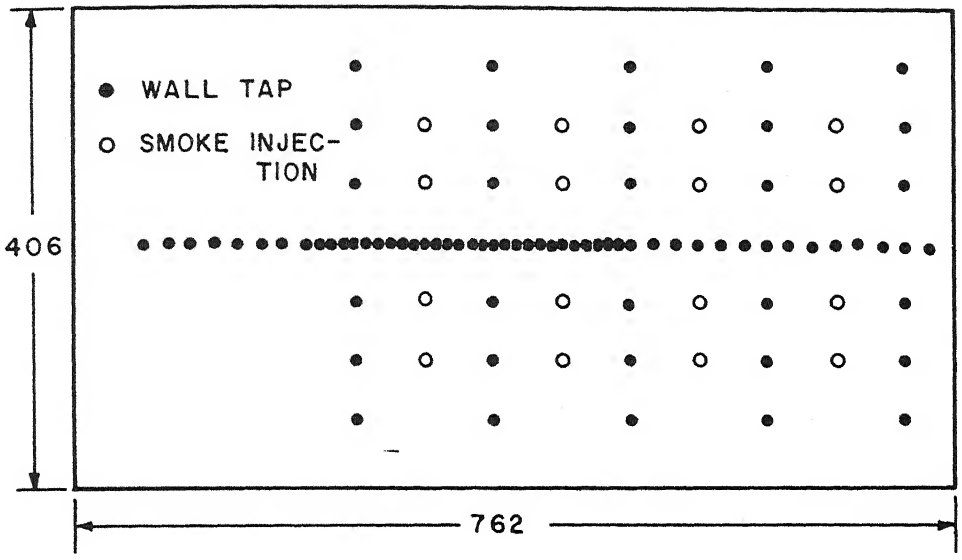

FIG.3 WALL TAP LOCATIONS

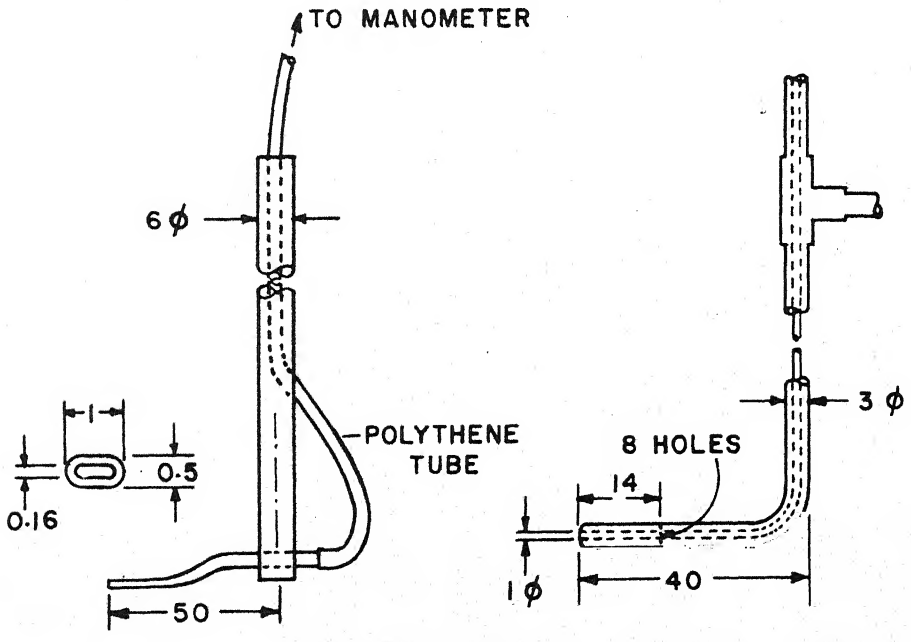

FLATTENED TOTAL-HEAD PROBE

PITOT-STATIC PROBE

FIG.4 STANDARD PROBES

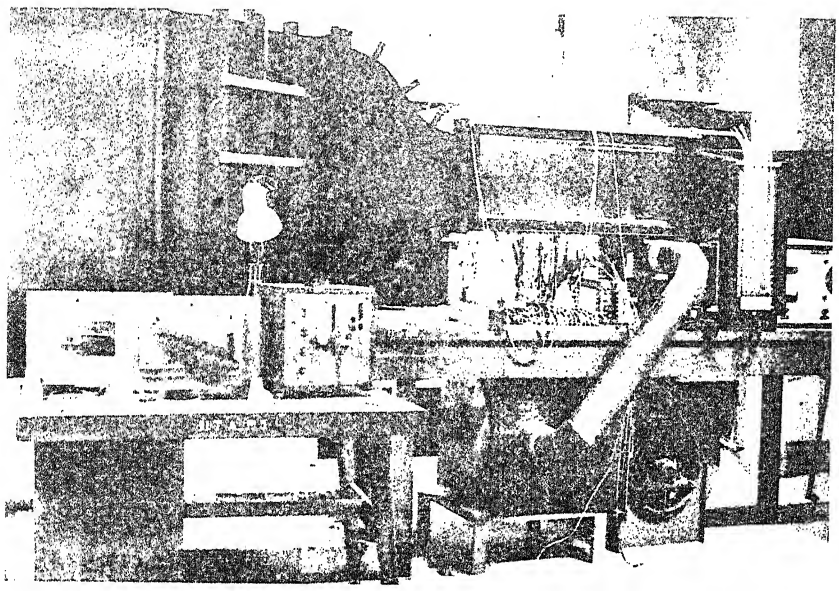

FIG.5 A VIEW OF THE EXPERIMENTAL SET UP

the sheet which determined the wall jet height t_j could be varied upto 12 mm in steps of 0.5 mm. The wall jet height t_j was kept 4 mm for all the experiments. A bypass valve near the first settling chamber controlled the wall jet velocity. The maximum jet velocity was 30 m/s and it gave a variation of λ from 1.5 to 7.2.

2.2 INSTRUMENTATION

Figure 4 shows two probes of conventional design employed in the experiments. The pitot-static tube was used to measure free stream dynamic pressure at a central reference point at the beginning of the test section. The flattened total-head probe was used for velocity measurements in the boundary-layers and near the wall jet exit.

The asymmetric probe, described in part I, was used for the measurement of velocity, flow direction and total pressure. A two-headed probe (Figure 6a) was used to locate the separation point. It consisted of two 1.2 mm outer and 0.8 mm inner diameter tubes, which were chamfered at 45° and soldered side by side, the chamfered ends facing opposite directions. It was held vertically with its tip touching the test surface and one chamfered end facing the freestream, and it was traversed along the centreline till the pressure difference between the tubes was zero. The separation point thus located with this probe was reproducible within $\pm$ 2 mm. This location typically agreed within $\pm$3 mm with the location

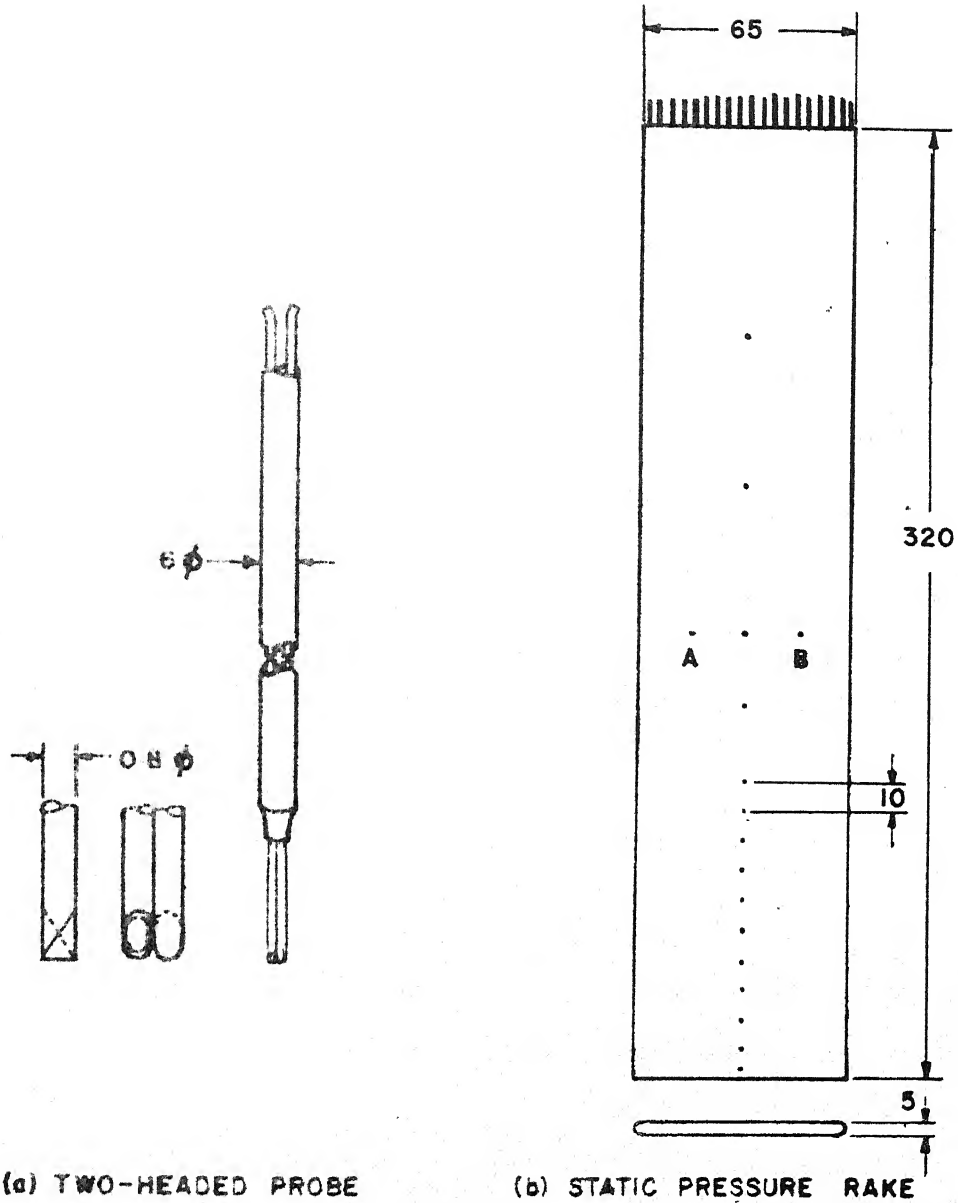

(a) TWO-HEADED PROBE (b) STATIC PRESSURE RAKE

FIG.6 TWO-HEADED AND STATIC PRESSURE PROBES

obtained by the flow visualisation method, which was obtained within ± 5 mm.

A static pressure rake (Figure 6b) was designed for rapid static pressure surveys. 19 tubes, suitably bent of 2 mm outer diameter were arranged in a plane and they were enclosed by 1.5 mm thick sheets, the interior space being filled with wax. The rake was thus 5 mm thick. The ends were covered with semicylindrical wooden strips. Wall taps of 0.5 mm were drilled centrally on one side at suitable locations to connect each hole with a tube. Four additional wall taps (A, B, C and D) were used to align the rake in the flow direction. The static taps on the centreline were 3.25 cm from the leading edge and a potential flow calculation showed that the measured static pressure would be less than the actual by 6% of the dynamic pressure.

Three manometers were used. A null-reading micromanometer with a movable inclined tube (Flow corporation, Model mm-3) had a resolution of 2.5×10^{-3} mm (10^{-4} in.) of ethyl alcohol over 50 mm (2 in.). The other two manometers were well-type fixed inclined tubes (Dwyer) with a resolution of 0.125 mm (5×10^{-3} in.) and 0.25 mm (10^{-2} in.) over 6 mm (0.25 in.) and 75 mm (3 in.) of water. The manometer with the smaller range was connected to a pitot-static tube at the reference point. It was also used for a preliminary survey. The manometer with the larger

range was used to measure the jet velocity at the wall jet exit. All other measurements like the wall pressures and velocity profiles were taken with the micromanometer.

A traversing mechanism provided three translational degrees of freedom to the probes. The vertical displacement was measured with a vernier (resolution 0.05 mm, range 240 mm) and also with a dial-gauge (resolution 0.01 mm, range 25 mm) for measurements close to the test surface. The measuring accuracy in the longitudinal and transverse directions was 1 mm. The probe and the traversing mechanism were sufficiently rigid to prevent detectable vibrations.

A constant-temperature anemometer (DISA 55A01) was used for turbulence measurements. Wollaston platinum wire (0.0075 mm dia., 2200 ohms/m) was used with single wire probe. Qualitative observations were made with a dual trace oscilloscope (Tektronix 545B) and RMS values were measured with an external voltmeter (GRC 1806A, 850) attached to the anemometer.

2.3 PRELIMINARY TESTS AND EXPERIMENTAL TECHNIQUES

The flow field of the experiment is shown in Figure 1 which was drawn on the basis of flow visualisation and velocity field survey which are described later. The sketch also shows the coordinate system and the symbols.

Before conducting the main experiments, the flow field was investigated for longitudinal pressure distribution, location of transition and two-dimensionality with only the free-stream ($U_j = 0$) and also with only the wall jet ($U_\infty = 0$). With the sand-paper trip, the boundary-layer velocity profile was found to follow the logarithmic law in wall coordinates in the overlap region for x greater than about 8 cm and was thus fully turbulent.

Mean velocity profiles, in the absence of wall jet, were measured with the flattened total-head tube and the wall tap as the boundary-layer thicknesses were of the order of 10 mm. A typical velocity profile is given in Figure 7. Figure 8 gives the development of the boundary-layer parameters.* Variations of the external velocity along the centreline were within one percent except at the last station. Displacement, momentum and energy thicknesses increased slowly with x upto about x = 55 cm and thereafter at a rapid rate, which was attributed to the pressure gradient created by the geometry of the wall jet exit at x = 73.2 cm. The friction coefficient decreased after x = 50 cm. Shape factor H remained about 1.4. These results suggest that the free-stream flow is to a good approximation a zero pressure gradient flow upto about x = 55 cm.

---

* Details of data reduction are given in Appendix B.

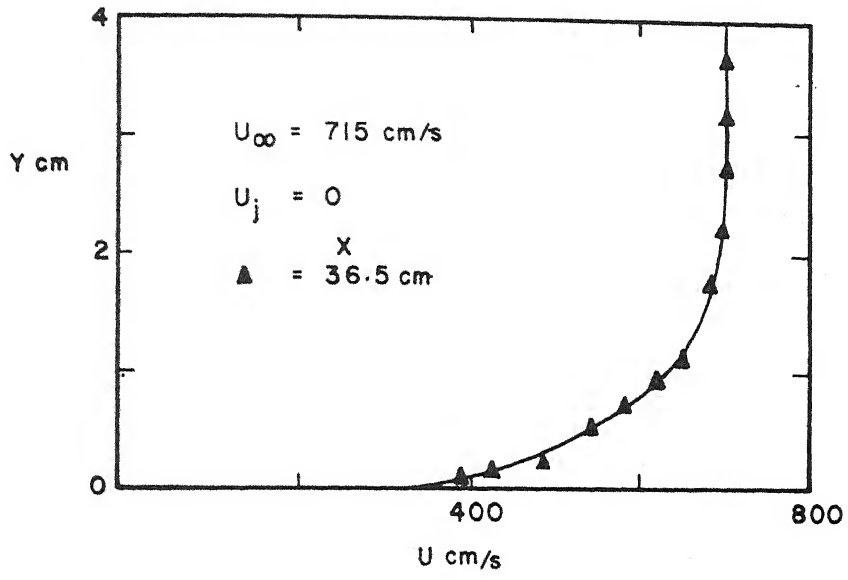

FIG.7 VELOCITY PROFILE

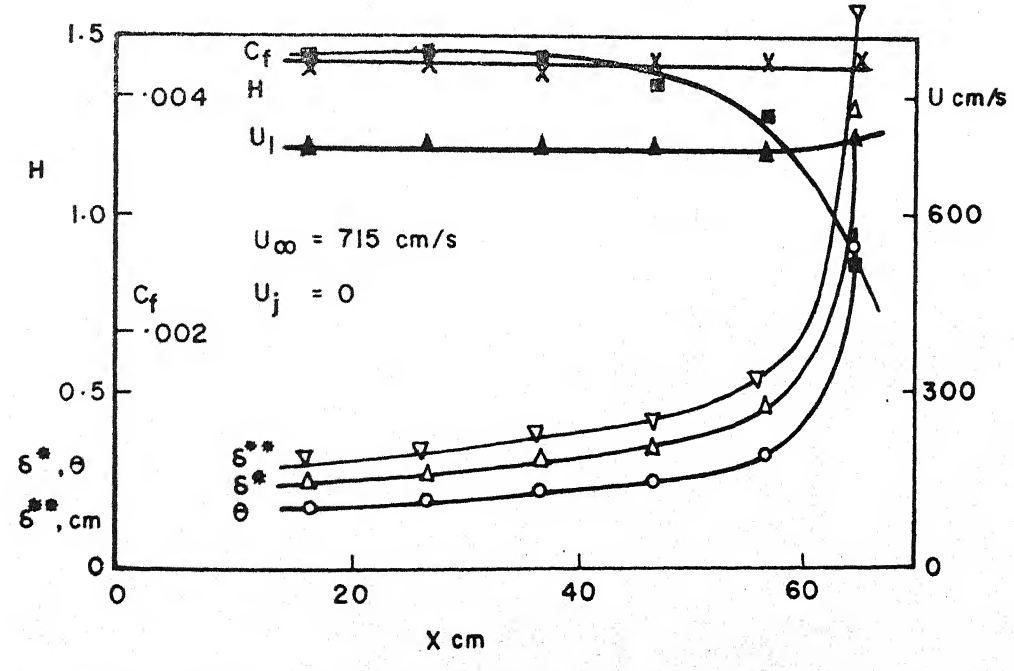

FIG.8 BOUNDARY LAYER PARAMETERS

Further checks were carried out to see possible effects of low unit Reynolds number or possible non-equilibrium effects. Figure 9 shows the velocity profile in wall coordinates. The agreement with the logarithmic law indicated that the boundary-layer was fully turbulent and the effects of low Reynolds numbers were not serious. The velocity defect profiles are plotted in Figure 10 in outer coordinates following Clauser (1954). The close agreement with the Clauser's equilibrium profile indicates that the boundary-layer was a normal fully-developed, zero pressure gradient, turbulent boundary-layer upto about x = 55 cm. The last profile (x = 64.5 cm) is quite different from the equilibrium profile indicating the effects of pressure gradient. A longitudinal wall pressure distribution along the centreline on the bottom surface also indicated its variation was within 2 percent of the free-stream dynamic head upto about x = 60 cm.

Turbulence intensity was measured in the boundary-layer at various stations. The results (Figure 11) are in good agreement with those of Klebanoff (1955). The agreement further substantiates the view that the boundary-layer was a normal fully-developed turbulent boundary-layer.

Some tests were made for checking the two-dimensionality of the flow. Figure 12 shows the spanwise variation of wall static pressures and dynamic pressures outside the boundary-layer, from the corresponding values at the reference

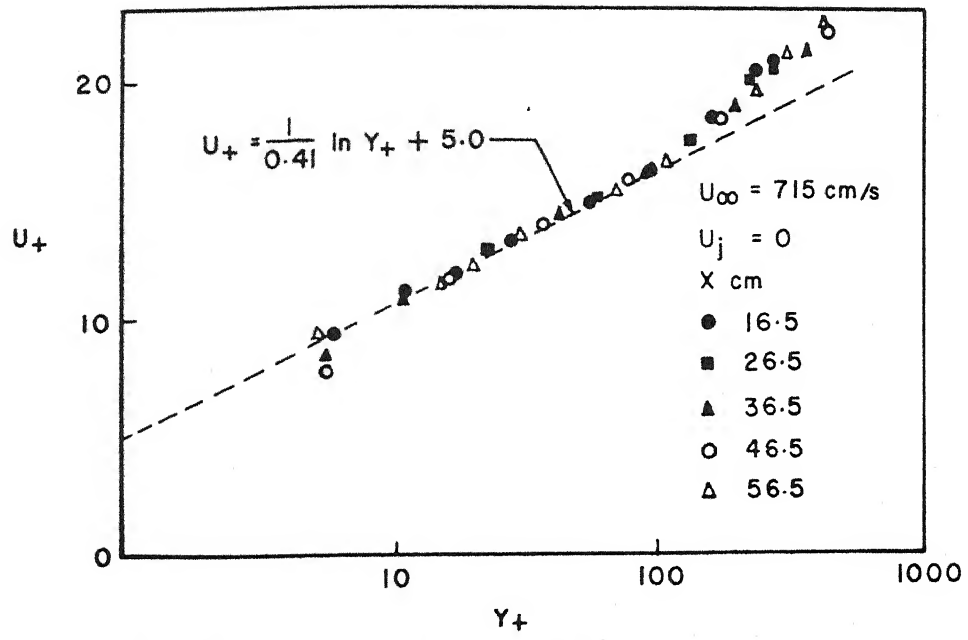

FIG.9 VELOCITY IN WALL COORDINATES

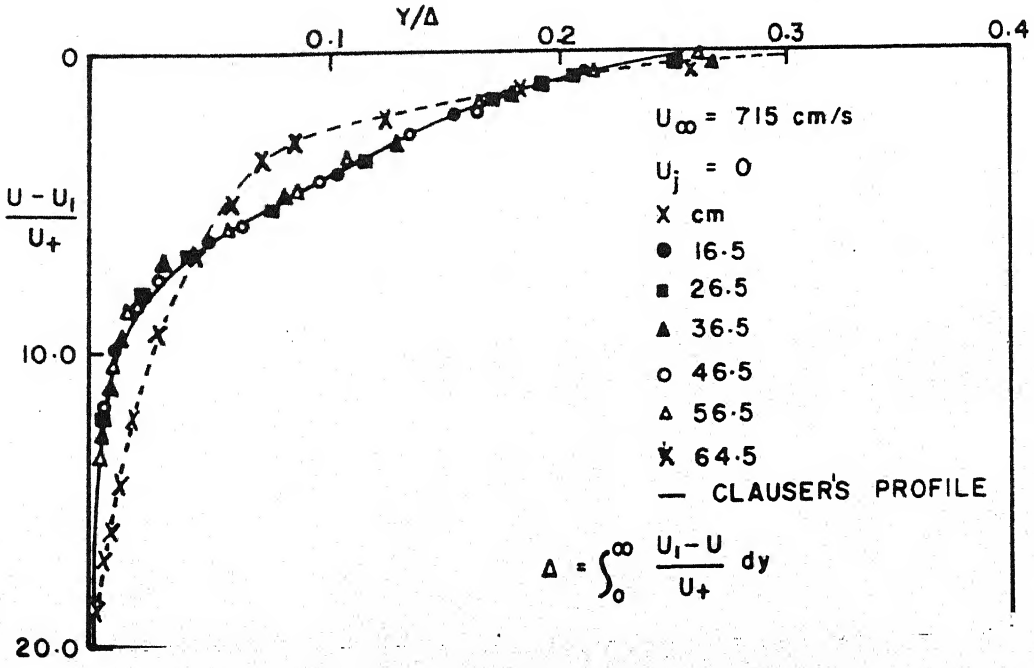

FIG.10 EQUILIBRIUM DEFECT PROFILE

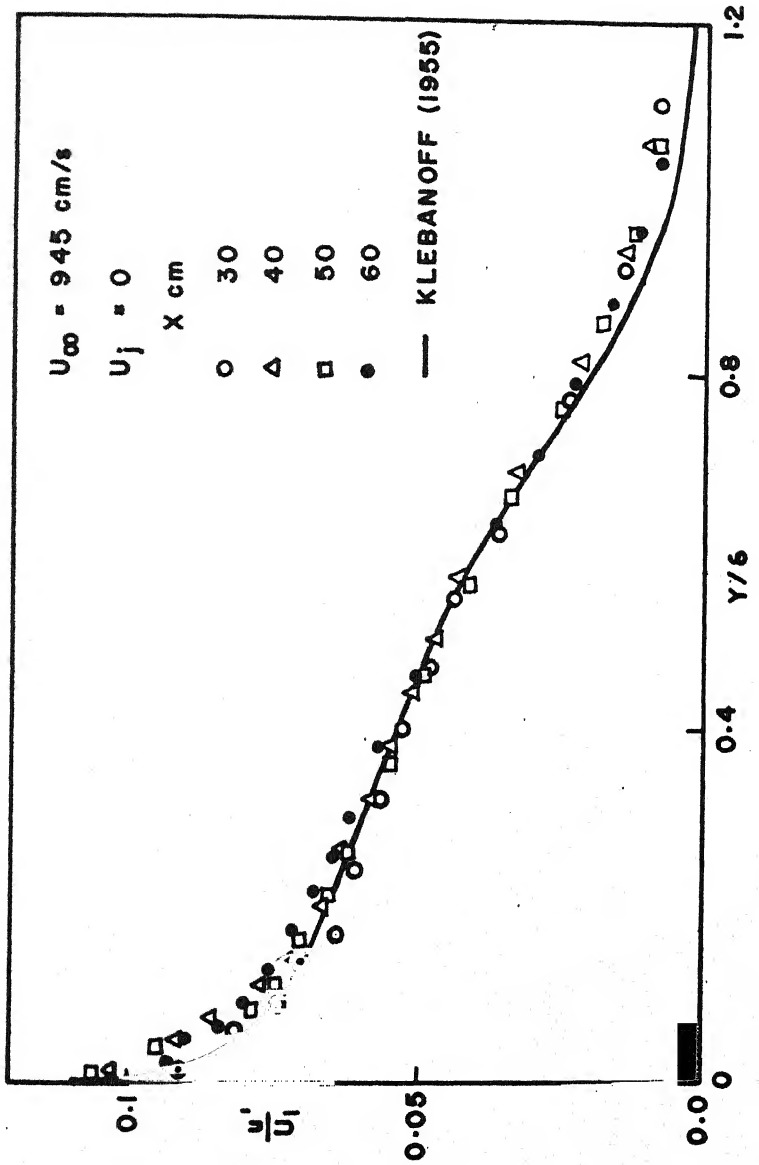

FIG.11 TURBULENCE INTENSITY

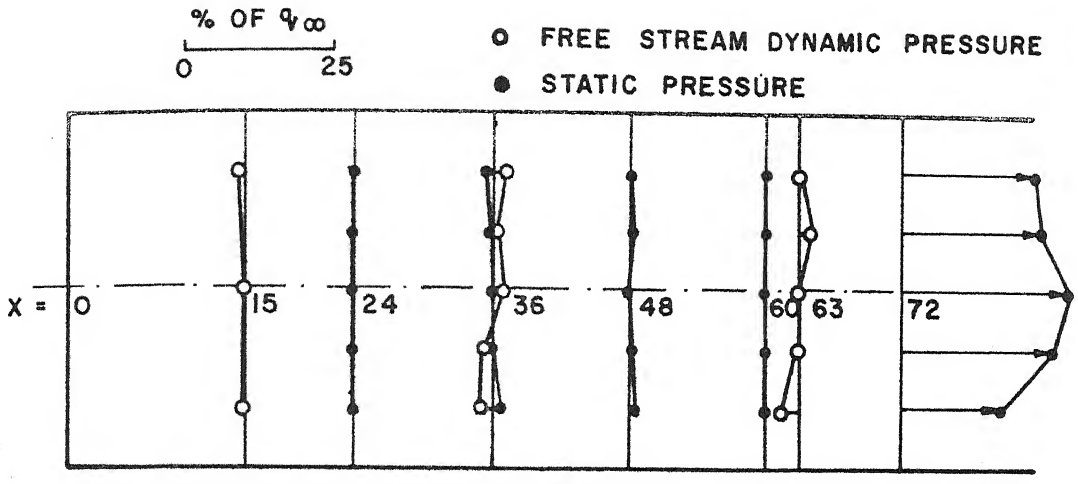

FIG.12 VARIATIONS IN SPANWISE DIRECTION

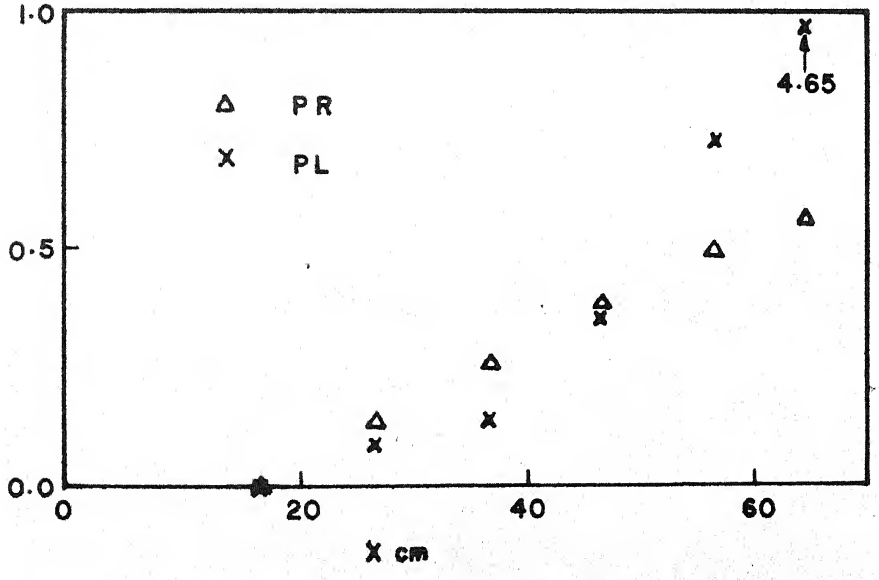

FIG.13 INTEGRAL MOMENTUM BALANCE

station, as a percent of free-stream dynamic pressure. The variations were less than about 5 percent in dynamic pressures and less than about 2 percent in static pressures. A momentum balance check as suggested by Coles (1968) was also made and Figure 13 show a good two-dimensionality of flow upto about x = 50 cm.

The wall jet profile and its development in the absence of free-stream are shown in Figure 14 and 15. The turbulence intensity in the jet flow was found to be of the order of 20%. The spanwise variation of jet flow at x location at 36 and 72 cm is shown in Figure 16. These figures show that the spanwise variations were less than 10 percent of the maximum velocity.

When neither U_∞ nor U_j was zero, the static pressure rake was used to measure the static pressures normal to the surface, and the asymmetric probe was used for the velocity field survey (Part I).

Various methods were tried to locate the separation point. The approximate location was indicated by a wool tuft attached to a thin rod. The smoke technique was not satisfactory due to limited smoke supply. Further, the china-clay technique was also not satisfactory due to inadequate spraying equipment for the volatile liquid. A liquid-film method employing a mixture at lamp-black and kerosene was successful. Elevation and plan of the flow

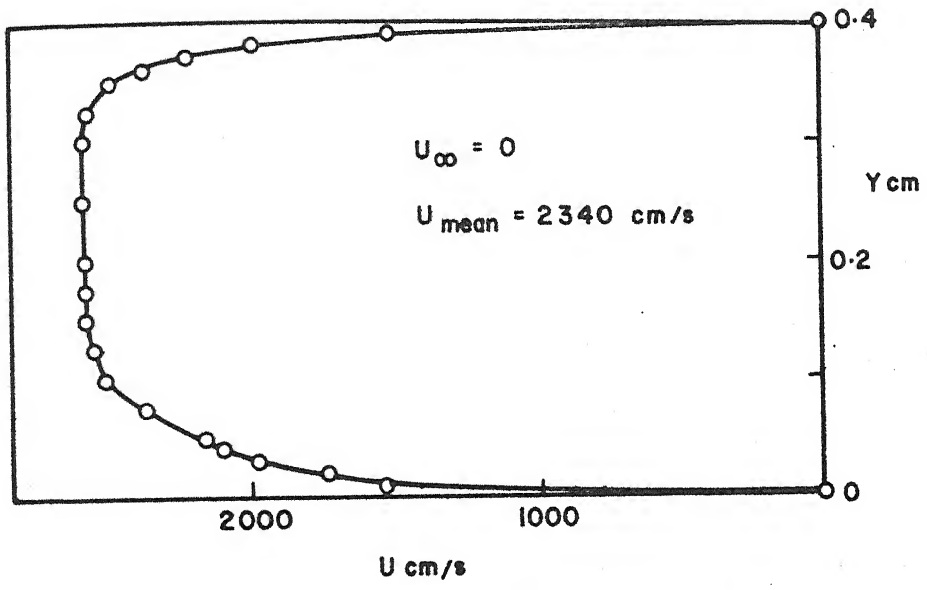

FIG.14 WALL JET PROFILE

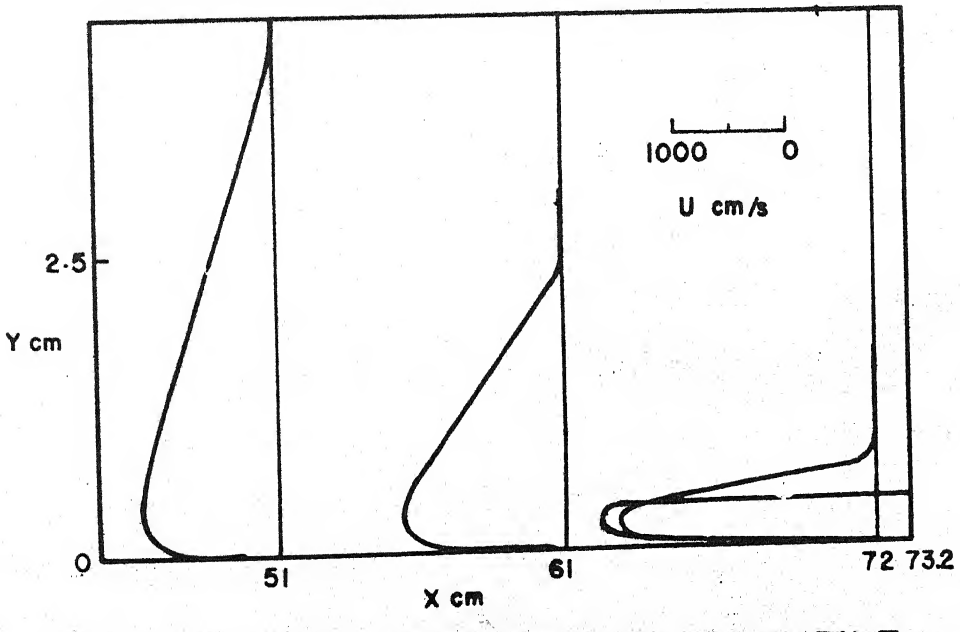

FIG.15 DEVELOPMENT OF JET PROFILE

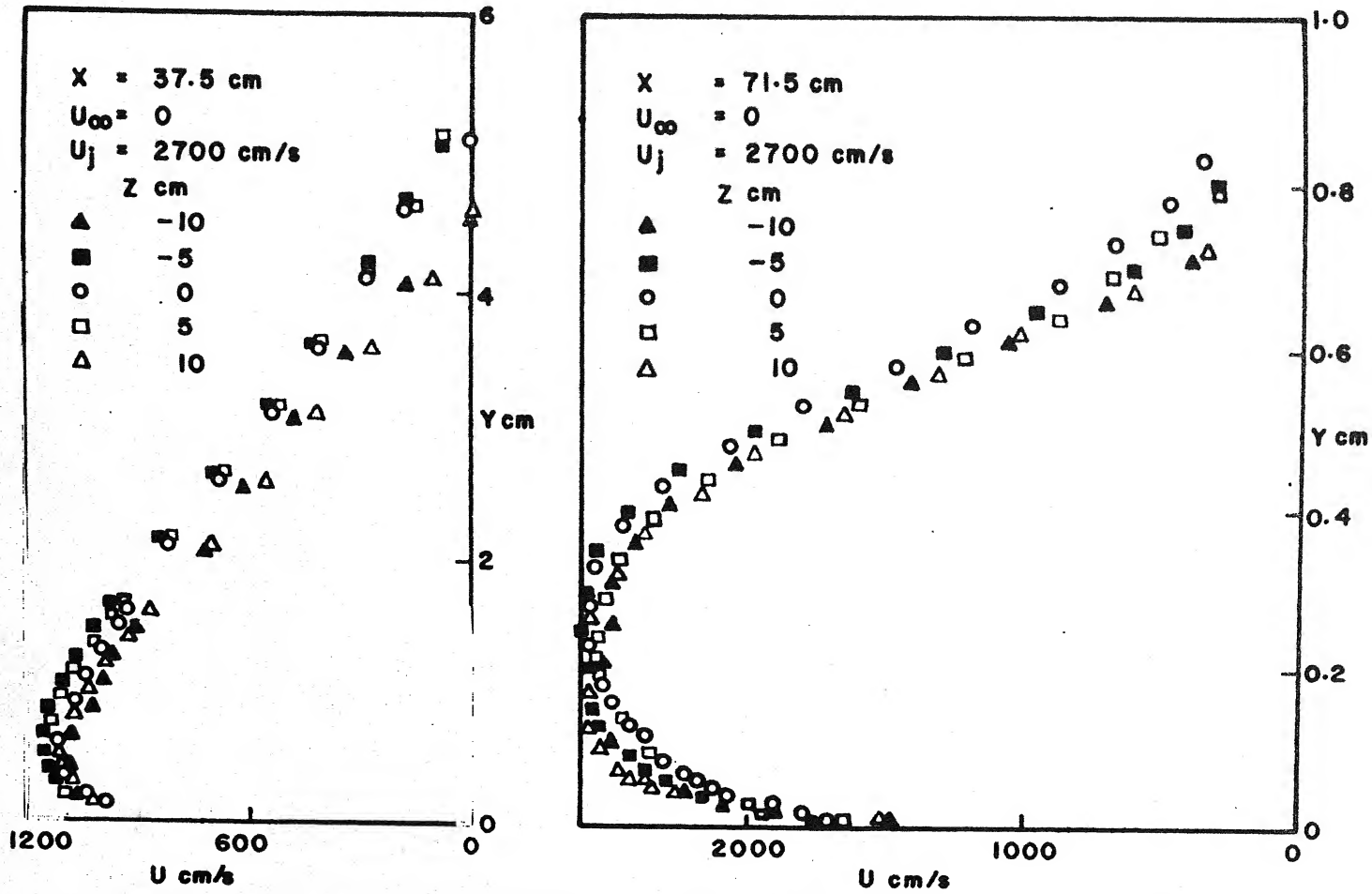

FIG.16 SPANWISE VARIATION OF JET VELOCITY PROFILE

patterns were obtained on two plates (Figure 17). The lower photograph shows the flow pattern obtained on a 0.4 mm thin aluminium plate attached to the test surface. A paste of lamp-black and kerosene was applied. With the flow, the paste flowed on the surface before the kerosene evaporated thereby giving the surface flow pattern. The upper photograph shows the flow pattern on a vertical aluminium plate which was placed symmetrically in the test section. The dark separation zone in the lower photograph was taken as the separation line and was located within ± 5 mm. The photograph also indicates that the flow was reasonably two-dimensional except in the close proximity of the side walls.

For the sake of completeness, some of the details of experimental techniques are given here. Initial attempts to locate the velocity profile origin (i.e. $y = 0$) by optical or electrical (continuity) methods were not entirely successful. Elastic deflection of the probe tip, as suggested by Prof. M.R.Head, was finally used. Displacements in steps of 0.1 mm near the wall indicated a minima in dynamic pressures which was taken to be the location $y = 0$ cm. It was reproducible within 0.1 mm. The total-head tube position was shifted by about 2 mm in the spanwise direction from the wall tap centreline to reduce the interference on the wall tap.

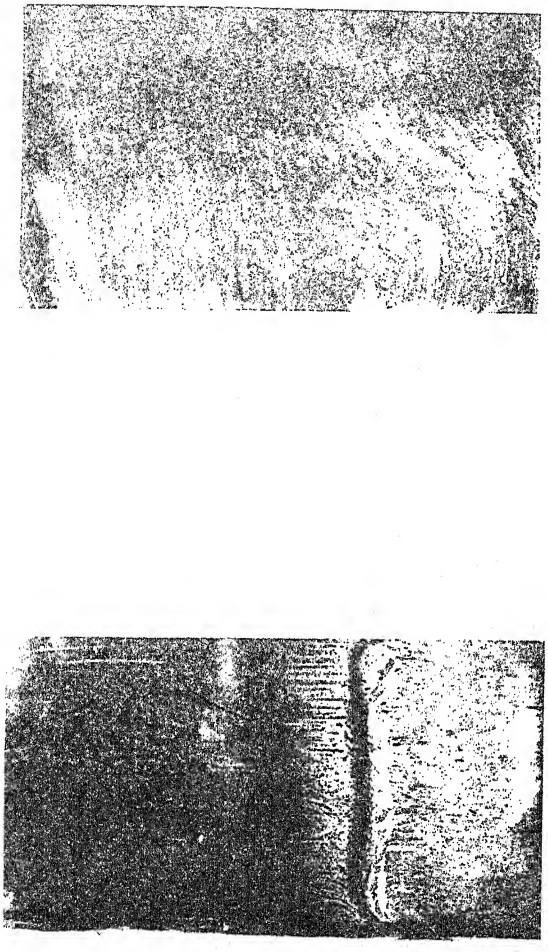

FIG.17 OIL FILM PATTERN OF WALL JET INDUCED SEPARATION

Wall pressure measurements were made by comparing the pressures with a reference pressure. Since the measurements were used to study the departures of wall pressures in separated flows from those in unseparated flows, it was desirable to use a wall point far upstream of separation as a reference pressure which itself would not be affected by separation. Limited length of the test surface resulted in some effects being experienced at the first wall tap on the test surface. A correction was applied to take this effect into account. $(p_{st} - p_{ref})$ was measured without separation. Then with the jet flow on and for the same free-stream velocity, $(p-p_{st})$ were measured to give $(p-p_{ref})$.

The control of λ was first attempted by varying the free-stream velocity and keeping the jet by-pass control valve fixed for a fixed value of jet velocity. However, the wall jet velocity varied significantly, thus requiring measurement and control of jet exit velocity for each set, for which a pitot-probe at the wall jet exit was provided.

rpg:lp.

CHAPTER 3

RESULTS AND DISCUSSION

3.1 INTRODUCTION

This chapter deals with results describing the nature of upstream effects in wall jet induced separation. Attention is focussed on the wall pressure distribution upstream of separation point, with emphasis on appropriate scales and similarity.

The general behaviour of wall pressure distribution for this flow field is described in section 3.2. As the free-stream boundary-layer was found to separate in favourable pressure gradient, the possibility of separation under favourable pressure gradient is examined in the next section.

Upstream wall pressure distribution and relevant parameters are considered in section 3.4. Section 3.5 considers the similarity of upstream pressure distribution, and applicability of the results to other configurations like a forward-facing step is also examined. The next two sections consider the inviscid flow models, their comparison with experimental results, and far and near upstream effects of separation.

These sections deal with the case of parallel opposite wall (Figure 1, $\alpha = 0$) where the pressure gradient associated with unseparated flow is zero in the region of interest and therefore the observed pressure gradient is due to separation. The case of convergent and divergent opposite walls ($\alpha \neq 0$) is considered in section 3.8 where separation modifies the pressure gradient which would have occured in the absence of separation.

Major conclusions are summarised in section 3.9.

3.2 WALL PRESSURE DISTRIBUTION

Preliminary experiments were conducted to obtain qualitative features of wall pressure distribution in a wall jet induced separation. Figure 18 shows that the wall pressure first attains a maximum and then drops. Further there are sometimes four local extrema in the reversed flow region of the jet near the jet exit. Locations of separation point obtained by the two-headed probe are also shown in the figure. The pressure distribution is qualitatively similar to that observed by Colin (1968) who used a forward-facing wall jet in the range $2.2 \leq \lambda \leq 9.4$ to simulate the recirculating region of jet lift VTOL aircraft flying or hovering in wind in ground proximity.

The wall pressures were sensibly steady upto the separation point but after the separation point, especially

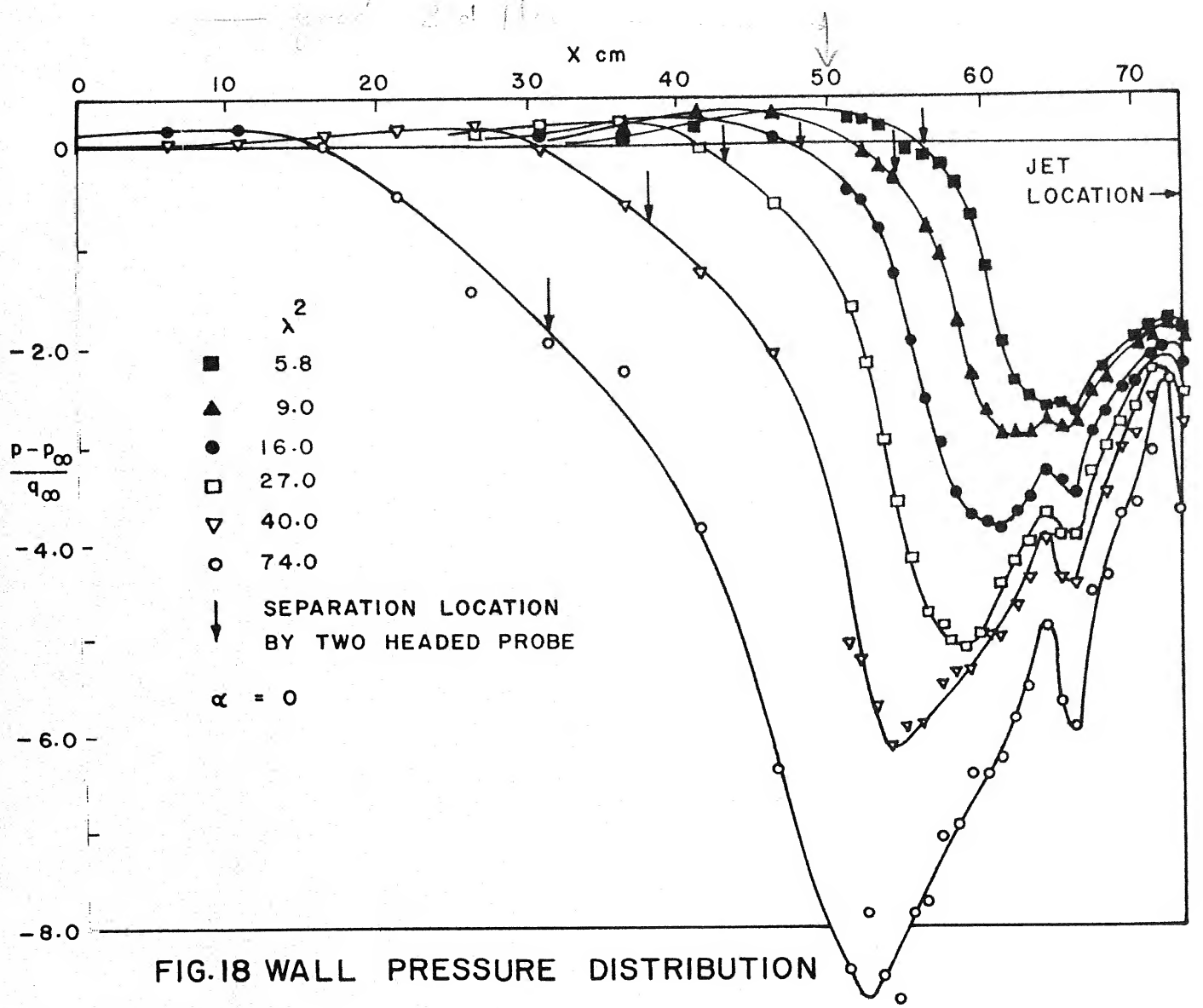

FIG. 18 WALL PRESSURE DISTRIBUTION

close to $C_{p_{min}}$ location, fluctuations of the order of 10 per cent of the free-stream dynamic pressure were observed. They seem to be due to the unsteadiness of the vortex. Further measurements of static pressure were made upstream of the separation point.

Figure 19 shows the wall pressure distributions for two values of λ obtained by several combinations of U_∞ and U_j. Clearly, the data suggests that

$$C_p = f(X/t_j, \lambda) \qquad (2)$$

describes to a good approximation the upstream effect slightly away from the separation point. This observation can be interpreted as the insensitivity of the wall pressure distribution to the Reynolds number of free-stream boundary-layer for given λ within the range of the experiments. Flow visualisation figures further showed that the location of the separation point X_s and the extent of the separation region h are determined by λ for given t_j, which was not varied during the experiments.

3.3 THE POSSIBILITY OF SEPARATION OF BOUNDARY-LAYER IN FAVOURABLE PRESSURE GRADIENT

Figures 18, 19 and 24 show that for the entire range of λ the separation point, as located by the two-headed probe, was in the region where the free-stream boundary-layer experiences favourable pressure gradient. This observation

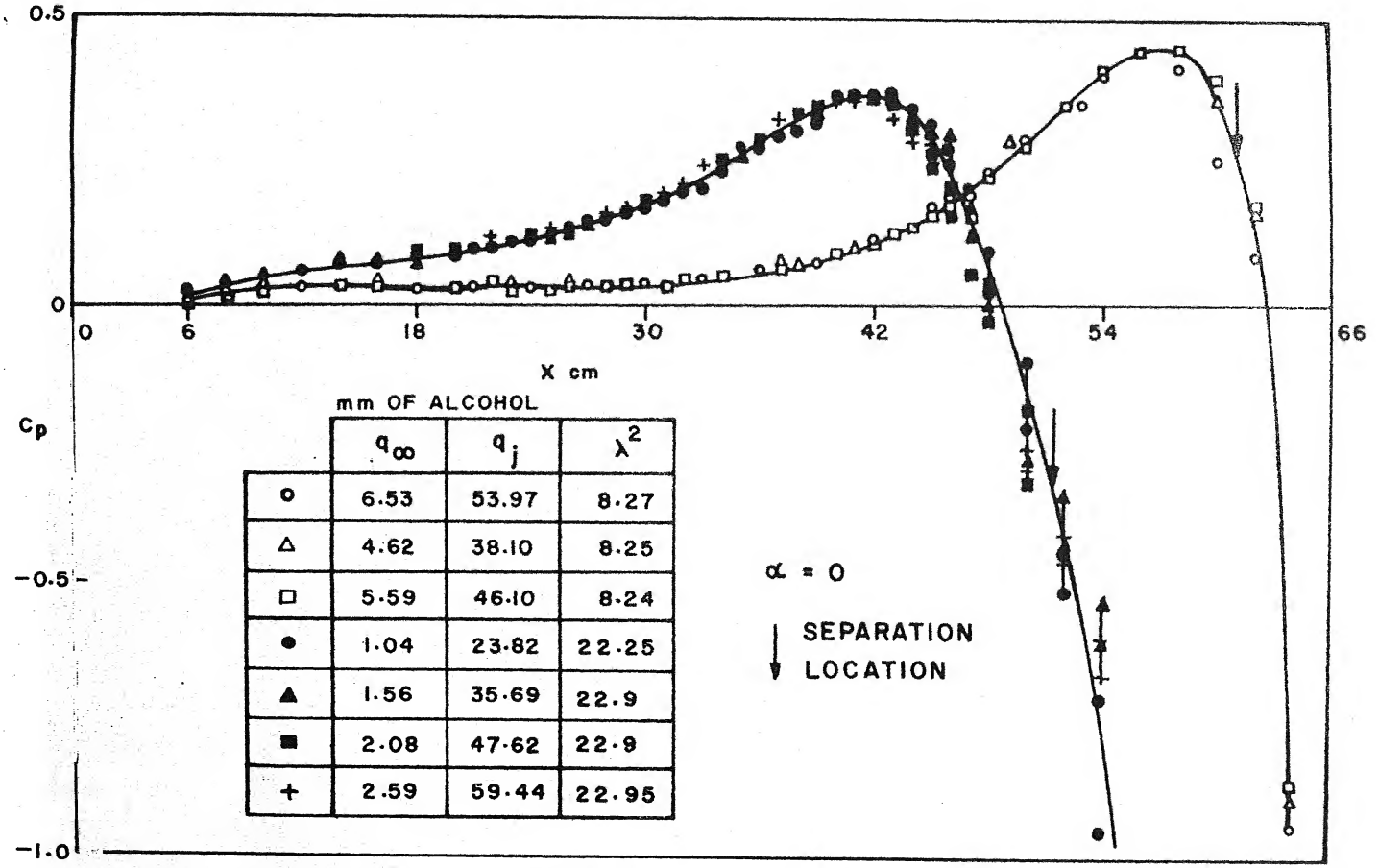

	q_∞	q_j	λ^2
o	6.53	53.97	8.27
△	4.62	38.10	8.25
□	5.59	46.10	8.24
●	1.04	23.82	22.25
▲	1.56	35.69	22.9
■	2.08	47.62	22.9
+	2.59	59.44	22.95

FIG.19 UPSTREAM WALL PRESSURE DISTRIBUTION
(VELOCITY RATIO KEPT FIXED)

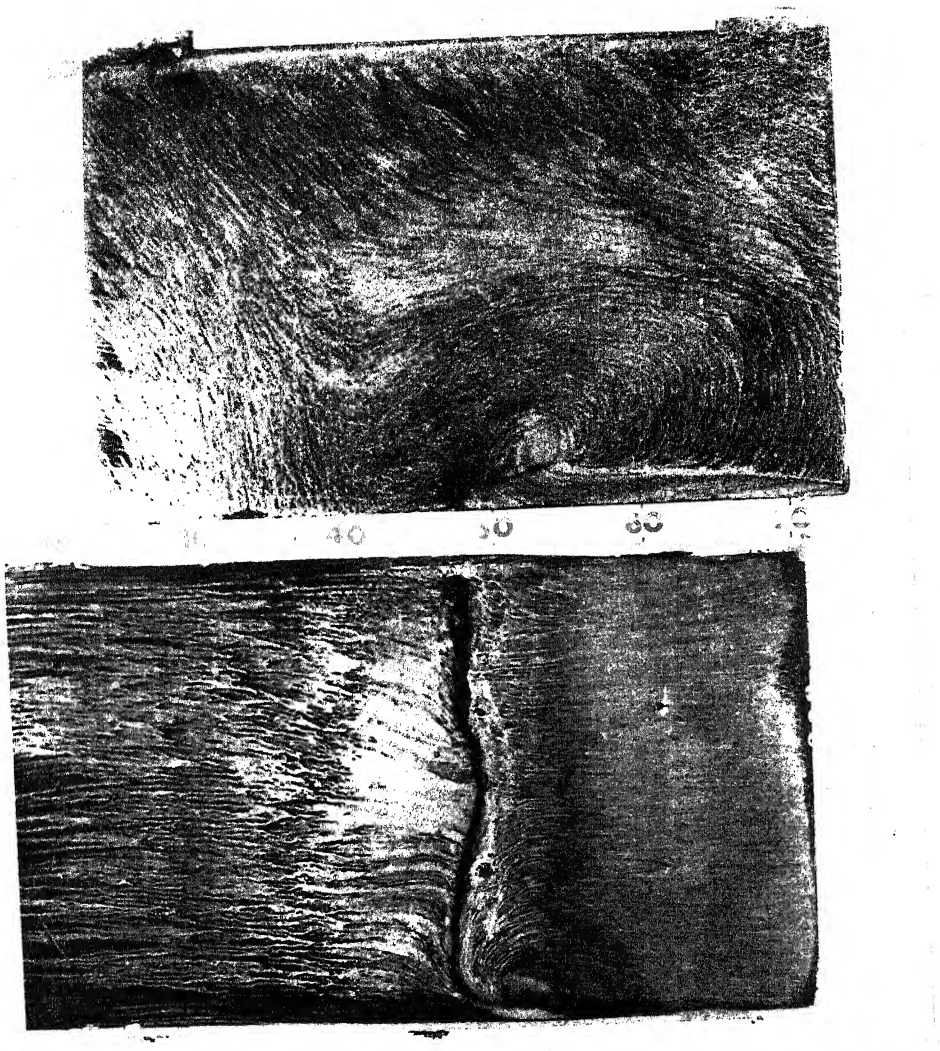

FIG. 20 SURFACE FLOW PATTERN WITH OIL FILM ($\lambda = 5{\cdot}1$)

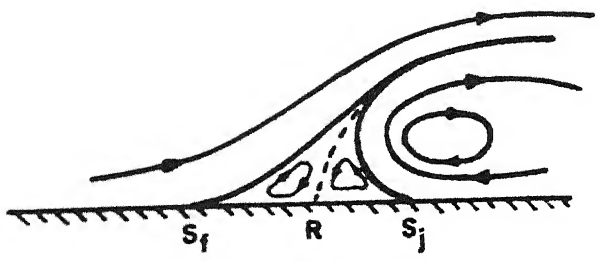

FIG.21 POSSIBILITY OF SECONDARY SEPARATION

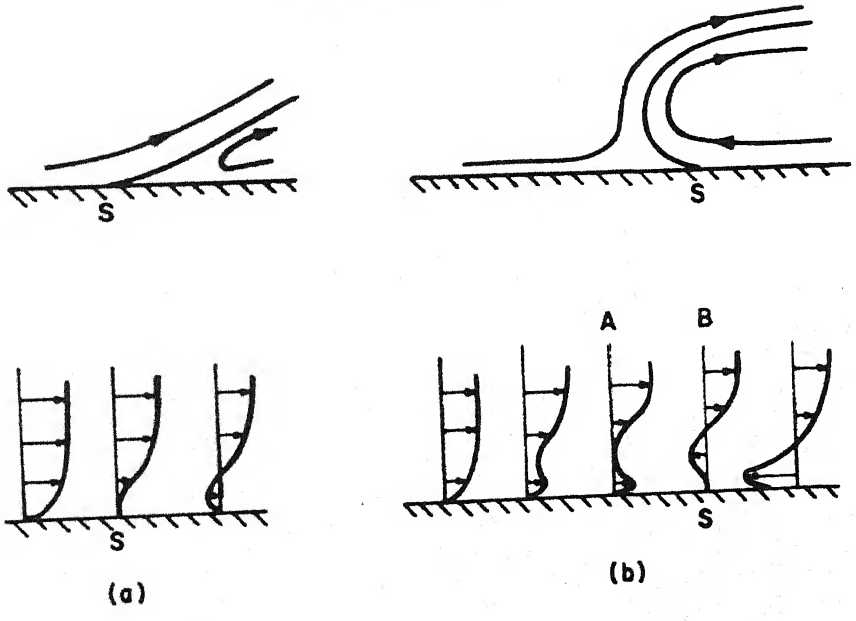

FIG.22 MONOTONIC AND NONMONOTONIC VELOCITY PROFILES BEFORE SEPARATION

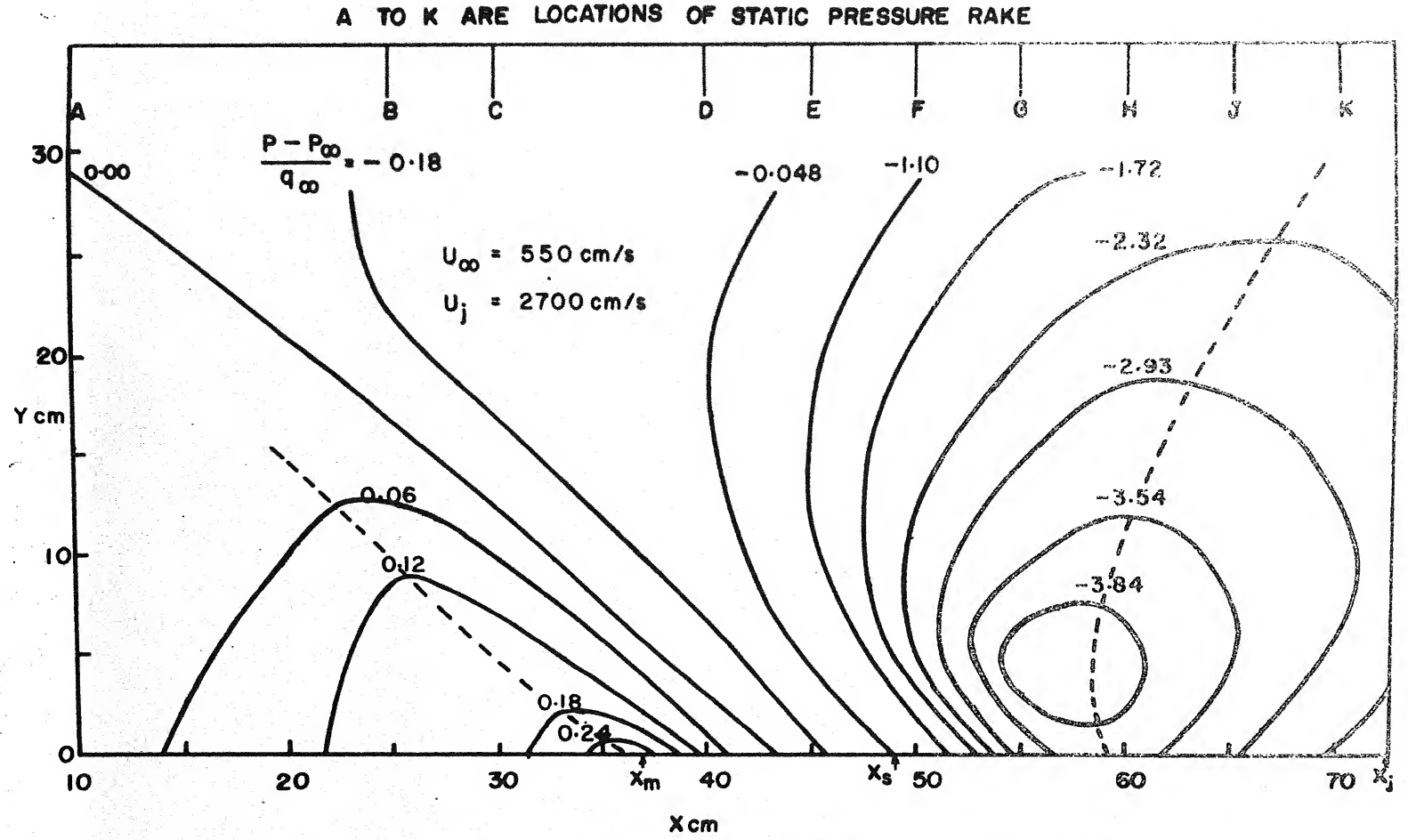

FIG. 23 ISOBARS IN WALLJET INDUCED SEPARATION

On the other hand, the pressure gradient experienced by the wall jet is adverse and its separation is compatible with the classical arguments. Further, the velocity field measurements (part 1, Figure 20) also indicate that the wall jet separated and curled up after proceeding a short distance upstream. The dividing streamline obtained by flow visualisation (Figure 17 and 20) also shows that it initially proceeds a short distance in upstream direction before turning around (part II, Figure 22(b)).

Although the above view makes the experimental observations understandable, some difficulties are not resolved by the arguments. As the vortical layer of the free-stream close to the wall plunges deep into the interior, the free-stream vortical layer separates in the usual sense. Further, any free-stream boundary-layer calculations based on a suitable turbulence model, and experimental initial conditions and wall pressure distribution cannot predict the separation of the free-stream boundary-layer if adverse pressure gradient is indeed necessary at the separation point as obtained by the classical argument.

While it is certainly possible to question the validity of boundary-layer approximation close to the separation point, it would be difficult to expect the calculations to predict even a tendency to separate, that is, a steady decrease in skin friction or rapid increase in δ. Further, the

experimental values of skin friction and parameters (Part I, Figure 17) are qualitatively like other turbulent boundary-layers near separation.

A simple argument can be given to show that the classical argument (Schlichting, 1960, p. 113) really applies to velocity profiles which are monotonic upstream of separation. In the present experiment, the velocity profile has a dip (Part I, Figure 16) which grows as the separation point is approached. Consequently the reversed flow begins at an interior point. Clearly, it is seen from the sketch (Figure 22(b)) that $\partial u/\partial y$ at sections between A and B decreases from positive values at the wall to a zero value at some interior point suggesting that $\partial^2 u/\partial^2 y$ is in all probability negative at the wall, which immediately implies a favourable pressure gradient.

Thus a theoretically important general conclusion emerges namely, that separation of a boundary-layer can take place in a favourable pressure gradient. Such a separation, which is permitted by the dynamics of the flow, is of course going to be realised in practice only under rather special types of initial and boundary conditions which give rise to non-monotonic velocity profiles upstream of the separation point.

3.4 PARAMETERS AND SIMILARITY OF UPSTREAM PRESSURE DISTRIBUTION.

Figure 24 shows the effect of λ on the upstream wall pressure distribution. Increase in λ resulted into shift of pressure maxima in the upstrear direction and the location of separation point away from $C_{p_{max}}$ position. $C_{p_{max}}$ decreased with increase in λ .

The gross effect of λ on wall pressure distribution can be readily seen by considering the behaviour of several parameters (Table 1). X_m and X_o where C_p is maximum or zero were obtained from pressure measurement to within ± 2 mm. The maximum height of the dividing streamline h was obtained from the flow visualisation plate and it was estimated within ± 3 mm.

The height h was found to be a suitable length scale for inviscid flow models (section 3.6). Visual observation was not attempted for all the values of λ . However it was noticed that h was approximately 1.2 times the distance $(X_o - X_m)$. Hence $(X_o - X_m)$ was used as a length scale for experimental data correlation. Figure 25 shows that $(X_s - X_m)$ and $(X_o - X_m)$ vary approximately linearly with λ^2. $C_{p_{max}}$ attains a value of approximately 0.2 for λ larger than 6, but for smaller values there is a marked rise in the value of $C_{p_{max}}$.

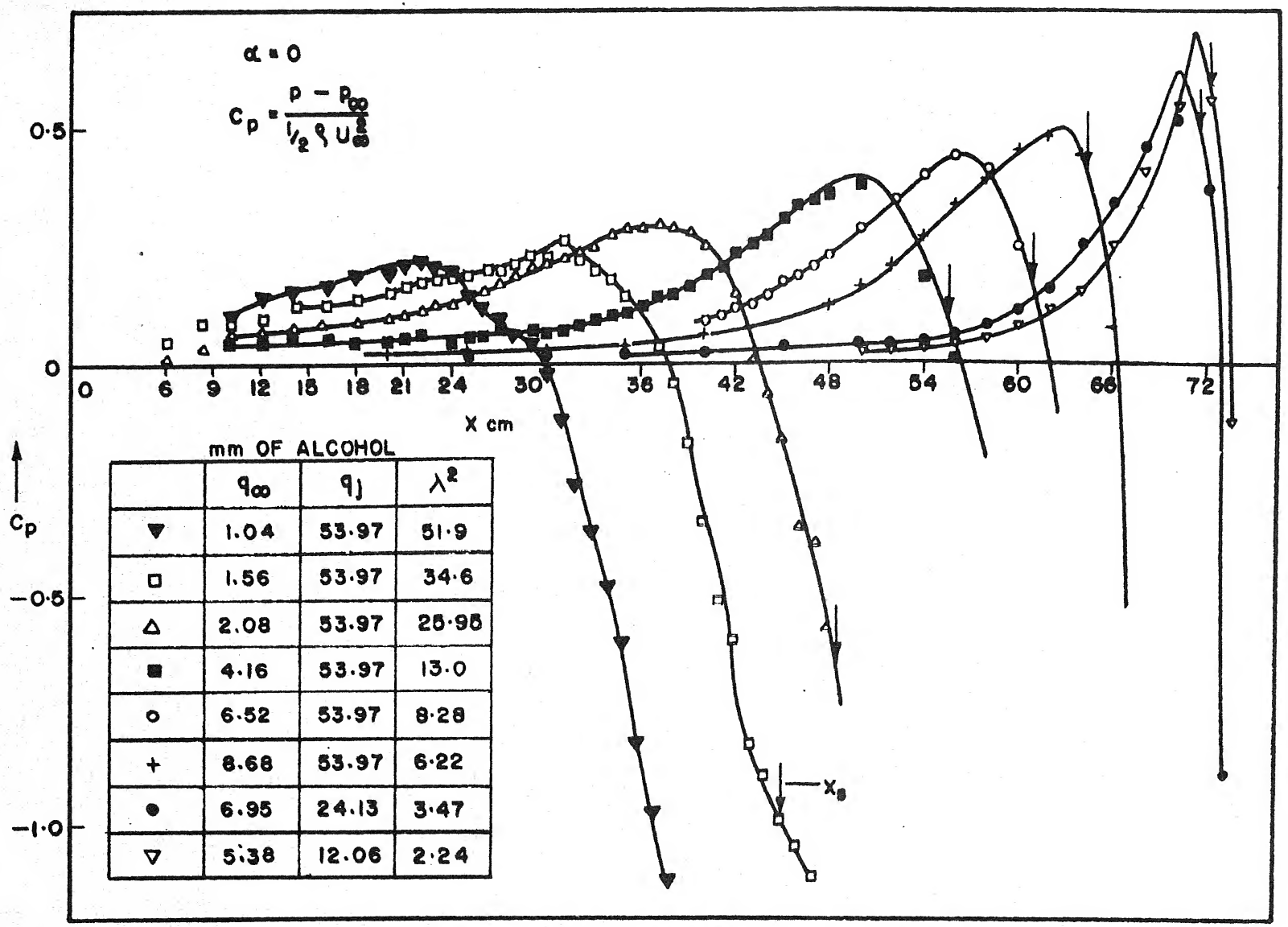

mm OF ALCOHOL

	q_∞	q_j	λ^2
▼	1.04	53.97	51.9
□	1.56	53.97	34.6
△	2.08	53.97	25.95
■	4.16	53.97	13.0
○	6.52	53.97	8.28
+	8.68	53.97	6.22
●	6.95	24.13	3.47
▽	5.38	12.06	2.24

FIG.24 UPSTREAM WALL PRESSURE DISTRIBUTION

TABLE 1

PARAMETERS OF UPSTREAM EFFECT
(zero pressure gradient)

q_ω mm of al.	q_j mm of al.	λ	$C_{p_{max}}$	X_s cms	X_o cms	X_m cms	h cms	$\frac{X_o - X_m}{h}$
1.04	54.0	7.20	0.220	41.5	30.5	21.5	10.9 ±.3	0.826
1.56	54.0	5.88	0.253	45.5	38.0	30.8	8.7 ±.2	0.828
2.08	54.0	5.09	0.300	48.6	43.5	37.0	7.8 ±.2	0.832
1.04	23.8	4.78	0.366	51.3	48.3	42.0	7.6 ±.3	0.828
1.56	35.7	4.78	0.358	51.3	48.3	42.0	--	--
1.04	47.6	4.78	0.360	51.3	42.9	48.3	--	--
2.60	59.4	4.79	0.353	51.3	48.3	42.0	--	--
4.17	54.0	3.60	0.384	55.7	56.5	51.2	6.4 ±.1	0.828
6.53	54.0	2.87	0.440	60.9 ±0.1	62.0	57.8	4.9 ±.1	0.817
8.70	54.0	2.49	0.500	64.5 ±0.5	66.2	62.5	--	--
7.0	24.1	1.86	0.620	71.3	73.1	70.0	--	--
5.38	12.0	1.50	0.700	72.2	73.6	71.0	--	--

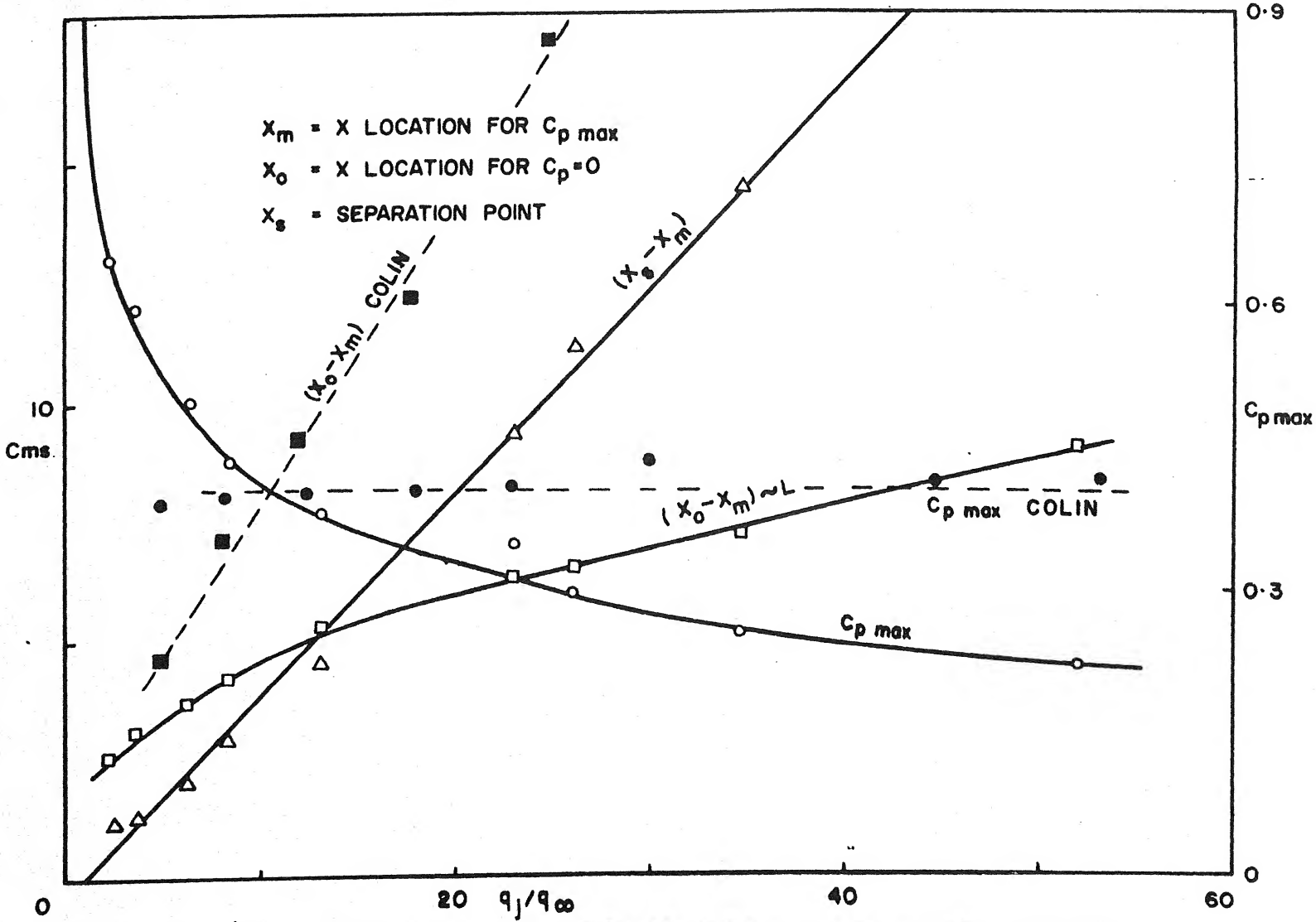

FIG.25 PARAMETERS OF UPSTREAM PRESSURE DISTRIBUTION

(X_o-X_m) and $C_{p_{max}}$ obtained from Colin's data (1968) are also plotted in the figure. (X_o-X_m) is roughly linear with λ^2 while $C_{p_{max}}$ is about 0.4.

The difference could be due to several reasons. First, the static pressure taps were spaced in Colin's experiment at 5 cm unlike the spacing of 1 cm in the present experiment. Wall jet exit height t_j was 2.3 mm in the former, while it is 4 mm in the present experiments. Interpolation near a sharp peak with large spacings evidently can cause significant errors in $C_{p_{max}}$ and X_m. Also, the ratio of wall jet thickness to test section height was 75 in the present experiment while it was 200 in Colin's experiment. Consequently blockage effect would be different. (X_s-X_m) could not be estimated from Colin's data as X_s was not measured.

Separation point was observed to move closer to the $C_{p_{max}}$ location with decrease of λ and they almost coincided at $\lambda = 1$. Figure 26 shows that the behaviour of $C_{p_{max}}$ can be approximated by $\lambda^{-3/4}$ and (X_o-X_m) behaves as $1.9\ \lambda^{3/4}$.

3.5 SIMILARITY OF UPSTREAM PRESSURE DISTRIBUTION

It is of interest to find out whether the upstream wall pressure distribution is governed by a similarity rule. The pressure distribution of Figure 24 suggests such a possibility. As mentioned earlier (X_o-X_m) was taken as a length scale for experimental pressure distribution. Figure 27 shows $C_p/C_{p_{max}}$

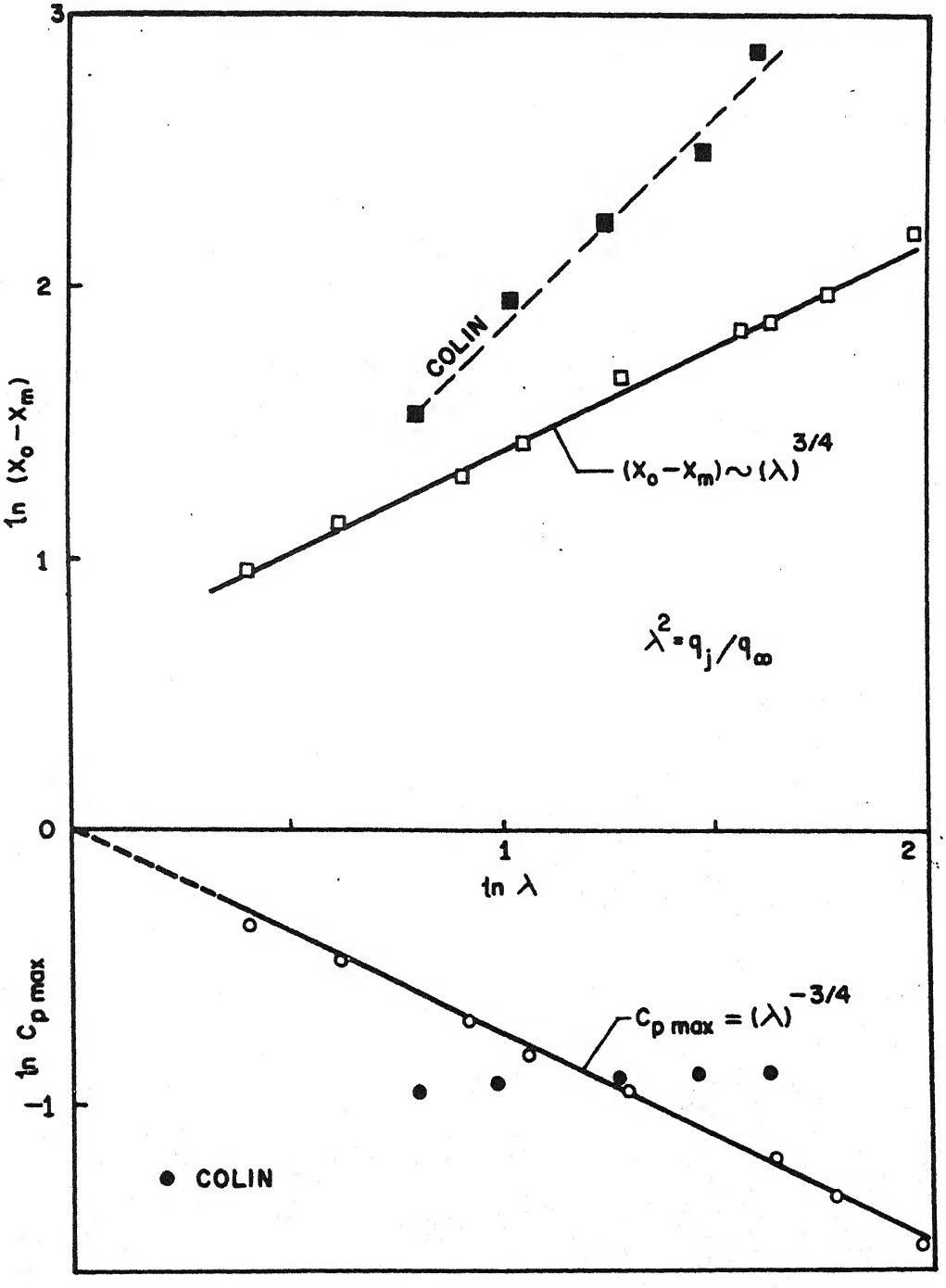

FIG.26 VARIATION OF $(X_o - X_m)$ & $C_{p\,max}$ WITH λ

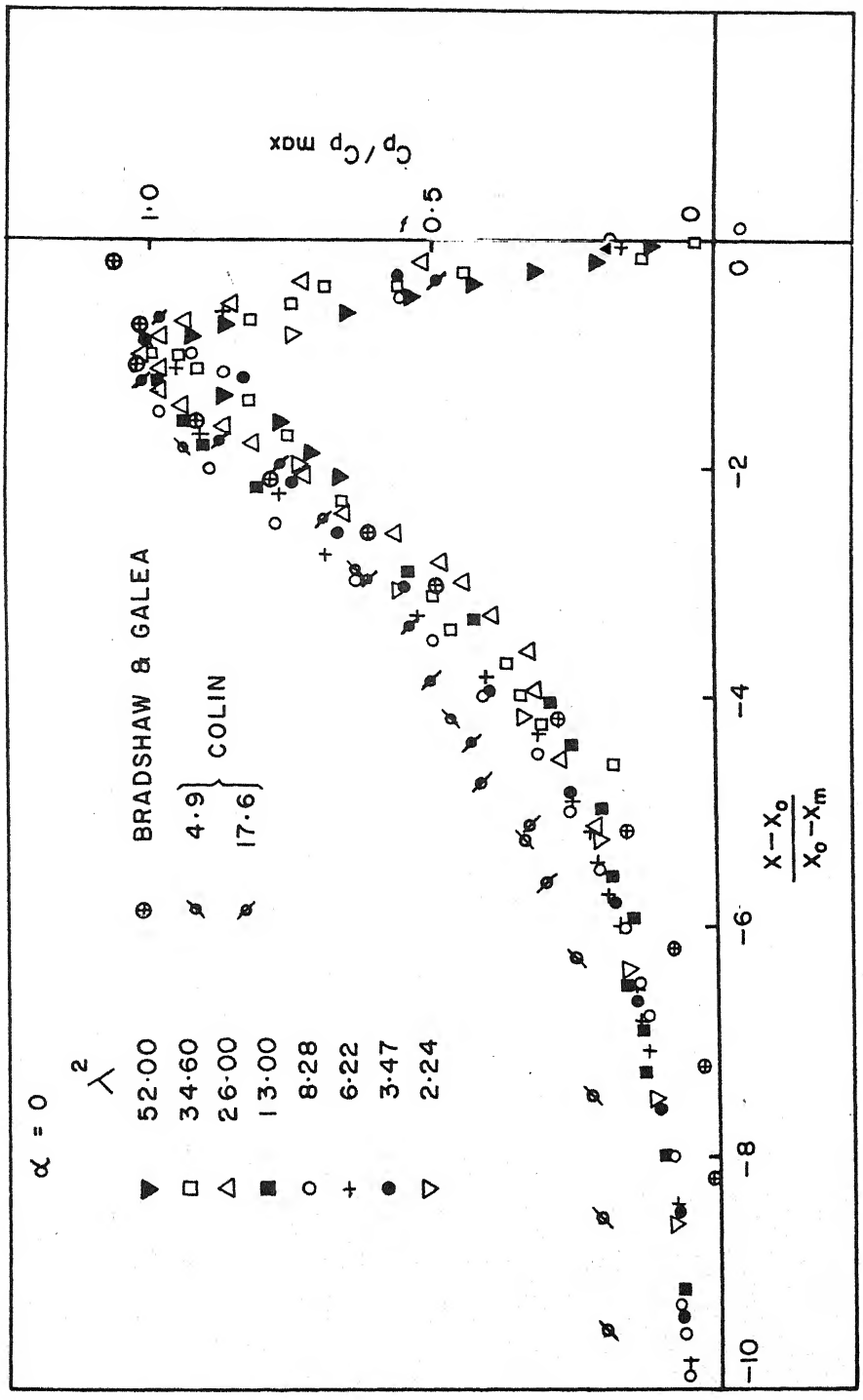

FIG.27 SIMILARITY IN WALL PRESSURE DISTRIBUTION

plotted against $(X-X_o)/(X_o-X_m)$ for various λ . For $(X_o-X)/(X_o-X_m) > 6$ the points lie close to a curve suggesting similarity to a good approximation. For lower values of $(X_o-X)/(X_o-X_m)$ there is a spread indicating a possible weak effect of λ . It is conceivable that if some other X_{ref} is taken as a reference point instead of X_o, or a slightly different length scale is choosen, the spread might diminish. This question was not investigated.

It was also noticed that for the present experiment

$$(X_m-X_{m/2}) \approx 2(X_o-X_m) \qquad (3)$$

where $X_{m/2}$ is the location of $C_{p_{max/2}}$ in the region upstream of $C_{p_{max}}$. So the former can also be used as a length scale in comparing data from other experiments which do not provide X_o. Figure 27 also shows the upstream effect in Colin's (1968) experiments. Colin's data for various λ also show that trend is of the same type as the present experiments. Colin's wall pressure measurements are however larger at far upstream distances. This could be the effect of W/t_j or W/L on pressure distribution, W being the height of the test section, or the effect of reference pressure used in calculating C_p.

Experimental data of Bradshaw and Galea (1967) for a forward-facing step is also shown in Figure 27. Equation(3) was used for getting these data and distances were measured from X_m. There is a close resemblence in far upstream effect

upto the maximum pressure. Points fall below the present experimental data for large upstream distances, but this could be due to choice of reference pressure, blockage effect, or the presence of a pressure gradient in corresponding unseparated flow past step.

These comparisons show that the far upstream effects observed in the present experiment are not confined to wall jet induced separation.

3.6 INVISCID FLOW MODELS AND FAR UPSTREAM EFFECTS

The upstream effects can in part be viewed as a displacement caused by the thick reversed flow region of the outer inviscid flow field which is governed by elliptic equations. This type of upstream effect can be studied in a simple way by considering various hypothetical models which describe indirectly the geometry of the dividing streamline. While the models may be crude in describing the geometry, they can still provide good approximations to upstream effects at sufficiently large upstream distances from the separation point.

Four flow models were considered (Figure 28). Complex potential ϕ and complex coordinate z are given by the following analytical expressions.

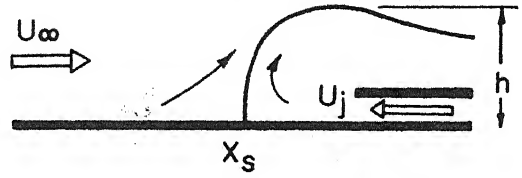

(A) EXPERIMENTAL SITUATION

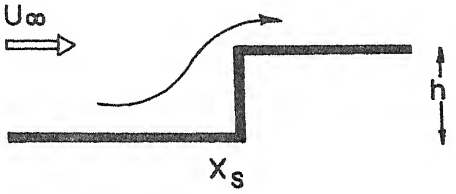

(M1) STEP MODEL

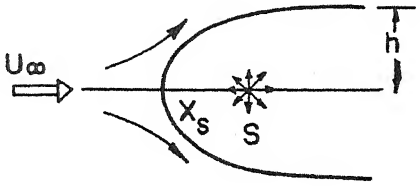

(M2) SOURCE MODEL

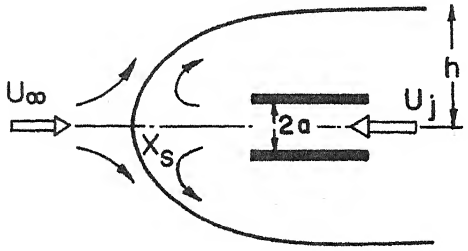

(M3) OPPOSED JET MODEL

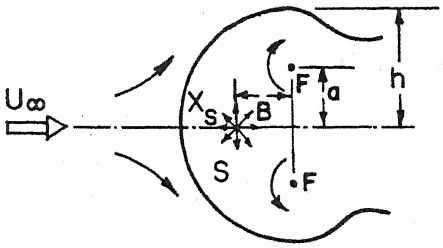

(M4) SOURCE & VORTEX PAIR MODEL

FIG.28 INVISCID FLOW MODELS

(1) STEP MODEL (Milne Thompson 1963, p.273)

$$z = \ln\left(\pi\omega + \sqrt{\pi^2\omega^2 - 1}\right) + \sqrt{\pi^2\omega^2 - 1} \qquad (4a)$$

where step height h is taken to be unity.

This gives

$$U_c = \frac{1-\pi\phi}{1+\pi\phi} \qquad (4b)$$

$$X = \frac{1}{\pi}\left\{\ln\left(\pi\phi + \sqrt{\pi^2\phi^2 - 1}\right) + \sqrt{\pi^2\phi^2 - 1}\right\} \qquad (4c)$$

Where U_c and X are nondimensional velocity and distances along the front stagnation line from the stagnation point.

(2) SOURCE MODEL (Milne Thompson, 1963, p.202)

$$\omega = -U_\infty z - S \ln z \qquad (5a)$$

where $h = \pi s/U_\infty$ is taken to be unity and s is the source strength.

This gives velocity along the front stagnation line as

$$U_c = 1 + \frac{1}{\pi X} \qquad (5b)$$

(3) OPPOSED JET MODEL (LAMB, 1945, p.74)

$$z = -\frac{\omega - U_\infty z}{U_\infty/m} + \frac{a}{\pi}\exp\left\{\frac{-\pi(\omega - U_\infty z)}{aU_\infty/m}\right\} \qquad (6a)$$

where $\frac{m-1}{m} = \lambda$ and 2a = channel width, and h = a/m = 1

The velocity U_c at X is given in terms of a parameter ϕ_1,

$$U_c = \frac{U_\infty}{m}\left[\frac{1-m\left\{1+\exp\left(\frac{-\pi\phi_1 m}{aU_\infty}\right)\right\}}{1+\exp\left(\frac{-\pi\phi_1 m}{aU_\infty}\right)}\right] \qquad (6b)$$

$$\text{and } X = \frac{\phi_1 m}{U_\infty} + \frac{a}{\pi}\exp - \frac{\pi\phi_1 m}{aU_\infty} \qquad (6c)$$

(4) SOURCE AND VORTEX PAIR MODEL (Milne Thompson, 1963, p.357)

$$\omega = U_\infty z - s\ln(z+B) + iF\ln\frac{z-ai}{z+ai} \qquad (7a)$$

where $U_\infty = F/2a = 1$ and $h = \pi s/U_\infty = 1$

s is the source strength and F is the vortex strength

This gives

$$U_c = \frac{1}{\pi(X+B)} + \frac{4a^2}{(X^2+a^2)} - 1 \qquad (7b)$$

B was varied from -1 to -9 and was found to have little effect on C_p.

A suitable length scale for describing the upstream effect by these inviscid models was found to be h, the maximum height of the dividing streamline from the line of symmetry. The pressure coefficient upstream of the stagnation point is shown in Figure 29 for step and the source model

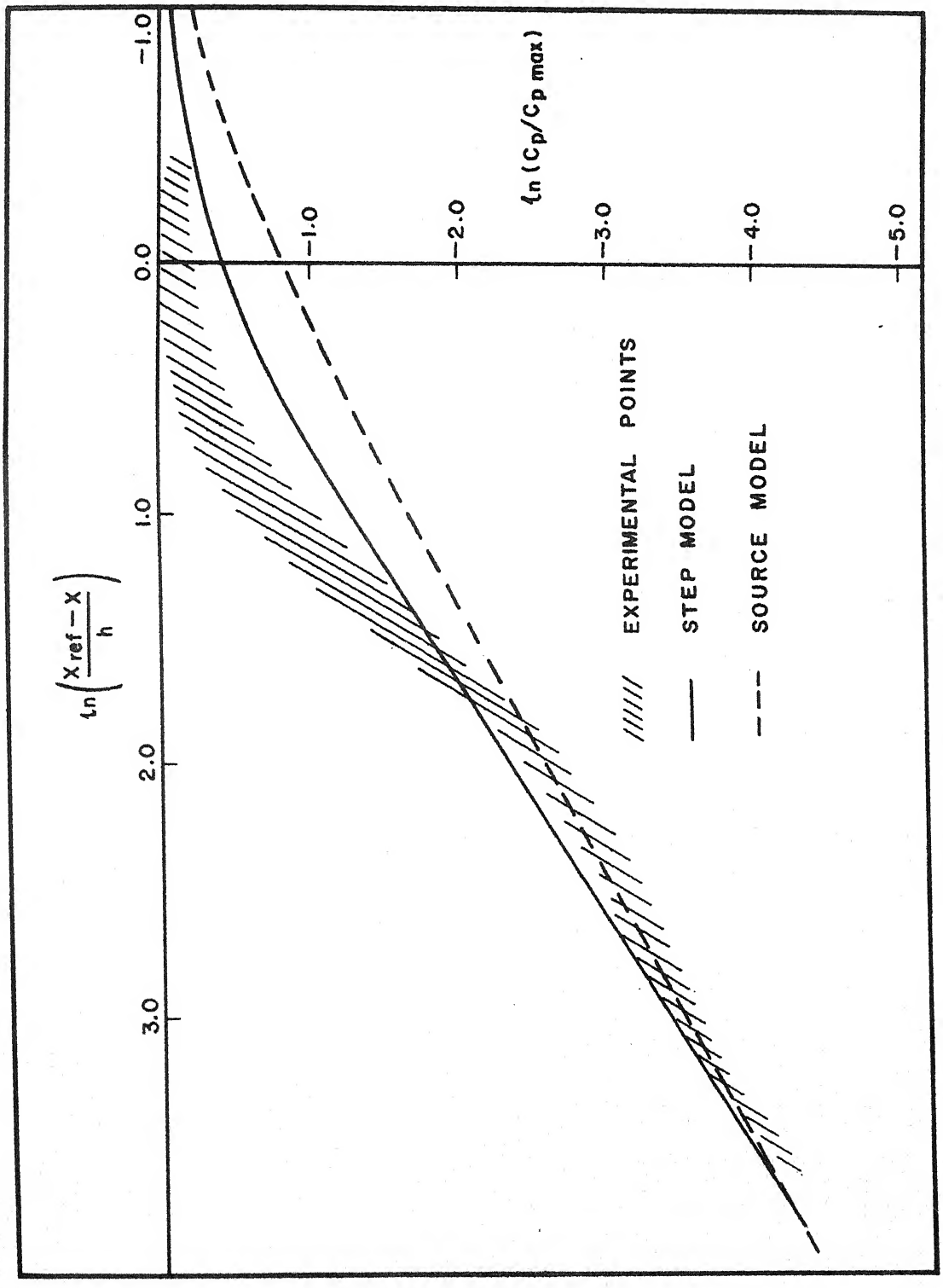

FIG.29 UPSTREAM EFFECT

where X_{ref} is taken to be the stagnation point ($C_{p_{max}} = 1$). Pressure distributions due to other models lie in between and are not shown. Thus the pressure distributions, scaled suitably, due to various models coincided at large upstream distances of the order of $(X_{ref}-X)/h > 6$.

This large distance behaviour is compatible with the experimental pressure data as indicated in Figure 29, agreement being greater with the source model. X_{ref} was taken to be X_o for experimental points and h was either taken from flow visualisation or taken as 1.2 (X_o-X_m).

3.7 NEAR UPSTREAM EFFECTS

There is a marked departure of experimental pressure distribution close to the separation point from all the inviscid flow models. This shows that in addition to the inviscid effect, there is an additional effect due to viscosity which is predominantly felt near the separation point. This effect has a scale smaller than the inviscid length scale. One is compelled to hypothesise that the vortical layer upstream of the separation point has a displacement effect on the inviscid flow field which gives rise to acceleration of the outer flow. Classical boundary-layer theory leads to the conclusion that the displacement effect and its effect on the pressure gradient are of a higher order. The action of boundary-layer on the outer flow is thus weak. The observed near upstream effect

requires a modification of the classical boundary-layer to permit a strong interaction over a limited distance. A strong interaction modification of boundary-layer has been made in supersonic flows (Lees and Reeves, 1964), as pointed out earlier.

The smaller length scale $(X_o - X_m)$ is shown in Figure 26 as a function of λ. It is seen that this behaves as $\lambda^{3/4}$ to a good approximation. If flow fields for different values of λ are obtained by holding the jet velocity fixed and varying the free-stream velocity, then $(X_o - X_m) \sim U_\infty^{-3/4}$ or as $(U_\infty L/\nu)^{-3/4}$ for a suitable length scale L for the free-stream boundary-layer. Thus the smaller length scale of upstream effect can be interpreted to behave as $R_\infty^{-3/4}$ $(R_\infty = U_\infty L/\nu)$ for fixed jet velocity.

3.8 INFLUENCE OF PRESSURE GRADIENT OF UNSEPARATED FLOW ON THE UPSTREAM EFFECT

As indicated in section 1.3, the effect of separation can be viewed as potential flow field $\Delta\psi$ added to an unseparated flow ψ'. The results given so far dealt with the case when ψ' was approximately uniform. To study possible effects of nonuniform ψ' on $\Delta\psi$, a straight false wall was placed near the roof of the test section. The inclination of the plate was varied by $\pm 2.5°$ ($\alpha = 0.0438$) to obtain adverse or favourable pressure gradient for the free-stream flow in absence of wall jet.

Experiments similar to zero pressure gradient case were carried out to find the effect of the recirculating region on the upstream wall pressure distribution. The pressure distributions were found to be similar to the zero pressure gradient case. Relevant parameters of the pressure distribution are given in Table 2.

Possible correlation of upstream pressure distribution for flow with pressure gradient with the pressure distribution of uniform flow was considered in the following way. If the static pressure is constant across the boundary-layer, the velocity at the edge of the boundary-layer is given by $U_1/U_\infty = \sqrt{1-C_p}$ (8)

Following the arguments of section 1.3, we regard the difference between external velocity distribution in presence of separation and that in absence of separation as the net effect of separation. We therefore consider

$$F(X-X_s;\ \lambda, \alpha) = \left[U_1(X-X_s;\ \lambda, \alpha) - U_1(X-X_s;\ 0, \alpha)\right]/U_\infty \quad (9)$$

The values of this function are shown in Figure 30 by unfilled symbols for two adverse and one favourable pressure gradient case. Filled symbols are for $\alpha = 0$ based on data discussed in earlier sections. Both terms on the right hand side were calculated from corresponding wall pressures by using (8). Clearly, for $X-X_s > 8$ cm curves for zero α coincide with those for non-zero α.

TABLE 2

PARAMETERS OF UPSTREAM EFFECT
(Adverse and favourable pressure gradient)

ADVERSE PRESSURE GRADIENT Wall slope = 2.5°, α = 0.0438 radians.

q_∞ mm of Al.	q_j mm of al.	λ	$C_{p_{max}}$	X_s cms	X_o cms	X_m cms
1.04	54.0	7.20	0.207	41.5	27.5	21.5
2.08	54.0	5.09	0.305	47.3	42.1	36.5
4.17	54.0	3.60	0.395	54.1	54.1	49.1
6.53	54.0	2.87	0.490	58.8	61.0	56.4
8.33	54.0	2.54	0.537	61.1	63.5	59.3
FAVOURABLE PRESSURE GRADIENT Wall slope =-2.5° α =-0.0438 radians						
1.04	54.0	7.20	0.256	45.4 $\pm$0.2	33.0	24.5
2.08	54.0	5.09	0.317	51.6	48.0	42.0
4.17	54.0	3.60	0.384	58.7	59.5	55.0
6.53	54.0	2.87	0.44	63.9	65.5	62.0

rg:lp/26473.

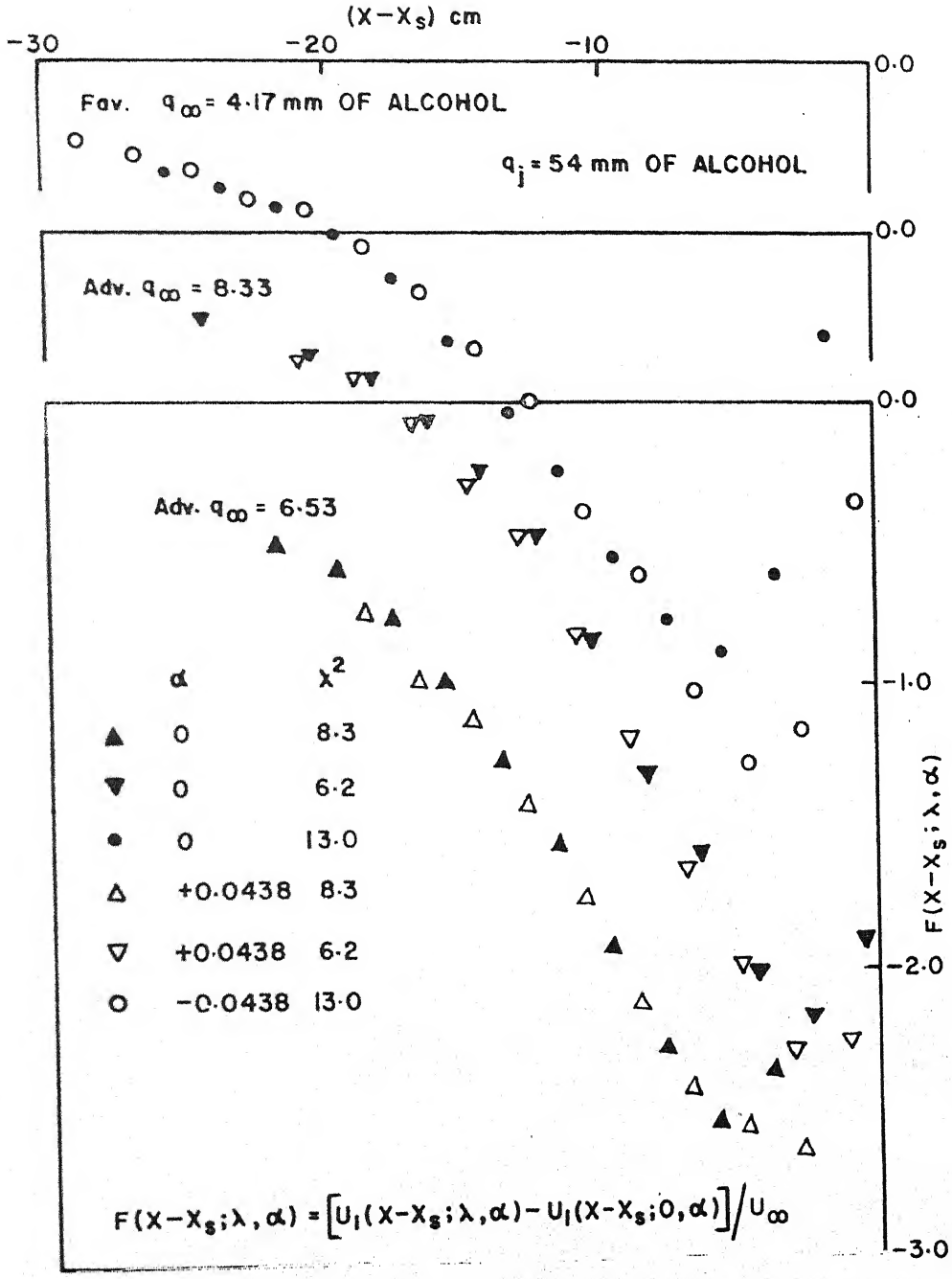

FIG.30 UPSTREAM EFFECT WITH EXTERNAL PRESSURE GRADIENT

This suggests that the far upstream effect is not significantly influenced by the pressure gradient of unseparated inviscid flow. Near the separation point however the differences are quite detectable. They are also compatible with the earlier conclusion that the near upstream effect is probably due to strong interaction of rapidly thickening vortical layer of the external flow.

3.9 CONCLUSIONS

The major conclusions are summarised below. It is clear from the previous sections that although there is scope for making more accurate measurements, the broad trends seem to have been definitely established.

(1) The upstream wall pressure can be described to a good approximation by

$$C_p = C_p(X/t_j, \lambda)$$

(2) Far upstream, the pressure rises, or the inviscid flow outside the boundary-layer is retarded. Near the separation point, the inviscid flow is accelerated. If the unseparated inviscid flow has an adverse pressure gradient, this local acceleration would decrease the magnitude of the adverse pressure gradient. This is known to be a fairly general feature of pressure distribution near the separation point (Townsend, 1962, Tani, 1964).

(3) Far upstream effect can be described by a similarity rule

$C_p/C_{p_{max}} = f\ (X_o-X/X_o-X_m)$ for $(X_o-X)/(X_o-X_m) > 6$. The length scale (X_o-X_m) in the above rule can be replaced by h, as for the present experiments $h \approx 1.2\ (X_o-X_m)$.

This effect can be very well described by inviscid flow models for $(X_s-X)/h \gtrsim 7$. The agreement improves with increasing upstream distance from the separation point. Clearly, the source model is the simplest and it is a very good approximation for $(X_s-X)/h > 7$. Also, the experimental data for a forward facing step resembles the present data suggesting that details of method of separation do not have a significant influence in this range.

When the unseparated inviscid ψ' was nonuniform, the far upstream effect $\Delta\psi$ of separation in the present experiment were found to be the same as in uniform flow for about $(X_s-X) > 8$ cm.

(4) The near upstream effect is qualitatively different from the description of all inviscid models. It therefore suggests that a different mechanism is needed to account for it. Observations seem to call for a strong interaction between the rapidly growing vortical layer a few boundary-layer thicknesses upstream of separation and the outer inviscid flow. Corresponding scales for

$C_{p_{max}}$ and $(X_o - X_m)$ behave like $\lambda^{-3/4}$ and $\lambda^{3/4}$. If U_j is kept constant, the scale would then behave like $R_\infty^{3/4}$ and $R_\infty^{-3/4}$.

When ψ' is nonuniform, the upstream effect $\Delta\psi$ is considerably different from the uniform flow. This is compatible with the view of strong-interaction.

(5) The free stream boundary-layer was observed to separate in favourable pressure gradient. A modification of classical argument shows that if velocity profiles upstream of separation point have a minimum, the dynamics of the flow permits pressure gradient at separation point to be favourable.

APPENDIX A

REMARKS ON DEFINITION OF SEPARATION POINT

Since there is a diversity of opinion on what constitutes a precise general definition of separation point or line, it seems desirable to make some preliminary remarks.

A steady two-dimensional flow of an incompressible fluid may be said to separate from a solid impervious boundary at rest when the streamlines close to surface do not follow the contour of the surface but leave it. Wall shear stress then changes sign at the separation point.

When one deals with (a) unsteady flow (b) a turbulent boundary-layer (c) porous boundaries (d) solid boundaries in motion (e) three-dimensional flow or (f) compressible flow, additional complications arise. At present there is no accepted definition of a separation point or line which is general enough to cover all the above types of flow situations. The lack of a precise general definition, which is probably due to incomplete understanding of the essential nature of separation, sometimes leads to consequential differences between the theoretical prediction of the location of the separation point (or line) and the experimentally observed point because they deal, in principle,

with different points. Differences could also arise between locations of separation points (or lines) found by different experimental techniques for the same reason.

A notable advance was made by Maskell (1955) who introduced the notion of 'limiting streamlines' on a stationary impervious body. As the wall is approached, although the velocity approaches zero, the direction of a streamline approaches a limit direction. Lines along these directions are termed 'limiting streamlines.' Maskell (1955) proposed to distinguish separation in three-dimensional flows by the locus of branching of limiting streamlines. Lighthill (1963) further studied separation in three-dimensional flows in terms of surface vorticity.

In the two-dimensional stationary turbulent boundary-layer on an impervious wall, the flow near separation is time dependent and one has to deal with instantaneous flow and mean flow. Thus as the mean wall stress begins to diminish, a point is reached beyond which the instantaneous wall shear stress is negative for some time interval and positive during the remaining time interval. There is an associated reversal of instantaneous flow close to wall. Kline (1959) working with dye in a water tunnel observed that the onset of instantaneous separation is characterised by small intermittent streaks of back flow occuring near the wall followed by their motion away from the wall and then being

washed downstream by the main flow. In such regions the upstream flow occurs for a certain fraction of the total time and the downstream flow for the rest of time. The mean wall shear stress may have positive, zero or negative values in such regions, as instantaneous wall shear stress at any point in this region takes positive and negative values. The region where instantaneous flow reversal takes place has been termed 'separation region' by Sandborn (1969). If mean wall shear stress changes its sign, the mean streamline would depart from the vicinity of the boundary and such a point may be called (mean) separation point.

When smoke, dye, or powder is injected from the wall in the separated region (Smith & Murphy 1955, Schubauer & Spangenberg 1960) the farthest point to which the tracer is found to move upstream is judged to be the point of interest. This is the beginning of the separation region and, at this point, mean wall shear stress would in general have a small positive value. In the oil-film technique there is an accumulation of oil near the mean separation point. Similarly, in an evaporative technique, such as the China-clay technique, the markedly slow evaporation rate of reversed mean flow gives rise to two sharply different colours and the boundary is judged to be the mean separation line.

Pressure probes and boundary-layer fence (Bradshaw and Galea 1967, Sandborn & Liu 1968) are sometimes used to

indicate the direction of mean flow. The point indicated by such a technique is interpreted as mean separation point. Sometimes two wire probes in the hot-wire anemometer (Downing 1972, Delleur 1966) are used to sense the flow reversal. Such a probe can show the instantaneous direction of flow.

APPENDIX B

DATA REDUCTION

The dynamic pressure data was used to calculate the velocity profiles and also the various integral parameters of the boundary-layer. Although the least count of the micromanometer was 2.5×10^{-3} mm (0.0001"), it was noticed that readings only upto 2.5×10^{-2} mm (0.001") could be obtained with reproducibility.

The temperature of the atmospheric air throughout the period of experiments varied from 18°C to 25°C but most of the experiments were done at about 21°C and as such the density and viscosity were taken corresponding to this temperature for calculation. A mean barometric pressure of 75.1 cm of Hg was taken. The specific weight and kinematic viscosity of air were taken to be 1.135 Kg/cm^3 and 0.152 cm^2/sec corresponding to this temperature and pressure. The specific gravity of the manometric fluid (butyl alcohol) was taken as 0.8166 as recommended by the supplier. With these values, the expression for velocity is

$$U = 1175\sqrt{\ell} \qquad (10)$$

where U and ℓ are velocity in cm/s and manometric height in cm of alcohol.

If extreme values of ambient temperature and pressures are considered, the calculated velocity will be affected by 1 percent.

The law of the wall in the logarithmic portion for turbulent boundary-layer is

$$U/U_* = (1/k)\ln(YU_*/\nu) + C \qquad (11)$$

where the friction velocity U_* is $\sqrt{\tau_w/\rho}$, and the wall coordinate is YU_*/ν. The values of k and C were taken to be 0.41 and 5.0 as recommended by Coles (1968).

It was noticed that the measured profile was in good agreement with the wall law, so a method suggested by Bradshaw (1957) for obtaining the local skin-friction coefficient from the velocity profile was used. It consists of plotting a curve U(y) from the law of the wall (logarithmic law) assuming a fixed value of Y_+ and varying U_+. The curve is a rectangular parabola. The intersection of the curve with the experimental curve U(Y) determines the actual value of U_+ and thus C_f. The fixed value of Y_+ was choosen as 100 since, as seen from Figure 9, experimental points corresponding to $Y_+ = 100$ are in the logarithmic part of the law of the wall.

The integral boundary-layer parameters were calculated applying a modified variable step size Simpson's rule to the

velocity profile data. A parabola was fitted through three adjacent points, and the contributions to various integrals between the intervals of first and second points and that between second and third points were computed. The central point was then moved one point outward and the process repeated. The contributions from the first and last intervals were doubled and added to the two values of each of the other intervals and averaged to give the values of the integral parameters. The process was expected to smoothen out the experimental data. The programme, written for the IIT/K IBM 7044 computer was checked for the Blassius flat plate data (Schlichting, 1960) and the agreement in the various thicknesses was within 0.01 percent. The procedure was also checked with some of the data given in the Stanford Conference (Coles, 1968) and the thicknesses were in agreement to within 0.2 percent.

After checking the programme, other parameters like shape factor, the thickness as defined by Clauser, Reynolds number based on displacement and momentum thickness etc. were calculated from these parameters. The friction velocity used for these calculations was obtained from Bradshaw's method. Friction velocity was also calculated from the Ludwieg-Tillman empirical relation and the agreement with that obtained from Bradshaw's method was within one percent.

Momentum balance check as suggested by Coles (1968) was applied to the zero pressure gradient data. For this method the momentum integral equation is normalised and integrated with respect to X, giving

$$\frac{U_\infty{}^2\theta}{(U_\infty{}^2\theta)_o} - 1 + \tfrac{1}{2}\int_{X_o}^{X} \frac{\delta^*}{\theta_o}\, d\left(\frac{U_\infty{}^2}{U_{\infty o}{}^2}\right) = \int_{X_o}^{X} \left(\frac{U_*}{U_{\infty o}}\right)^2 d\left(\frac{X}{\theta_o}\right) \quad (12)$$

The left and right sides (denoted by PL and PR) of this equation were determined by computer programme using trapezoidal integration of unsmoothed data. This comparison represents a qualitative guide to the accuracy of C_f and to the degree of two-dimensionality of the flow.

REFERENCES

1. Batchelor GK 1956, A proposal concerning laminar wakes behind bluff bodies at large Reynolds number. J. Fluid Mechanics, Vol. 1, 388-398.

2. Bradshaw P and Galea PV 1967, Step induced separation of a turbulent boundary-layer in incompressible flow, J. Fluid Mechanics, Vol. 27, part 1, 111-130.

3. Brown SN and Stewartson K 1969, Laminar Separation, Annual Rev. Fluid Mechanics, Vol. 1.

4. Brown KC and Joubert PN 1969, The measurement of skin friction in turbulent boundary-layers with adverse pressure gradients, J. Fluid Mechanics, Vol. 35, part 4, 737-757.

5. Carpentor PW 1968, Survey and evaluation of supersonic base flow theories, NASA CR 97129.

6. Catherall D and Mangler KW 1966, The integration of two-dimensional laminar boundary-layer equations past the point of vanishing skin friction, J. Fluid Mechanics. Vol. 26, part 1, 163-182.

7. Catherall D et al 1965, Viscous flow past a flat plate with uniform injection, Proc. Roy. Soc. A, Vol. 284, 370.

8. Clauser F. 1954, Turbulent boundary-layer in adverse pressure gradient, J. Aero. Sci, Vol. 21, No. 2, 91-108.

9. Chapman DR et al 1958, Investigation of separated flows in supersonic and subsonic streams with emphasis on the effect of transition, NACA R 1356.

10. Coles DE and Hirst EA 1968, Conference, Computation of Turbulent boundary-layers, Stanford AFOSR-IFP, Vol. 2.

11. Colin PE 1968, The wall jet beneath a counter-flowing stream, von Karman institute of fluid dynamics, Rep.

12. Crocco L and Lees L 1952, A mixing theory for the interaction between dissipative flows and nearly isentropic streams, J. Aero. Sci, Vol. 19, 649-676.

13. Delleur JW 1966, Flow direction measurements by hot-wire anemometry, J. Engg. Mechanics Division, ASCE Vol. 92, 45-70.

14. Downing PM 1972, Reverse flow sensing hot-wire anemometer, J. Phy. E: Scientific Instruments, Vol. 5.

15. Drinkuth RF and Pierce EJ 1966, Directional heat meter for wall shear stress measurements in turbulent boundary-layers. Rev. Sci. Instruments, Vol. 37, 740-741.

16. Fraser HR 1958, Study of an incompressible turbulent boundary-layer in a conical diffuser, Proc. ASCE 84 (J. Hydr. Division).

17. Goldstein S 1948, On boundary-layer flow near a position of separation, Q.J.Mech. Appl. Maths., Vol. 1, 43.

18. Good MC and Joubert PN 1968, The form drag of two-dimensional bluff plate immersed in turbulent boundary-layer, J. Fluid Mechanics, Vol. 31, part 3, 547-582.

19. Hartree DR 1939, The solution of the laminar boundary-layer equation for retarded flow, Aero. Res. Council Rept. Mem. 2426 (Also 2427).

20. Helmholtz H Von 1968, See Laminar boundary-layers by Rosenhead L, p.2.

21. Howarth L 1938, On the solution of the laminar boundary-layer equation Proc. Roy. Soc. A, 164, 547.

22. Kirchoff G 1869, See Laminar boundary-layers by Rosenhead L, p. 2.

23. Klemp JB and Acrivos A 1972, A method for integrating the boundary-layer equations through a region of reverse flow, J. Fluid Mechanics, Vol. 53, part 1, 177-191.

32. Ludwieg H and Tillman W 1950, Investigations of the wall shearing stress in turbulent boundary-layers, NACA TM 1285.

33. Maskell EC 1955, Flow separation in three dimensions, RAE Rep. No. Aero. 2565.

34. McCroskey WJ and Durbin EJ 1972, Flow angle and shear stress measurements using heated films and wires, Trans. ASME, J. Basic Engg, 46-52.

35. Milne-Thomson LM 1963, Theoretical Hydrodynamics (Macmillan).

36. Moses HL 1964, The behaviour of turbulent boundary-layer in adverse pressure gradient, MIT Gas turbine Lab., Rep. 73.

37. Newman BG 1951, Some contributions to the study of turbulent boundary-layer near separation, Austr. Dept. Supp. Rep. ACA-53.

38. Nishioka M and Iida S 1972, Separation of turbulent boundary-layer (Wall pressure distribution near separation), Bulletin of the Japan Soc. Mech. Engg. Vol. 15, 1084-1092.

39. Ojha SK 1967, An experimental study of laminar separation bubbles, IISc., Bangalore, Rep. No. AE-186/A.

40. Perry A 1966, Turbulent boundary-layer in decreasing adverse pressure gradient, J. Fluid Mechanics, Vol. 26, 481-506.

41. Robertson JM and Taulbee DB 1969, Turbulent boundary-layer and separation flow ahead of a step, Development in Mech. Vol. 5.

42. Roshko A 1955, On the wake and drag of bluff bodies, J. Aero. Sci., Vol. 22, 124-132.

43. Sandborn VA 1969, Characteristics of boundary-layers at separation and reattachment, RM 14, Colorado State University.

44. Sandborn VA and Liu 1968, On turbulent boundary-layer separation, J. Fluid Mech. Vol. 32, part 2, 293-301.

45. Schubauer GB and Klebanoff PS 1951, Investigation of separation of the turbulent boundary-layer, NACA TR 1030.

46. Schubauer GB and Spangenberg WG 1960, Forced mixing in boundary-layers, J. Fluid Mechanics, Vol. 8, 10-32.

47. Smith AMO and Murphy JS 1955, A dust method for location of the separation point, J. Aero. Sci., Vol. 22, 273.

48. Spangenberg WG et al 1967, Measurements in a turbulent boundary-layer maintained in a nearly separating condition, Fluid Mech. of internal flows. (Elsevier)

49 Stewartson K 1958, On Goldstein's theory of laminar separation, Q.J. Mech. Appl. Maths, Vol. 11, 399.

50. Stratford BS 1959, An experimental flow with zero skin friction throughout its region of pressure rise, J. Fluid Mechanics, Vol. 5, 17-35.

51. Tani I 1964, Low-speed flows involving bubble separations, Prog. Aero. Sciences, Vol. 5 (Pergamon).

52. Townsend AA 1962, The behaviour of turbulent boundary-layer near separation, J. Fluid Mechanics, Vol. 12, part 4, 536.

53. Terril RM 1960, Laminar boundary-layer flow near separation with and without suction, Phil. Trans. Roy. Soc. A, Vol. 253, 55-100.

54. Zukoshi EE 1967, Turbulent boundary-layer separation in front of a forward facing step, AIAA J. Vol. 5, 1746-1753.

rpg:lp.

Date Slip

This book is to be returned on the date last stamped.

.....	.....
.....	.....
.....	.....
.....	.....
.....	.....
.....	.....
.....	.....
.....	.....
.....	.....
.....	.....
.....	.....

CD 6.72.9